Fakultät für Medizin

Abteilung für Hämatologie und internistische Onkologie

The role of anti-apoptotic BCL-2 proteins for the development and continued survival of T cell lymphoma

Sabine Rosemarie Spinner

Vollständiger Abdruck der von der Fakultät für Medizin der Technischen Universität München zur Erlangung des akademischen Grades eines Doktors der Naturwissenschaften genehmigten Dissertation.

Vorsitzender:	Prof. Dr. Jürgen Ruland
Prüfer der Dissertation:	1. Priv.-Doz. Dr. Philipp Jost
	2. Prof. Angelika Schnieke, Ph.D.

Die Dissertation wurde am 02.05.2016 bei der Technischen Universitat München eingereicht und durch die Fakultät für Medizin am 07.12.2016 angenommen.

Wesentliche Teile dieser Arbeit sind in folgender Publikation veröffentlicht:

Re-activation of mitochondrial apoptosis inhibits T cell lymphoma survival and treatment resistance

S Spinner, G Crispatzu, J-H Yi, E Munkhbaatar, P Mayer, U Höckendorf, N Müller, Z Li, T Schader, H Bendz, S Hartmann, M Yabal, K Pechloff, M Heikenwalder, G L Kelly, A Strasser, C Peschel, M-L Hansmann, J Ruland U Keller S Newrzela M Herling and P J Jost

Leukemia accepted article preview 8 March 2016; doi: 10.1038/leu.2016.49

http://www.nature.com/leu/journal/vaop/naam/abs/leu201649a.html

Ich versichere hiermit an Eides statt, dass die vorliegende Dissertation selbständig und ohne unerlaubte Hilfe angefertigt wurde. Weiterhin erkläre ich, dass die Dissertation nicht ganz oder in wesentlichen Teilen einer anderen Prüfungskommission vorgelegt worden ist und dass ich mich nicht anderweitig einer Doktorprüfung ohne Erfolg unterzogen habe.

München, den 02.05.2016

Danksagung

Mein Dank gilt allem voran PD Dr. Philipp Jost für die Chance, an diesem spannenden Projekt zu arbeiten und seine engagierte Betreuung während meiner Promotion. Bei Frau Prof. Dr. Angelika Schnieke bedanke ich mich vielmals für die Bereitschaft die Funktion als Zweitgutachterin zu übernehmen. Meine Mentorin, Dr. Monica Yabal stand mir stets mit Rat und Tat zur Seite, wofür ich mich ebenfalls herzlich bedanken möchte. Prof. Dr. Christian Peschel, Prof. Dr. Jürgen Ruland und Prof. Dr. Mathias Heikenwälder danke ich für die Bereitstellung der Räumlichkeiten und Ressourcen, die meine Forschung erst ermöglichten, sowie für ihre beratende Tätigkeiten. In unserem Team herrschte stets eine goße Hilfsbereitschaft und ein herzlicher Umgang miteinander, auch in stressigen Situationen, weshalb ich mich ganz besonders bei meinen Kolleginnen Stephanie Rott, Nicole Müller, Enktsetseg Munkhbaatar und Ulrike Höckendorf bedanken möchte. Zu Beginn meiner Promotion wurde ich herzlich von allen Labormitarbeitern der AG Ruland aufgenommen und eingewiesen, wobei ich hier vor allem Dr. Nathalie Knies, Dr. Stefan Wanninger, Kristina Brunner und Verena Laux hervorheben möchte. Dr. Konstanze Pechloff danke ich sehr für ihre Unterstützung und Unterweisung in die Mausanalysen. Ich danke allen, die durch Experimente oder beratende Funktion zum Gelingen dieses Projekts beigetragen haben: Giuliano Crispatzu, Dr. Zhoulei Li, PD Dr. Silvia Hartmann, Dr. Ji-Hee Yi, Petra Mayer, Tim Schader, Dr. Henriette Bendz, Dr. Gemma L Kelly, Prof. Dr. Andreas Strasser, Prof. Dr. Dr. h.c. Martin-Leo Hansmann, Prof. Dr. Ulrich Keller, Dr. Sebastian Newrzela und Prof. Dr. Marco Herling. Auch Dr. Marco Herold möchte ich hier dankend erwähnend, da er mir zu Beginn meines Projekts durch seine Beratung sehr weiter geholfen hat. Ebenso bedanke ich mich bei allen Mitarbeitern des Zentrums für präklinische Forschung (ZPF), der AG Ruland, AG Groß, AG Haas/Pöck, AG Krackhardt und AG Oostendorp. Mein ganz besonderer Dank gilt meiner Familie: meinen Eltern Dr. Thomas und Rosemarie Spinner für ihre Förderung und Unterstützung auf meinem gesamten bisherigen Lebensweg, sowie meinen Geschwistern Sarah, Sebastian und Stephanie. Zuletzt danke ich meinem Lebensgefährten Almamy Ahmed Bangoura, der mich auch in schwierigen Zeiten immer unterstützt und motiviert hat.

Zusammenfassung

T-Zell Non-Hodgkin Lymphome (T-NHL) bilden eine heterogene und aggressive Untergruppe der Non-Hodgkin Lymphome aus. Patienten mit T-NHL zeigen eine hohe Rezidivanfälligkeit und schlechte Langzeitüberlebensraten. Die zugrunde liegenden molekularen Mechanismen sind bis heute nur unzureichend bekannt. Lymphomzellen sind, wie alle transformierten Zellen, meist durch genetische Instabilität gekennzeichnet. Dadurch werden die Zellen enormem Stress ausgesetzt, was sie prinzipiell für den programmierten Zelltod, auch Apoptose genannt, anfällig macht. Durch Fehlregulationen innerhalb des Apoptose-Signalweges entkommen die Lymphomzellen diesem Schicksal jedoch. Eine Überlebensstrategie transformierter Zellen besteht oft darin, anti-apoptotische Bcl-2 Proteine (BCL-2, BCL-X_L, BCL-W, MCL-1 und A1) verstärkt zu exprimieren wodurch die Reizschwelle für den Zelltod erhöht wird. In manchen hämatologischen Krebserkrankungen zeigte sich bereits, dass das anti-apoptotische Bcl-2 Protein MCL-1 obligatorisch für das Überleben der transformierten Zellen ist (1). Weiterhin steuern MCL-1, sowie teilweise auch BCL-2 und BCL-X_L, das Überleben von normalen hämatologischen Zellen, darunter auch T-Zellen (2,3).

Ziel dieser Arbeit war es herauszufinden, ob anti-apoptotische Bcl-2 Proteine auch essenzielle Kompontenten für das Überleben von T-NHL Zellen darstellen und so als geeignete Angriffspunkte für die Therapie der T-NHL dienen. Dazu wurde das Prinzip der konditionellen genetischen Deletion verwendet, um *Mcl-1* bzw. *Bcl-x_L* gezielt nach Etablierung der Lymphome zu eliminieren. Zur Etablierung der T-NHL wurden vier Wochen alte Mäuse viermal einer 150 rad γ-Strahlung ausgesetzt. Erfahrungsgemäß entwickeln diese bestrahlten Mäuse dann in einem Zeitraum von wenigen Monaten T-Zell Lymphome, die dem humanen T-NHL gleichen (4). Sobald die Mäuse klinische Anzeichen einer Erkrankung zeigten, wurden aus Lymphknoten, Thymus und Milz die T-NHL Zellen gewonnen.

Heterozygoter Verlust von *Mcl-1* führte zu einer signifikanten Reduktion der Viabilität der T-NHL Zellen ex vivo. Die homozygote Deletion von *Bcl-x$_L$* rief ebenfalls Apoptose in den T-NHL Zellen hervor, zeigte allerdings weniger Potential als der Verlust eines Allels von *Mcl-1*. In beiden Situationen konnte die Re-Expression der verschiedenen anti-apoptotischen Proteine einem Sterben der Zellen entgegen wirken. Weiterhin waren die Zellen resistent gegen ABT-737, einem BH3-Mimetic das BCL-2, BCL-X$_L$ und BCL-W inhibiert, MCL-1 und A1 aber nicht binden kann. Nur bei gleichzeitiger Reduktion von MCL-1 konnte ABT-737 den Zelltod von T-NHL Zellen herbeiführen.

Die heterozygote Deletion von *Mcl-1* konnte außerdem die Rekonstitution nach Transplantation von T-NHL Zellen in Empfängermäusen signifikant verzögern. Reduktion von MCL-1 führte weiterhin zu einem verstärkten Effekt verschiedener Chemotherapeutika ex vivo und erhöhtem Ansprechen auf Doxorubicin in vivo, was darauf schließen lässt, dass MCL-1 geeignet ist um die Chemoresistenz von T-NHL Zellen zu überwinden.

Um die Wichtigkeit von MCL-1 für die Lymphomagenese zu untersuchen, wurde außerdem ein zweites Mausmodell, basierend auf der Expression der ITK-SYK Fusionskinase, benutzt. Diese Kinase wird, unter Kontrolle des CD4 Promoters, ausschließlich in CD4 positiven Thymozyten, also ab dem Doppelt Positiven (DP) Stadium der T-Zell-Entwicklung im Thymus exprimiert (5). ITK-SYK vermittelt ein ständiges Aktivierungssignal an die T-Zellen, wodurch diese vermehrt proliferieren und fungiert so als Onkogen. In dieser Arbeit wurden *ITK-SYK$^{+/-}$CD4Cre* Mäuse mit *Mcl-1$^{fl/fl}$* oder *Mcl-1$^{fl/+}$* Mäusen gekreuzt, um gleichzeitig zur Aktivierung des Onkogens ITK-SYK eine *Mcl-1* Deletion herbeizuführen. Sowohl der komplette Verlust als auch die Reduktion von MCL-1 führten zu einer signifikanten Verzögerung der Lymphomagenese. Dies zeigte, dass MCL-1 auch eine Rolle bei der Lymphominitiierung spielt.

Während eine homozygote Deletion von MCL-1 in gesunden Mäusen toxische Effekte zeigte, konnte nach heterozygotem Verlust, die eher der Situation nach Behandlung mit einem Inhibitor entspricht, keine nennenswerte Toxizität für normale B- und T-Zellen festgestellt werden.

Um die Rolle von MCL-1 im Vergleich zu den anderen Bcl-2 Proteinen in humanen T-NHL Zellen zu erkunden, wurden T-NHL Zelllinien mit induzierbaren BIM_S Konstrukten transduziert. Diese BIM_S Konstrukte verfügten über verschiedene Bindungseigenschaften, wobei BIM_SWT alle anti-apoptotischen Bcl-2 Proteine, BIM_S2A nur MCL-1, BIM_SBAD nur BCL-2, BCL-X_L sowie BCL-W und BIM_S4E keines der BCL-2 Proteine binden kann. Die Rolle von MCL-1 in den verwendeten humanen T-NHL Zelllinien war sehr heterogen, was wahrscheinlich auf die unterschiedliche Expression in diesen Zellen zurückzuführen war.

RNA Expressionsdaten von primären T-NHL Proben aus Patienten zeigte, dass MCL-1 als einziges anti-apoptotisches Bcl-2 Protein in allen Subgruppen überdurchschnittlich stark exprimiert wurde. Weiterhin konnte die Expression von MCL-1, als auch seinem positiven Regulator USP9X, auf Proteinebene nachgewiesen werden, was eine funktionelle Bedeutung von MCL-1 für das Überleben von humanen T-NHL wahrscheinlich macht.

Abstract

T-lymphocyte Non-Hodgkin Lymphoma (T-NHL) represents a heterogeneous and aggressive subtype of Non-Hodgkin Lymphoma. Patients with T-NHL frequently relapse after chemotherapy and overall survival of patients with advanced stage disease is poor. Despite a wealth of genetic data on T-NHL, the molecular mechanisms of lymphomagenesis or treatment resistance remain poorly understood. We hypothesized that anti-apoptotic Bcl-2 proteins protect T-NHL cells from cell death, cause resistance to therapy, and therefore represent an attractive therapeutic target.

The Bcl-2 family member MCL-1 possesses potent pro-survival activity in healthy T lymphocytes, but its function in transformed T cells remains unclear. To better understand the requirement for MCL-1 in T-NHL cell survival, we functionally characterized MCL-1 in comparison to other Bcl-2 family members in a T-NHL mouse model. This model is based on four consecutive low-dose whole-body γ-irradiations in 4 week-old mice, resulting in the development of T-NHL mimicking human peripheral T cell lymphoma not otherwise specified (PTCL-NOS). We utilized mice harboring loxP-flanked *Mcl-1* or *Bcl-x*$_L$ and an inducible Cre recombinase (*Mcl-1*$^{fl/+}$ *CreERT2*$^{ki/+}$ and *Bcl-x*$_L{}^{fl/+}$ *CreERT2*$^{ki/+}$) to conditionally delete *Mcl-1* or *Bcl-x*$_L$ after lymphoma induction. Interestingly, conditional deletion of only one allele of *Mcl-1* in fully established primary T-NHL cells *ex vivo* led to a significant and specific loss of viability that could be rescued by ectopic (re-) expression of MCL-1, BCL-2, BCL-X$_L$, or BCL-W. Complete *Bcl-x*$_L$ deletion showed a similar, still not as profound effect. Reduced MCL-1 levels resulted in substantially elevated sensitivity to standard chemotherapeutics such as anthracyclins, cyclophosphamide and etoposide, which was lacking in cells after *Bcl-x*$_L$ deletion.

In addition, mono-allelic deletion of *Mcl-1 in vivo* prolonged survival of lymphoma-bearing mice and augmented the effect of doxorubicine treatment. In a second mouse model, based on the constitutive T cell receptor signal from the fusion kinase ITK-SYK, the importance of MCL-1 for lymphoma initiation was investigated. *Mcl-1*

deletion at the same time-point as ITK-SYK induction lead to a significant delay in lymphoma development, indicating that MCL-1 is important for the survival of transforming T cells.

Although the role of MCL-1 for the the survival of human T-NHL cell lines was less clear, *in silico* meta-analyses of available gene expression data on human primary T-NHL identified MCL-1 as the primary Bcl-2 family member that is highly expressed across most T-NHL subsets. Expression of MCL-1 was restricted to its anti-apoptotic full-length splice variant as opposed to its pro-apoptotic short isoform. Together, these data argue that anti-apoptotic Mcl-1 is the most important Bcl-2 family member mediating the survival of T-lymphocyte Non-Hodgkin Lymphoma (T-NHL).

Contents

List of Figures

List of Tables

Abbreviations

Instance	Expansion
A	adenine
A1	BCL-2 like protein A1
ABC-DLBCL	Activated B cell like diffuse large B cell lymphoma
AITL	angioimmunoblastic T cell lymphoma
ALCL	anaplastic large cell lymphoma
ALL	Acute lymphoblastic leukemia
ALK	anaplastic lymphoma large cell lymphoma receptor tyrosine kinase
AML	Acute myeloid leukemia
Apaf-1	Apoptotic protease activating factor 1
APC	Allophycocyanin
ATL	adult T cell leukemia/lymphoma
BAD	BCL-2 associated death promoter
BAK	BCL-2 antagonist/killer 1
BAX	BCL-2 associated X protein
BCL-2	B cell lymphoma 2
BCL-W	BCL-2 like protein 2
BCL-X	BCL-2 like protein 1
BCMA	B cell maturation antigen
BH	BCL-2 homology
BID	BH3 interacting-domain death antagonist
BIM	BCL-2 like protein 11
BM	bone marrow
bp	base pair
C	cysteine
CAD	caspase-activated DNAse
CD	cluster of differentiation
cDNA	complementary deoxyribonucleic acid

Instance	Expansion
CHAPS	3-[(3-cholamidopropyl)dimethylammonio]-1-propanesulfonate
CHOP	Cyclophosphamide, Doxorubicine, Vincristine, Prednisone
CLL	chronic lymphoblastic leukemia
cm	centimeter
Cre	protein recombinase of the phage P1
CT	computed tomography
CTCL	cutaneous T cell lymphoma
CVR	Vincristine
CYCLO	Cyclophosphamide
DLBCL	diffuse large B cell lymphoma
DMEM	Dulbecco's Modified Eagle Medium
DN	double negative
dNTP	deoxyribonucleoside triphosphate
DP	double positive
DEXA	Dexamethasone
DOX	Doxycycline
DOXO	Doxorubicine
EATL	Enteropathy-associated T-cell lymphoma
eGFP	enhanced green fluorescent protein
ER	estrogen receptor
EPOCH	CHOP plus Etoposide
ETO	Etoposide
EtOH	ethanol
FADD	Fas-associated protein with death domain
FBW7	F-box and WD repeat domain-containing 7
FCS	fetal calf serum
FDG	fluorodeoxyglucose
FFPE	formalin-fixed paraffin-embedded
FITC	fluorescein isothiocyanate
fwd	forward
G	guanine
H & E	haematoxylin eosin

Instance	Expansion
HTCL	hepatosplenic T cell lymphoma
HRP	horseradish peroxidase
IC50	half maximal inhibitory concentration
IS	ITK-SYK
ITK	IL-2 inducible T cell kinase
kDa	kilo Dalton
KI	kidney
KO	knockout
LGL	large granular lymphocyte
LIV	liver
LN	lymph node
loxP	locus of crossover in P1 bacteriophage
MCL-1	myeloide cell leukemia 1
min	minute
miRNA	micro RNA
ml	milliliter
MOMP	mitochondrial outer membrane permeabilization
mRNA	messenger RNA
MSCV	murine stem cell virus
NSCLC	non small cell lung cancer
NHL	non-Hodgkin Lmyphoma
NK	natural killer
nm	nanometer
nM	nanomolar
No	number
NOXA	Phorbol-12-Myristate-13-Acetate-Induced Protein 1
ns	non significant
OMM	outer mitochondrial membrane
OS	overall survival
PBS	phosphate buffered saline
PCR	polymerase chain reaction
PDK	Phosphoinositide-dependent kinase-1

Instance	Expansion
PE	Phycoerythrin
pen	penicillin
PET	positron emission tomography
PEST	proline (P), glutamic acid (E), serine (S), and threonine (T)
PI	propidium iodide
pMIG	pMSCV-IRES-GFP
PTCL-NOS	peripheral T cell lymphoma, not otherwise specified
PUMA	p53 upregulated modulator of apoptosis
rev	reverse
RIPA	Radioimmunoprecipitation assay buffer
RNA	ribonucleic acid
ROI	region of interest
RT	room temperature
RT	reverse transcriptase
rpm	rounds per minute
s	second
SCLC	small cell lung cancer
SDS	sodium dodecyl sulfate
SNP	single nucleotide polymorphism
SP	single positive
SPL	spleen
strep	streptomycin
SYK	spleen tyrosine kinase
T	thymine
TMX	(4´Hydroxy) tamoxifen
TCR	T cell receptor
TNF	Tumor necrosis factor
vs	versus
WT	wild type
XIAP	X-linked inhibitor of apoptosis

1 Introduction

1.1 The apoptotic pathways

1.1.1 Programmed cell death

Programmed cell death is an essential mechanism for maintaining tissue homeostasis and for the elimination of damaged cells. This process is also called apoptosis and is morphologically characterized by chromatin condensation and shrinkage of the nucleus and cytoplasm, followed by fragmentation of the cell into plasma membrane-bound "apoptotic bodies" (6). These bodies are subsequently engulfed by phagocytic cells and ultimately digested in lysosomes. In contrast to other types of cell death, apoptosis does not rupture the plasma membrane, thereby minimizing the release of inflammatory cellular contents and the risk of autoimmune reactions (7). Apoptosis consists of two distinct pathways: the intrinsic apoptotic pathway which is activated upon intracellular stress like cytokine withdrawal or DNA damage and the extrinsic apoptotic pathway which is initiated by death receptors on the cell surface.

The extrinsic apoptotic pathway is engaged on the plasma membrane by ligation of members of the tumor necrosis factor (TNF) receptor family such as FAS and TNF-R1. These receptors contain an intracellular "death domain" that, upon activation, is bound by the adaptor protein FADD which recruits and activates Caspase 8 (Caspase 10 in humans) and thus leads to the activation of the effector caspases (8).

Regardless of the initiating death stimulus, apoptosis always culminates in the activation of effector Caspases (aspartate-specific cysteine proteases) that are responsible for proteolysis as well as the activation of CAD (caspase-activated DNAse) that causes DNA fragmentation.

The effector caspases 3, 6 and 7 are synthesized as single-chain zymogens with short pro-domains and are catalytically inactive. They get activated when the initiator caspases 8 or 9 cleave their pro-domains. The initiator caspases themselves also have long pro-domains. Upon a death stimulus they are targeted to scaffold proteins where conformational changes provoke their activation (9).

1.1.2 The intrinsic apoptotic pathway

The intrinsic apoptotic pathway is mainly regulated by proteins, which belong to the Bcl-2 family. There are three different groups of Bcl-2 proteins that show structural similarities and harbor 1-4 Bcl-2 homology (BH)- domains that allow their interaction among each other. The first group comprises of the pro-apoptotic Bcl-2 proteins BAK and BAX, which are localized at the outer mitochondrial membrane (OMM). Upon activation, they oligomerize and form pores in the OMM, which leads to the release of cytochrome C from the mitochondrial inner-membrane space. Cytochrome C can then bind to the scaffold protein APAF-1 in the cytosol, which enables additional binding and activation of Caspase 9, culminating in the activation of the effector caspases. In addition to cytochrome C, there are also other apoptotic factors that are released from the mitochondria such as SMAC/DIABLO, which prevents the inhibitor of apoptosis protein XIAP from neutralizing caspases.

In healthy cells devoid of death stimuli, BAK and BAX are bound by anti-apoptotic Bcl-2 proteins, which form the second group of Bcl-2 proteins. This class consists of BCL-2, BCL-X_L, MCL-1, BCL-W and A1. They prevent activation of BAK and BAX by sequestering them and therefore impeding mitochondrial outer membrane permeabilization (MOMP). Upon intracellular stress the third category of Bcl-2 proteins is activated: the BH3-only proteins. This group includes PUMA, NOXA, BIM, BAD and BID, which all harbor the BH3-domain only and are able to activate BAK and BAX either via inhibiting the anti-apoptotic Bcl-2 proteins (indirect activation model) or direct binding and activation of BAK and BAX (direct activation model), depending on their binding affinities (Figure 1.1 A and B) (10). Most of the BH3-only proteins are unstructured prior to binding to the Bcl-2 proteins except BID,

which forms an alpha-helical bundle which resembles BAK or BCL-2 (11). It is able to link the death receptor pathway with the intrinsic pathway because its cleavage by Caspase 8 can create an active C-terminal segment (tBID) that can directly activate BAK and BAX. This amplification mechanism is essential for death-receptor induced killing in so called type 2 cells, as hepatocytes, but dispensable in type-1 cells, as thymocytes (12,13). The apoptotic pathways are depicted graphically in Figure 1.2.

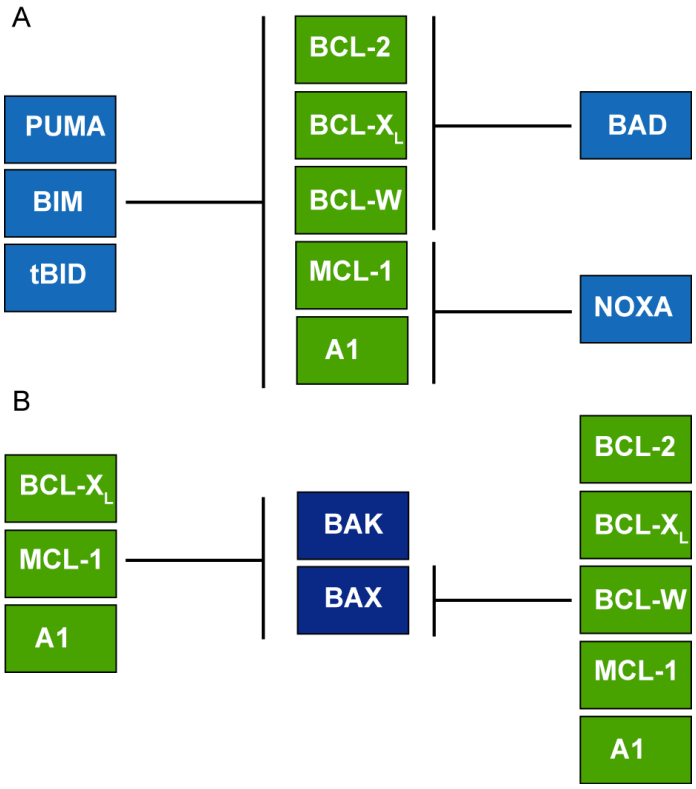

Figure 1.1 Interaction of pro-and anti-apoptotic Bcl-2 proteins A) Interaction of the BH3-only proteins (blue) with the anti-apoptotic Bcl-2 proteins (green). B) Interaction of BAK and BAX (dark blue) with the anti-apoptotic Bcl-2 proteins.

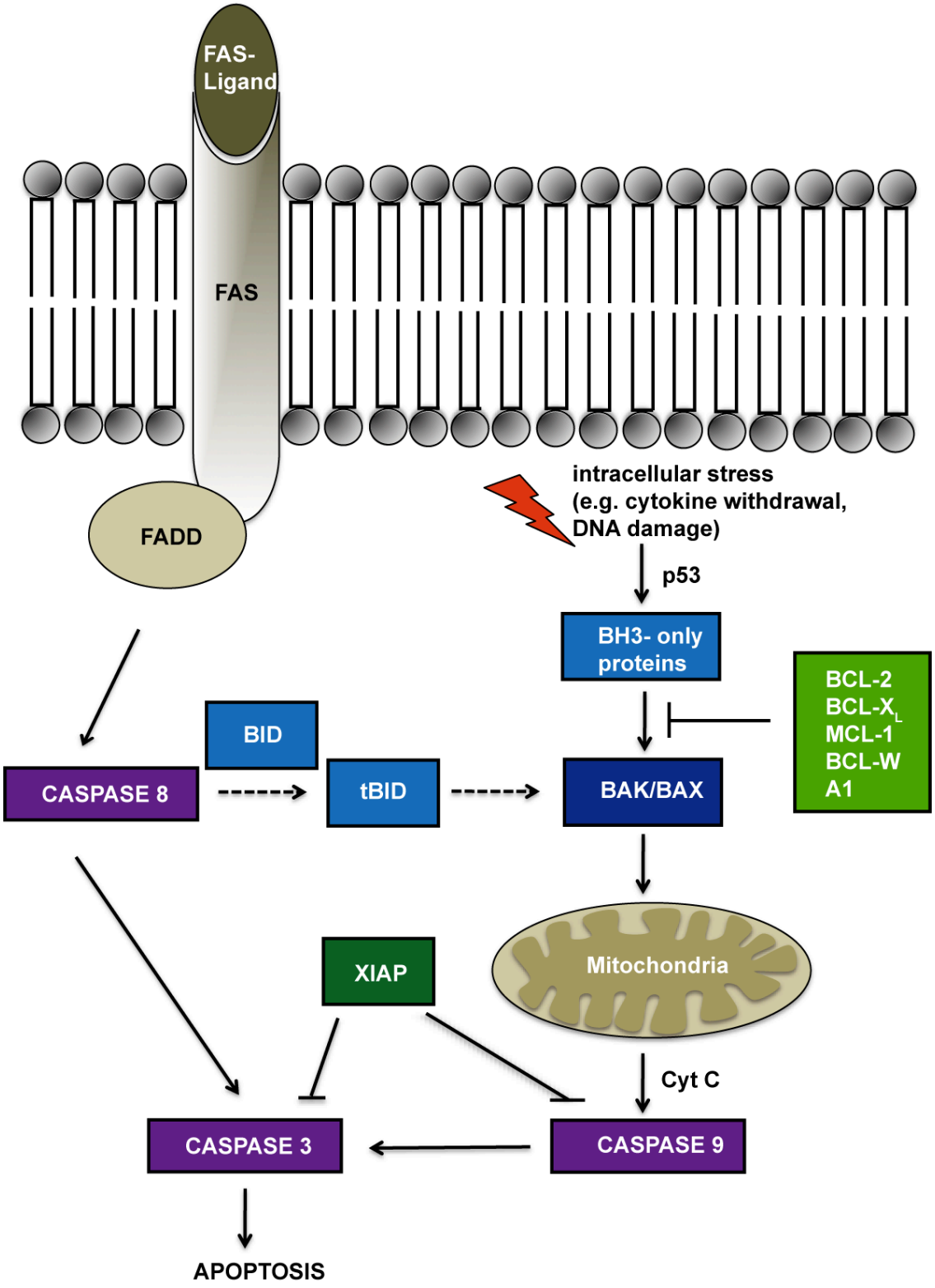

Figure 1.2 Graphic depiction of the apoptotic intrinsic and extrinsic pathways. Shown is an overview of the apoptotic extrinsic and intrinsic pathways. Pro-apoptotic proteins are depicted in blue, anti-apoptotic Bcl-2 proteins and xIAP are green and the caspases are highlighted in violet.

1.1.3 Activation models

How the Bcl-2 proteins exactly regulate MOMP and cytochrome C release is still a matter of debate. According to the "direct activation model", the BH3-only proteins BIM, tBID and probably PUMA function as "activators" and transiently bind and activate BAK and BAX, whereas the remaining BH3-only proteins serve as "sensitizers" and capture the anti-apoptotic Bcl-2 proteins. In this model the anti-apoptotic Bcl-2 proteins are mainly bound to the activators, preventing their interaction with BAK and BAX. When the sensitizers capture the anti-apoptotic Bcl-2 proteins, the "activators" are released and can bind to BAK and BAX (14,15).

The "indirect activation" model postulates that BAK and BAX are able to oligomerize without previous activation, which is prevented by the anti-apoptotic Bcl-2 proteins. The BH3-only proteins can liberate BAK and BAX by capturing the anti-apoptotic Bcl-2 proteins themselves and therefore enable BAK and BAX to oligomerize (16). This model was supported by the finding that BAX molecules with mutations in their BH3 domains that disable its binding to the other Bcl-2 proteins provoke unrestrained apoptosis (17,18).

A third model, called the "priming-capture-displacement model", is based on findings indicating that physiological cell death follows both models (19) and was also suggested by Strasser et al. (20). This model posits that direct activation of BAK and BAX is at least one way of generating "primed" molecules but that anti-apoptotic Bcl-2 proteins immediately capture these "primed" molecules of BAK and BAX. Those can only be freed upon replacement by the BH3-only proteins, as in the indirect activation model (20).

Independent of the underlying model, the ratio of anti- and pro-apoptotic proteins determines whether a cell lives or dies and disturbance of this balance can have profound consequences for the organism (21).

1.2 The anti-apoptotic Bcl-2 proteins

1.2.1 Physiological role of anti-apoptotic Bcl-2 proteins

The anti-apoptotic Bcl-2 proteins are pivotal for the survival of cells. However, different cell types vary in their dependence on individual Bcl-2 proteins presumably due to different expression patterns and selectivity of interactions. Knockout (KO) studies have given insights into the dependency of different cell types on the individual Bcl-2 proteins. *Bcl-2* KO mice develop a fatal polycystic kidney disease (PKD), due to the death of renal epithelial stem and progenitor cells in the embryonic kidney, premature greying due to the death of melanocyte progenitors and immunodeficiency because of B and T cell reduction (22).

Knockout of *Bcl-x_L* leads to the loss of fetal erythroid progenitors, certain neuron populations, male germ cells, immature (CD4+ CD8+) thymocytes, hepatocytes and platelets. *Bcl-x_L* KO mice die around E14-15 due to severe anemia and neuronal degradation (23) (24,25). Loss of MCL-1 has the most severe effects as *Mcl-1* KO causes pre-implantation embryonic lethality (26). MCL-1 is essential for survival of hematopoietic stem cells (27), immature B and T lymphoid progenitors and mature cells (28), activated germinal centre B cells (29), granulocytes and activated macrophages (30).

BCL-W KO leads to defects in adult spermatogenesis (31,32) and in apoptosis of epithelial cells in the small intestine only (33), even though BCL-W is broadly expressed in various tissues. The role of A1 is still not completely illuminated for there are at least three expressed mouse *a1* genes, which makes it hard to perform knockout studies. Loss of one *a1* gene however accelerated apoptosis in granulocytes (34) and mast cells (35). Some more recent findings furthermore showed that A1 is essential at some stages of T cell development (36) and it plays a role for survival of activated T cells (37).

1.2.2 Bcl-2 proteins in T cells

The anti-apoptotic Bcl-2 proteins play, as mentioned before, a pivotal role for the survival of various cell types and the importance of the individual Bcl-2 proteins varies depending on the respective tissue. For T cells, it has been shown that MCL-1 is an important player for the survival at different stages of T cell development.

The life of T cells can be divided into several distinct stages, starting in the thymus were T cells are differentiated from precursor cells generated in the bone marrow. Thymocyte precursors are CD4-CD8- double negative (DN), mature into CD4+ CD8+ double positive (DP) and after negative selection into either CD4+ or CD8+ single positive (SP) cells. Those SP thymocytes then exit to the periphery as naive T cells. When a naive T cell comes across its cognate antigen, it undergoes activation, proliferation and differentiation into an effector T cell (38). MCL-1 and BCL-2 are both expressed in DN thymocytes, whereas expression of BCL-X_L is largely inversely correlated with BCL-2, i.e. BCL-2 is downregulated in DP and upregulated in SP thymocytes whereas BCL-X_L is strongly upregulated in DP and less expressed in SP cells (39). Additionally, BCL-2 is highly expressed in naive T cells and down-regulated in effector CD8+ cells and BCL-X_L in contrast is rapidly up-regulated upon activation of T cells (40). Consistent with the expression data, genetic studies with mice lacking BCL-2 or conditionally lost BCL-X_L revealed that these proteins support survival of T cells at different stages (41). Although BCL-X_L is highly expressed in activated T cells it has been shown to be dispensable for the survival of effector T cells (42).

Another important player for the survival of hematopoietic cells is MCL-1. In addition to being critical for the viability of neutrophils and hematopoietic stem cells (27,43) it also possesses an obligate role for the development and maintenance of T lymphocytes (28). It has been demonstrated that MCL-1 is expressed throughout T cell development and that its overexpression rescues autoreactive thymocytes from negative selection (44). Furthermore conditional knockout studies revealed, that MCL-1 is required for the survival of T cells at multiple stages (2).

MCL-1 deficient thymocytes die largely through a BAK-specific mechanism which can not be rescued by BCL-2 overexpression (45). Only in the DP stage the deletion of Mcl-1 is not sufficient to kill, as the additional deletion of *Bcl-x*$_L$ is required to induce cell death (2).

The question that arises is whether MCL-1 has the same obligate role mediating survival in T cell derived lymphoma and if it comprises a suitable target for future lymphoma therapy.

1.2.3 MCL-1 regulation

MCL-1 was originally identified because it is upregulated upon phorbolester-induced maturation of ML-1 AML cells (46). Furthermore MCL-1 is special among the anti-apoptotic Bcl-2 proteins concerning its short half-life. The rapid turnover of MCL-1 can be explained by its unique structure. It harbors so called PEST sequences at its N-Terminus, which are sequences rich in proline, glutamic acid, serine and threonine that target it for rapid proteasomal degradation (47). For that reason, MCL-1 is highly regulated not only by transcriptional and translational mechanisms but also by a range of kinases which can either stabilize MCL-1 or target it for ubiquitinylation by E3 ligases and subsequent degradation (48,49). Still, the constitutive half-life of MCL-1 cannot be defined in detail because the turnover may be shortened or lengthened depending on the cellular conditions and varies between the cell types, but is estimated to about 30 min.

One important positive regulator of MCL-1 expression is USP9X, a deubiquitinase, which is also overexpressed in some malignancies (50). Furthermore, MCL-1 expression is regulated by micro RNAs (miRNAs), which can regulate both mRNA stabilization and translation. One important example for a miRNA regulating MCL-1 is miR29b which appears to reduce MCL-1 protein levels upon being overexpressed (51), whereas its loss is a mechanism for enhanced MCL-1 expression (52). Another mode of MCL-1 regulation is alternative splicing. In contrast to the other Bcl-2 proteins BCL-2 and BCL-XL, MCL-1 consists of three Exons instead of two. Exon 2 can be skipped by splicing, which results in expression of a truncated

isoform that lacks the BH2 and BH1 domains. In contrast to full-length MCL-1, this truncated form of MCL-1 promotes apoptosis in human cell lines (53).

There is accumulating evidence that MCL-1 is not exclusively an apoptotic modulator but has other functions. A fast mobility isoform of MCL-1, resulting from cleavage of its N-terminus, is localized to the inner mitochondrial membrane, suggesting other mitochondrial functions (54). MCL-1 expression is furthermore controlled by additional mechanisms than apoptotic stimuli. Elevated glycolysis e.g. affects Bcl-2 family proteins to suppress the induction of pro-apoptotic proteins (55) and it has been shown that Glucose metabolism promotes MCL-1 synthesis (56). MCL-1 expression can be regulated via several signaling pathways. For example, in germinal centre derived plasma cells, which have been shown to be dependent on MCL-1, signaling via BCMA leads to an increase in MCL-1 mRNA and protein level (57). Furthermore in ABC-DLBCL cells, constitutive STAT3 signaling leads to increased MCL-1 expression (58).

1.2.4 The role of anti-apoptotic Bcl-2 proteins in cancer

One of the most prominent hallmarks of cancer is escaping apoptosis (59). In this context, the first Bcl-2 protein discovered was BCL-2, which was shown to be involved in the t[14;18] chromosomal translocation found in most human follicular lymphomas (60). Furthermore, it protects hematopoietic cells from cell death after cytokine deprivation and cooperates with MYC for immortalization of lymphoid cells (61) and in lymphomagenesis (62). *BCL-2* gene amplifications were found in non-Hodgkin lymphoma (63) and Small Cell Lung Cancer (SCLC) (64), where it also plays a role in transformation of lung cells exposed to carcinogens (65).

BCL-X_L showed to be frequently genetically amplified in various kinds of cancers (66). Overexpression of BCL-X_L together with c-MYC promotes the development of fatal acute lymphoblastic leukemia (67). Moreover it is often up-regulated in solid tumors (68), acute myeloid leukemia (AML) (69) and some subsets of B cell non-Hodgkin lymphoma (70). Aside from that, it has been implicated in the chemoresistance of myeloma (71). One study showed that loss of BCL-X_L

abrogated the development of Eμ-MYC induced B cell lymphoma in mice (72). In contrast to these data shows a more recent finding that BCL-X_L is dispensable for the maintenance of Eμ-MYC induced B cell lymphomas (1).

The *MCL-1* gene is not only frequently amplified (66), but MCL-1 is also often highly expressed in various kinds of cancers as multiple myeloma (73) and hepatocellular carcinoma (74). Some findings demonstrated, that murine AML cells are critically dependent on expression of MCL-1 (75). In human AML, MCL-1 levels are often elevated at the timepoint of leukemic relapse (76) and miR29b, which negatively regulates MCL-1 protein translation, induces apoptosis in AML cell lines and primary samples (52). MCL-1 is furthermore up-regulated in high-grade B cell non-Hodgkin lymphoma (77) and in subgroups of diffuse large B cell lymphoma (58). MCL-1 overexpression has shown to predispose mice to develop B cell lymphoma and haematopoietic stem/progenitor cell tumors (78). Consistent with that, Kelly et al. found, that MCL-1 is critical for the maintenance of Eμ-MYC induced B cell lymphoma (1). Expression data also indicate that MCL-1 might play a role for at least a subgroup of T cell non-Hodgkin lymphoma (79).

1.3 T cell Non-Hodgkin Lymphoma

1.3.1 Definition, Classification and Outcome

T lymphocyte non-Hodgkin lymphoma (T-NHL) accounts for approximately 15% of all NHL worldwide (80). It comprises a heterogeneous group of diverse disorders from T lymphocyte or more rarely NK/T cell origin (80). The disease can either originate from T cell precursors or thymocytes (T cell lymphoblastic leukemias/lymphomas) or derive from mature post-thymic T cells, which are also called peripheral T cell lymphoma (PTCL). Referring to the World Health Organization (WHO) PTCL are classified by their primary site of disease into nodal, extranodal, cutaneous and leukemic cases. The nodal lymphoma group consists of peripheral T cell lymphoma not otherwise specified (PTCL-NOS), anaplastic large cell lymphoma (ALCL) and angioimmunoblastic T cell lymphoma (AITL). ALCL is further subdivided into anaplastic lymphoma kinase (ALK) negative (ALK-) and ALK positive (ALK+) entities. The extranodal group includes hepatosplenic γδ T cell lymphoma (HTCL), which is mainly a disease of children and young adults, enteropathy-associated T cell lymphoma (EATL) and nasal-type NK/T cell lymphomas. The cutaneous T cell lymphomas constitute the third group and comprise of αβ and γδ type lymphoma. The leukemic group consists of adult T cell lymphoma (ATL), T cell chronic large granular lymphocytic (LGL) leukemia, aggressive NK cell leukemia and T cell prolymphocytic leukemia (81).

Characterization of different T-NHL subtypes is notoriously difficult and recurrent genetic aberrations within the different subgroups are rare (82,83). Gene expression profiling has substantially advanced the understanding of the molecular composition of this disease. It has added a novel resource to differentiate between morphologically similar T-NHL entities (84-88) and provides a new prognostic tool (89-91). Still, despite substantial progress in understanding the aberrantly activated signaling pathways in different T-NHL entities, the molecular mechanisms of disease initiation and maintenance are not well understood (92). Differentially expressed genes within the different subgroups comprise a large range of pathways and functions, what makes it hard to find targets that are feasible in most T-NHL

subsets. With the exception of anti-CD30 antibodies and ALK inhibitors, the wealth of novel genetic data on various T-NHL subtypes has so far not translated into effective novel therapeutic concepts. There are several studies ongoing, testing new therapeutic approaches like anti-CD4 antibodies or denileukin diftitox, which is a fusion protein that combines the IL-2 receptor binding domain with dipheria toxin. Still, the potency of the tested drugs is mostly restricted to small subgroups of T-NHL or shows severe side effects.

The only available standard therapy so far is a combination chemotherapy regimen of cyclophosphamide, doxorubicin, vincristine and prednisone (CHOP), with eventually added etoposide (EPOCH) and stem cell transplantation for the most aggressive forms (81). Most patients initially respond to standard chemotherapy, but the majority of the patients with most subtypes of T-NHL show a bad long-term disease-free survival (93). Relapse is common and there are few effective options for salvage therapy.

1.3.2 Peripheral T cell lymphoma not otherwise specified (PTCL-NOS)

The most undefined and heterogenous subgroup of T-NHL comprises PTLC-NOS. They account to about 26 % of all PTCL and it is the most frequent subgroup in North America and Europe (93). Although there have been described some subgroups, like lymphoepithelioid, T-zone and follicular variants (94), PTCL is still mostly categorized by exclusion, due to its inhomogeneous histological features (90). To date, not much is known about factors that favor the development of PTCL-NOS. No immunological defects, hereditary components or viral infections have been proven to affect the occurrence of PTCL-NOS.

PTCL-NOS typically occurs in adults with a median age of 55- 60 years and shows a higher prevalence in males. The standard therapeutic option is conventional anthracycline-containing chemotherapy, with an overall response rate of more than 60%. Still, relapses are frequent and the prognosis of patients is poor with a 5-year

overall survival (OS) of 20 to 30 %. The only option for relapsed patients is high-dose chemotherapy supported by autologous or allogeneic stem cell transplantation (SCT), which is able to achieve a long-term survival of 35 to 45 %. Recently there are clinical trials using combination of CHOP with an anti CD52 antibody, Alemtuzumab. Although there were some promising results so far, only 30 − 40 % of PTCL-NOS express CD52 (95). PTCL-NOS are described to have a primary nodal presentation, but frequent infiltration of extranodal sites as spleen, liver, skin, the gastrointestinal tract and involvement of the bone marrow can be observed. The cells show an aberrant T cell phenotype with frequent loss of CD5 and CD7. They are predominately $CD4^{+}/CD8^{-}$ but also $CD4/CD8^{-/-}$ or $^{+/+}$ is seen in some cases and the Ki-67 rate is typically high. TCRβ chain is usually expressed and the TCR genes are mostly clonally rearranged. In comparison to normal T lymphocytes, PTCL-NOS cells show an aberrant gene expression profile of genes involved in diverse cell functions e.g. cytoskeleton organization, matrix deposition, cell adhesion, proliferation, transcription, signal transduction and apoptosis (96) .

On the cellular level, the commonly observed histological involvement of inflammatory components in PTCL-NOS hints towards a supportive role of chemokines and other inflammatory factors. Also chronic antigen receptor stimulation has been discussed in the pathology of PTCL. Furthermore, 30% of cases are positive for Epstein-Barr virus although the role in pathogenesis is still unknown (95). However, no experimental proof has been provided so far that confirms either of these aspects as an etiological component in the pathology of PTCL-NOS (95).

1.3.3 Two T-NHL mouse models

1.3.3.1 Irradiation induced thymic lymphoma

The development of irradiation induced thymic lymphoma is based on the massive DNA damage caused by exposing mice to four weekly doses of 150 rad gamma-irradiation. The mutagenic effect drives thymic lymphomagenesis by transformation of hematopoietic stem/progenitor cells in the bone marrow (4,97). This irradiation protocol has been shown to result in a variety of chromosomal aberrations and activating mutations such as mutations in *N-ras* (98), *Notch-1*, *Fbw7* and *Tp53* (99). This model therefore reflects the genetic and chromosomal heterogeneity observed in T-NHL, specifically PTCL-NOS, patients (92). The mice have severe infiltration of spleen, lymph nodes and bone marrow with T lymphoblastic cells, arising from the thymus. It was been demonstrated that tumorigenesis in this model is markedly enhanced by deficiency of p53, a critical DNA-damage sensor that plays a pivotal role in induction of cell cycle arrest, DNA repair and apoptosis (100). Furthermore the phenotype was aggravated when BIM and BAD are deleted (101), indicating that the apoptotic pathway is critical for lymphoma development in this mouse model.

1.3.3.2 ITK-SYK induced T-NHL

Approximately 17% of human unspecified T cell lymphoma harbor the t(5;9)(q33;q22) chromosomal translocation which leads to the fusion of the N-terminal pleckstrin homology domain and proline rich region of ITK (Interleukin-2-inducible T cell kinase) to the tyrosine kinase domain of SYK (spleen tyrosine kinase), resulting in an ITK-SYK fusion transcript (102). ITK-SYK showed to be a catalytically active tyrosine kinase, associated with lipid rafts, which leads to a strong constitutive TCR signal. ITK-SYK expression in CD4 cells i*n vivo* leads to a peripheral T cell lymphoma with a latency time of 12- 27 weeks, characterized by infiltration of T cells in lymphoid organs, but also liver and kidney (5). Furthermore it has been shown, that ITK-SYK expression leads to diminished apoptosis in CD4

T cells *in vitro* (103). This indicates that apoptotic resistance might be a pivotal feature of ITK-SYK induced T cell lymphoma cells and that targeting apoptotic key players might abrogate the lymphoproliferative effect of ITK-SYK expression.

2 Research Objective

T cell non-Hodgkin lymphoma (T-NHL) is an aggressive disorder that is characterized by high relapsing rates and poor prognosis. Novel promising therapeutic approaches are rare and therefore essential to generate. Conventional cytogenetics, comparative genomic hybridization and SNP array studies of large cohorts of human T-NHL patients have revealed that defined recurrent genetic aberrations in T-NHL are rare, whereas most patients carry multiple genomic imbalances or complex karyotypes (92). This identifies T-NHL as a genetically heterogeneous group of lymphoid malignancies and underscores the need to identify common molecular vulnerabilities that might be targeted for T-NHL therapy in the majority of T-NHL patients.

Bcl-2 proteins play an important role for survival of normal tissue cells and have shown to be important drivers of persistence of various tumor cell types (see section 1.2.4). It is further known that T cells strongly depend on the expression of Bcl-2 proteins, especially MCL-1. Additionally, there have been findings that show strong Bcl-2 protein expression in T-NHL samples and correlation of expression with proliferation and apoptosis (79).

The aim of this thesis was to find out whether the importance of MCL-1 and BCL-X_L observed in normal T cells also exists in T cell lymphoma cells and whether it is a suitable target for global therapy of T-NHL. The two mouse models used in this thesis constitute eligible tools that reflect the situation in human T-NHL. Both models furthermore gave hints in previous publications that lacking apoptosis is an important factor for lymphoma development and survival. This work addresses the question whether the targeting of MCL-1 or BCL-X_L is sufficient to induce cell death in T cell lymphoma cells.

3 Material

3.1 Reagents

If not stated otherwise, all chemicals were purchased from Sigma-Aldrich. Additional reagent and kit information is provided in the respective methods section.

3.2 Employed Antibodies

3.2.1 Western Blot Analysis

Identification	**clone**	**species**	**Company**
αMCL-1 (hs and mm)	19C4-15	rat	gift
αBCL-2 (mm)	3F11	hamster	BD
αBCL-2 (hs)	7/Bcl-2	mouse	BD
αBCL-XL (mm)	DF7	rabbit	BD
αCreER	HC-20	rabbit	Santa-Cruz
αCASPASE 3 (hs and mm)	8G10	rabbit	Cell Signaling
αACTIN, HRP tagged (mm)	13E5	rabbit	Cell Signaling
αFLAG	M2	mouse	Sigma-Aldrich
αBIM/BOD	polyclonal	rabbit	Enzo
αBCL-W (hs)	H-139	rabbit	Santa-Cruz
αA-TUBULIN (hs)	DM1A	mouse	Sigma-Aldrich
αMouse IgG, HRP tagged	polyclonal	goat	South.-Biotech
αRabbit IgG, HRP tagged	polyconal	goat	Jackson IR
αRat IgG, HRP tagged	polyclonal	goat	Jackson IR
αhamster IgG, HRP tagged	polyclonal	goat	Jackson IR

3.2.2 Flow Cytometry

Identification	conjugate	clone	species	Company
αCD4	PerCP	GK1.5	rat	eBioscience
αCD8a	APC	53-6.7	rat	eBioscience
αTCRb	PE	H57-597	hamster	eBioscience
αB220	APC	RA36B2	rat	eBioscience
αCD19	APCFluor780	1D3	rat	eBioscience
αCD62L	PeCy5	MEL-14	rat	eBioscience
αCD25	PE	PC61.5	rat	eBioscience
αCD44	APCFluor780	IM7	rat	eBioscience
αCD69	Pe-Cy7	H1.2F3	hamster	eBioscience
αCD16/32	purified	93	rat	eBioscience

3.2.3 Immunhistochemistry

Identification	clone	species	company
αCD3, mouse	SP7	rabbit	Abcam
αCleaved Caspase 3, mouse	Asp175	rabbit	Cell Signaling
αMcl-1, human	22	rabbit	Enzo
αUSP9X/FAM, human	2G7	mouse	LSBio

3.3 Employed Primers

Primers were synthesized at Sigma-Aldrich or MWG-biotech.

3.3.1 Genotyping primers

Identification	**sequence 5´> 3`**
Mcl-1 loxP fwd (Opferman)	GCAGTACAGGTTCAAGCCGAT
Mcl-1 loxP rev (Opferman)	CTGAGAGTTGTACCGGACAA
ITK-SYK fwd	GATGGATGGGAAGTGGAGGTG
ITK-SYK rev	GGACCAAGTTCTGCCATCTC
CD4Cre fwd	ACCAGCCAGCTATCAACTCG
CD4Cre rev	TTACATTGGTCCAGCCACC
Rosa 26 wt fwd	GTAGTAAGGATCTCAAGCAGG
Rosa 26 wt rev	AGTCGCTCTGAGTTGTTATCAG
Mcl-1 loxP fwd (Vikström)	GCACAATCCGTCCGCGAGCCAA
Mcl-1 loxP rev (Vikström)	GCCGCAGTACAGGTTCAAG
CreERT2scUP3	GAATGTGCCTGGCTAGAGATC
CreERT2scLP1	GCAGATTCATCATGCGGA
Gabra1_UP	AACACACACTGGAGGACTGGCTAGG
Gabra1_LP	CAATGGTAGGCTCACTCTGGGAGATGATA
Bcl-x_L loxP fwd	CGGTTGCCTAGCAACGGGGC
Bcl-x_L loxP rev	CTCCCACAGTGGAGACCTCG

3.3.2 Detection of target gene deletion

Identification	**sequence 5´> 3`**
Mcl-1 del fwd (Opferman)	GCACAATCCGTCCGCGAGCCAA
Mcl-1 del rev (Opferman)	GTCCAGTTTCCGGAGCATG
Mcl-1 del fwd (Vikström)	CGACACAGATCAGCAGGCGTTC
Mcl-1 del rev (Vikström)	GAGTCAGCGCGATCATTCAGCT
Bcl-x_L del fwd	AATGGCCAGTACTAGTGAACC
Bcl-x_L del rev	TCAGAAGCCGCAATATCCCC

3.3.3 Real Time Primers

Identification	**sequence 5´> 3`**
Actin fwd	AAGAGCTATGAGCTGCCTGA
Actin rev	TACGGATGTCAACGTCACAC
Mcl-1 fwd	TGTAAGGACGAAACGGGACT
Mcl-1 rev	AAAGCCAGCAGCACATTTCT
Bcl-x_L fwd	GGATGGCCACCTATCTGAAT
Bcl-x_L rev	TGTGGATCTCTACGGGAACA
Bcl-2 fwd	CTGGAAACCCTCCTGATTTT
Bcl-2 rev	AAATATTTCAAACGCGTCCA

3.4 Plasmids

3.4.1 Ectopic Bcl-2 protein expression

Identification	backbone	source
pFLAG-hsBCL-2-IRES-GFP	pMSCV	gift, WEHI
pFLAG-mmBCL-W -IRES-GFP	pMSCV	gift, WEHI
pFLAG-hsBCL-X_LCass-IRES-GFP	pMSCV	gift, WEHI
PFLAG-hsMCL-1-IRES-GFP	pMSCV	gift,WEHI
Env	pMSCV	Addgene
Gag/pol	pMSCV	Addgene

3.4.2 BIM_s-construct expression

Identification	backbone	source
TetO-BIM_SWT-Ubq-rtTA-IRES-GFP	pTRIPZ	gift, WEHI
TetO-BIM_S2A-Ubq-rtTA-IRES-GFP	pTRIPZ	gift, WEHI
TetO-BIM_SBAD-Ubq-rtTA-IRES-GFP	pTRIPZ	gift, WEHI
TetO-BIM_S4E-Ubq-rtTA-IRES-GFP	pTRIPZ	gift, WEHI
pPAX2	psPAX2	Addgene
pMD2.G	pMD2.G	Addgene

4 Methods

4.1 Work with eukaryotic cells

4.1.1. Basic cell culture

Lymphoma cells (T-NHL) from irradiated mice and all human T cell lymphoma/leukemia cell lines were cultured in high-glucose Dulbecco´s modified Eagle´s medium (DMEM) (Gibco, Invitrogen), supplemented with 20% fetal calf serum (FCS) (Gibco, Invitrogen), 10 µM β-mercaptoethanol (Life technologies), 100 µM L-Glutamine (Life Technologies), 100 mg/ml Penicillin and Streptomycin (Life Technologies). Virus producing HEK 293T cells were cultured in DMEM supplemented with 10% FCS (Gibco, Invitrogen), 10 µM β-mercaptoethanol (Life technologies), 100 µM L-Glutamine (Life Technologies), 100 mg/ml Penicillin and Streptomycin (Life Technologies). All cells were maintained at 37°C and 5% CO_2.

4.1.2 Cell purification of murine T-NHL cells

Lymphoid tissue as well as liver and kidney of diseased mice were harvested in RPMI 1640 medium (Gibco, Invitrogen), supplemented with 5 % FCS and kept on ice. Single-cell suspensions were made by smashing organs with a plunger and passing cells through a nylon mesh. Red blood cells were lysed using G-DEX^{TM} II RBC lysis buffer (iNtRON Biotechnology). Cells were counted in a Neubauer Counting Chamber (Omnilab) in 0.2% Trypan Blue (Life Technologies).

4.1.3 Cre-mediated deletion of target genes

2 x 10^5 mouse T-NHL cells, suspended in 150 µl medium, were seeded in 96-Well plates and treated with either 50 µl 400 nM 4´OH-Tamoxifen (Sigma-Aldrich) or 50 µl 8% Ethanol (Carl Roth) for 0, 12, 24, 48, 72 and 96 hours. The cells were then washed once with FACS-Buffer (PBS, 5% FCS) and incubated 20 min with AnnexinV-GFP (purified) on ice. 5 Minutes prior to Flow Cytometry 5 µM Propidium Jodid (Sigma-Aldrich) was added to the cells.

4.1.5 Chemotherapeutic treatment of T-NHL cells

For treatment with chemotherapeutic drugs 2 x 10^5 cells suspended in 150 µl medium were seeded in 96-Well plates and treated with either 25 µl 800 nM 4´OH-TMX (Sigma-Aldrich) or 25 µl 8% Ethanol (Carl Roth) and co-treated with 25 µl different concentrations (final: 1 nM to 5 µM) of etoposide, vincristine, dexamethasone, doxorubicine, cyclophosphamide or ABT-737 (Active Biochem). After 0,12, 24, 48, 72 or 96 hours of treatment 50 µl of cell suspension was transferred into white 96-Well plates (Peqlab) pre-filled with 50 µl of room-tempered Cell Titer Glo (Promega). Plates were incubated on a shaker for 15 min and then luminescence was measured using a Mithras LB 940 plate reader (Berthold).

4.1.6 Flow Cytometry

Fc receptors of single cells were blocked by 15 min incubation with anti mouse CD16/CD32 Fc-block (eBiocsience) on ice. Cells were stained for 20–30 min with antibodies to various surface markers (CD4, CD8, TCRβ, B220, CD19, CD11b, CD11c, GR-1) directly conjugated to the fluorochromes FITC, PE, PE/Cy5, PE/Cy7, APC, or APC/Cy7. All antibodies were obtained from eBioscience (San Diego, CA, USA) and were used at a dilution of 1:250- 1:400 in 50 µl FACS Buffer (PBS, 5% FCS; both from Gibco) per 7 x 10^5 cells. For analysis, cells were washed and resuspended in FACS buffer for run on a BD FACSCanto cytometer (BD

Biosciences, San Jose, CA, USA). All analyses were performed on FlowJo software (Tree Star Inc., Ashland, OR, USA).

4.2 Work with Nucleic Acids

4.2.1 Genotyping

DNA was extracted from T-NHL cells using the Qiagen DNAeasy tissue Kit or the Nucleospin Triprep Kit (Machery-Nagel) according to the manufacturer's instructions and DNA concentration was quantified using the Nanodrop 670 assay. All PCRs were performed with GoTaq green mastermix (M712, Promega). PCR on *Mcl-1* or *Bcl-x$_L$* flox or wild type alleles and *Rosa26CreER* were performed, using 3.3 mM primers with 32 cycles of 1 min at 96°C, 1 min at 55°C, and 1 min at 72°C followed by a 5 min extension at 72°C. The primer combinations used to PCR-amplify mouse *Mcl-1* from irradiated mice were “Mcl-1 loxP rev” (Vikström) and “Mcl-1 loxP fwd” (Vikström). The loxP allele resulted in a 340 bp band, whereas wild type *Mcl-1* was represented by 280 bp. *Rosa26CreER* PCR was performed using the primers “CreERT2scUP3”, “CreERT2scLP1”, “Gabra1_UP” and “Gabra1_LP”, resulting in a 330 bp band for wild type Rosa26 locus and 190 bp for *CreER^{T2}*. *LoxP Bcl-x$_L$* was detected using “Bcl-x$_L$ loxP fwd” and “Bcl-x$_L$ loxP rev” which resulted in a 300 bp fragment for *Bcl-x$_L$ loxP* and a 200 bp fragment for *Bcl-x$_L$* wild type. For detection of *Mcl-1 loxP* in ITK-SYK induced T-NHL the primer combination used was “Mcl-1 loxP fwd (Opferman)” and “Mcl-1 loxP rev (Opferman)”, resulting in a 330 bp band for *Mcl-1* wild type and a 360 bp band for *Mcl-1 loxP*. The *Cre* allele from *CD4-Cre* mice (104) was identified with the primer pair “CD4Cre fwd/CD4Cre rev”, yielding a 200 bp fragment for the recombinant locus. The PCR conditions for both genes were 95°C for 2s, 15 cycles of 95°C for 30s, 64°C for 30s, 72°C for 30s followed by 20 cycles of 95°C for 30s, 58°C for 30s, 72°C for 30s, as well as an end-elongation step at 72°C for 10min. The presence of the *ITK-SYK* transgene was tested using “Rosa26 wt fwd” and “Rosa26 wt rev” for detection of the wild type locus which was represented by a 506 bp band and using “ITK-SYK fwd” and “ITK-

SYK rev" in a separate reaction to detected the transgenic Rosa26 locus, harboring *ITK-SYK*, resulting in a 569 bp fragment.

4.2.2 Detection of recombined *Mcl-1*

For the detection of several recombined *Mcl-1* alleles, PCR conditions were 35 cycles with 30 sec at 96°C, 30 sec at 50°C and 1,5 min at 72°C, followed by 5 min extension at 72°C. The primer combination to detect recombined *Mcl*-1 in irradiation-induced T-NHL, were "Mcl-1del fwd (Vikström)" and "Mcl-1 del rev (Vikström)", resulting in a 850 bp fragment. For detection of recombined *Mcl-1* in ITK-SYK induced T-NHL, "Mcl-1 del fwd (Opferman)" and "Mcl-1 rev (Opferman)" were used, resulting in a 250 bp fragment.

4.2.3 Quantitative real-time PCR

RNA was isolated from lymphoma-burdened tissue using the Nucleospin Triprep Kit (Machery-Nagel) according to the manufacturer´s instruction and RNA concentration was quantified using the Nanodrop 670 assay. 1 µg of RNA was reverse transcribed, using Reverse Transcriptase II (Invitrogen) according to the manufacturer´s instructions and cDNA was diluted 1:10 in nuclease-free water (Promega). Quantitative RT-PCR was performed using GoTaq Green Mastermix (Promega) with 2,5 µl cDNA per sample. The PCR was run in a LightCycler 480 II (Roche). For qPCR analysis of primary lymphoma tissues, following primer combinations were used: Actin fwd/Actin rev as reference, "Mcl-1 fwd/Mcl-1 rev" for *Mcl-1* detection, "Bcl-x_L fwd/Bcl-x_L rev" for *Bcl-x_L* detection, "Bcl-2 fwd/Bcl-2 rev" for *Bcl-2* cDNA detection. All primer sequences are listed in Section 3.3.3.

4.3 Work with Viruses

4.3.1 Retroviral transduction with BCL-2 proteins

HEK293T cells were seeded into 10 cm^2 dishes (Biochrome) with 4 x 10^6 cells/plate and incubated for 24 hours. Cells were transfected with 2,4 µg env, 4,8 µg gag and 14,4 µg plasmid DNA and 50 µl Metafectene Pro (Biontex) for 8 hours. Prior to transfection, supplemented DMEM medium was changed to antibiotics-free DMEM. 8 hours after transfection, the medium was changed to 15 ml DMEM, supplemented with 20% FCS and incubated for 24 hours. After 24 hours, the supernatant was taken and fresh medium was added to the HEK293T cells. After another 24 hours, the supernatant was collected again, pooled with the first batch and filtered through a 45 µm sterile pipet filter (Carl Roth). After addition of 4 µg/ml Polybrene (Sigma-Aldrich), 15 ml of supernatant were added to 10^5 T-NHL cells in a 15 ml Falcon tube (Greiner) and incubated at 37°C and 5% CO_2 for 30 min, regularly inverting the tubes. After incubation the cells were centrifuged for 1 hour at 2200 rpm at RT and subsequently 1 hour at 32°C. Afterwards, the supernatant was removed and the cells diluted in 500 µl fresh DMEM with 20% FCS and seeded into 12-Well-plates. The cells were propagated until they comprised a cell number of 5 x 10^6 cells and then cell sorting on GFP-positive cells with a FACS Canto II (BD) was performed.

4.3.2 Lentiviral transduction with BIM_S-constructs

6,75 x 10^6 HEK293T cells were seeded in 15 cm^2 dishes and incubated over night. Medium was changed to antibiotics-free DMEM, supplemented with 10% FCS, 10 µM β-mercaptoethanol and 100 µM L-Glutamine and cells were transfected with 15 µg TRIPZ-TetO-BIM_S-Ubq-rtTA-IRES-GFP (BIM_S2A, BIM_SWT, BIM_S4E or BIM_SBAD), 7,5 µg pPAX2 and 7,5 µg pMD2G. Cells were incubated for 6 hours and then medium was changed to supplemented DMEM with 20% FCS. Viral supernatant was harvested 24 and 48 hours after transfection, filtered through a 45 µm sterile pipet filter and supplemented with 4 µg/ml Polybrene. 2 x 10^5 human

T-NHL cells were resuspended in 10 ml virus-supernatant and centrifuged for 30 min at 32°C. Subsequently the T-NHL cells were resuspended again and incubated for 24 hours in viral supernatant before cells were centrifuged again and supernatant was replaced by fresh medium. After 2 weeks of propagating, the cells were sorted on GFP.

4.4 Work with proteins

4.4.1 Western Blot analysis

For whole cell protein analysis, T-NHL cells were lysed with RIPA buffer and subsequently subjected to Western blot analysis as previously described (105). Protein from primary lymphocytes was isolated, by using the Nucleospin Triprep Kit (Machery-Nagel). After washing the protein was resolved in RIPA, supplemented with 2% SDS. The antibodies used for western blot analysis are listed in Section 3.2.1.

4.4.2 Histological analysis

All organs were fixed in 4% formaldehyde and paraffin embedded. 3–5-µm-thick sections were cut and stained with H&E. Immunohistochemistry was performed on an automated immunostainer (Ventana Medical Systems, Inc.) according to the company's protocols for open procedures with slight modifications. The antibody panel used included is listed in section 3.2.3.

4.5 Work with mice

4.5.1 Mouse Husbandry

All animals were housed under standardized, specific pathogen free conditions in individually ventilated cages (Thoren MaxiMixeR caging systems or TechniPlast IVC). Studies were conducted in compliance to federal and institutional guidelines. Animal protocols were approved by the government of Oberbayern.

4.5.2 Mouse breeding

For generation of irradiation induced T-NHL, *Rosa26CreER^{T2}* mice (106) were either crossed with *Bcl-x$_L^{fl/fl}$* (107) or *Mcl-1$^{fl/fl}$* mice (29). All mouse strains had a C57BL/6-LY5.2 background. For the experiments with ITK-SYK induced T-NHL, ITK-SYK transgenic mice (5) were crossed to CD4Cre transgenic (104) and *Mcl-1$^{fl/fl}$* mice (28). Toxicity of *Mcl-1* deletion was examined crossing *Rosa26CreER^{T2}* transgenic mice (108) to *Mcl-1$^{fl/fl}$* mice (28). At an age of 12 weeks the mice were treated once per day with 4 mg TMX, each for 2 days per oral gavage. At day 3 the mice were sacrificed and the lymphoid tissues were analyzed. Some mice were analyzed 4 weeks after the first TMX administration. All mice were treated and held according to the ethics commitee of the Klinikum rechts der Isar and approved by the government of Oberbayern.

4.5.3 Irradiation

At day 30 after birth mice were irradiated with 150 rad γ-irradiation, repeatedly every seven days to a total of four irradiations. At first signs of disease the mice were sacrificed and spleen, lymph nodes and thymus isolated.

4.5.4 Transplantation

10^7 T-NHL cells were transplanted into the tail vein of 12-16 weeks old C57BL/6 wild type mice (Jackson Laboratories). At day 16 after transplantation the mice were treated with 150 µg TMX by i.p. Injection on day 16, 18, 20, 22, 24 and 26. At first signs of disease the mice were sacrificed and spleen, lymph nodes and thymus isolated and analyzed.

4.5.5 Chemotherapeutic treatment

For doxorubicine treatment of T-NHL transplanted mice, recipient C57BL/6 mice were treated with 4 mg/kg TMX at day 16 and 17 by oral gavage. On day 17 100 µg doxorubicine were injected i.p. and PET/CT was performed on day 16 and 18.

4.5.6 PET/CT Analysis

PET analysis was performed on day 16 and 18 after T-NHL cell transplantation. [18F]FDG was synthesized as previously described (109) and was obtained from the radiopharmacy unit of the TU Munich. Imaging was done using a dedicated micro PET/CT system (Inveon, SIEMENS Preclinical Solutions). Before administration of the tracer, the mice were narcotized with Isofluran. Subsequently 100µl [18F]FDG with an activity dose of 5-10 MBq was administered via tail vein injection. The accumulation of the radiotracer in the lymphoma tissue was allowed for 45 min. Subsequently, mice were imaged for 15 min (static data acquisition). Percentage of Injected dose per gram (%ID/g) were calculated to semi-quantitatively assess the tracer accumulation in the lymphoma tissue. Circular 3D regions of interest (ROIs) were placed manually in the area with the highest tumor activity. The diameter was not covering the entire tumor volume to avoid partial volume effects. For determination of background activity, two 3D ROIs were placed in the spinal muscle.

4.6 Histological analysis of human biopsies

Histological analysis of human biopsies has been done in collaboration with Dr. Sylvia Hartmann (Dr. Senckenberg Institute of Pathology, Goethe Universität, Frankfurt am Main) as described below.

4.6.1 Preparation of tissue sections

2 µm thick cuts of Formalin-fixed parafin-embedded (FFPE) tissue were mount on Superfrost plus OT for 15 min on a stretching slide and left at 37°C over night. To deparaffinize, slides were put two times for 10 min each in Xylol before 2 times incubation in 100 % isopropanol for 3 min, followed by 96% and 70% ethanol. Afterwards the slides were rinsed three times with aqua dest.

4.6.2 MCL-1 Staining

Slides were boiled in 1x target retrieval solution high pH9 (DAKO EnVision Flex(K8000)) for 10 min. After cooling down they were rinsed two times with 1x wash buffer. Peroxidase blocking was applied and after 10 min the slides were again rinsed two times with 1 x wash buffer. A 1:150 dilution (antibody diluent Fa Zytomed systems) of the anti-MCL-1 antibody (pAb ADI-AAP-240 Enzo Life Sciences) was added and incubated for 1 h.

4.6.3 USP9X Staining

Slices were boiled in Citrate buffer pH6 for 10 min. After cooling down the slides were rinsed two times with 1 x wash buffer, followed by incubation in peroxidase-blocking for 10 min. Subsequently the slides were again washed two times and the anti-USP9X antibody was added in a dilution of 1:150.

4.6.4 Further procedures

After staining with the primary antibody the slides were rinsed off 3 times with 1 x wash buffer. Subsequently the slides were incubated for 30 min in HRP-conjugated polymer (Dako EnVision Flex/HRP (K8000)) and afterwards again rinsed 3 times with 1 x wash buffer. The chromogen DAB (Dako EnVision Flex/Substrate Buffer (K8000)) was added for 10 min followed by three washing steps. The slides were finally counterstained with Hematoxylin for 15 s (Gill´s Hematoxylin No 3) and were blued under floating mains water for two min. Slides were finally covered with Aquatex. Pictures were taken with a Nikon Eclipse ti 3000.

4.7 In silico integrative analysis of gene expression data set on human T-NHL

The integrative analysis of gene expression data has been done in collaboration with Giuliano Crisptatzu (Department I of Internal Medicine, Center for Integrated Oncology (CIO) Köln Bonn, University of Cologne, Cologne, Germany) as follows.

4.7.1 Data sets

Out of 45 reports on gene expression studies of mature T cell leukemias/ lymphomas (MTCL)/T cell non-Hodgkin lymphomas (T-NHL) (84,85,87-89,96,102,110-146), 19 on array-based profilings were found, to carry open-access available and integrable primary data sets. Data from the *CNIO Human Oncochip 1.1a-c* (142) as well as those from the *Agilent-014850 Whole Human Genome Microarray 4x44K G4112F* (146) were not considered due to non-standardization and difficulties in normalization. Data from the HT_HG-U133_Plus_PM chip (119) was not considered, because it was not annotatable via biomaRt_2.16.0 in R-3.0.0 (with Rcurl_1.95-4.1 and XML_3.98-1.1). *MCL1* isoforms were also not distinguishable in the respective annotation csv file obtained from the Affymetrix

Support Site. Out of 16 residual profilings, 11 (84,85,88,89,96,110-113,116,118) were hybridized on *Affymetrix Human Genome U133 Plus 2.0 Arrays [HG-U133_Plus_2]* and 5 (86,87,114,115,117) on the older *[HG-U133A] Affymetrix Human Genome U133A Array*.

4.7.2 MCL1 probe(set)s

According to the biomaRt_2.16.0 annotation there are 3 probes assigned to *MCL1* and its different transcripts in the Affymetrix HG-U133A chip:
- 200796_s_at for *MCL1-001* (MCL1l) *& MCL1-002* (only probe that can be used for second pro-apoptotic isoform MCL1s)
- 200797_s_at for *MCL1-001* (unique for first isoform; anti-apoptotic)
- 200798_x_at for *MCL1-001* & *MCL1-003* (can be filtered)

For the Affymetrix HG-U133 Plus 2.0 chip there is one additional probe:
- 241722_x_at for *MCL1-001*

4.7.3 Expression profiling and clustering

All Affymetrix platform derived data sets were retrieved from GEO or ArrayExpress, separately background-corrected and pre-annotated using the BioConductor package „affy_1.38.1" in R 3.0.0. Replicates were combined with their original samples and the mean of both was calculated. After that, the data set was quantile normalized. Genes were annotated (updated) via Ensembl ID using „biomaRt". The residual unambiguous probe sets, assigned to a gene, were then reduced by calculating their mean. *BCL2L11* has only two probes, one hybridizes 2 protein-coding and 6 NMD (nonsense-mediated decay) transcripts, the other one 2 protein-coding and 8 NMD transcripts and due to its ambiguity is to be looked at with caution. The 15 marker genes (*GSK3B, BCL2, BAD, BCL2L1, BCL2L2, BAX, GSK3A, BBC3, BAK1, BID, PMAIP1, BCL2L11, BCL2A1, HUWE1, USP9X*) and two *MCL1* transcripts selected for the analysis were then retrieved from the data sets and integrated. The approach used samples from Affymetrix expression array

platforms, imputes non-spotted genes by the median across the other samples, quantile normalizes a matrix of average gene expressions across entities from different experiments and finally gives a visual approximation. If one has a tumor suppressor gene and an oncogene in the gene set to be evaluated, one can expect a similar expression range as the whole-transcriptome. The more genes are used, the more stable the normalization. Probe sets of a gene that map to more retained/dysfunctional transcripts, than other probe sets of the same gene, were removed. Expression values from all data sets were merged into one matrix and again quantile normalized to account for variability in platform specifications and noise. The resulting heatmap (generated by R 3.0.0, function "heatmap.2") shows the expression of these 15 genes and 2 transcripts in their respective original data set additionally subdivided by the different entities (median across samples of an entity). For further subsets of genes the same normalized expression range was used, to get stable patterns across all heatmaps. The data set of Eckerle et al. 2009 (116)/ GSE 14879 was excluded in this approach, because the lymphoma cells acquired a gene expression pattern hampering an assignment to a CD4+, CD8+ or CD30+ T cell origin.

4.8 Statistical analysis

Graphpad Prism V software was used for generating Kaplan-Meier curves and performing statistical analysis (using Mantle-Cox test) to compare the survival of mice. Graphpad Prism was also used to carry out unpaired two-tailed t-tests on the viability assays with T-NHL cells.

5 Results

5.1 The role of Bcl-2 proteins for murine T-NHL cell survival

5.1.1 Heterozygous deletion of *Mcl-1* impairs T-NHL cell survival *ex vivo*

As described before, γ-irradiation of young mice with 150 rad leads to development of T-NHL (4). To address the question whether MCL-1 plays a role for survival of murine T-NHL, lymphoma cells from irradiated, diseased *Mcl-1*$^{fl/+}$*CreER* and *Mcl-1*$^{+/+}$*CreER* mice (termed „controls") were harvested and cell survival was measured *ex vivo* after 48 h of tamoxifen (TMX) treatment and thereby caused Cre induction. Deletion of one allele of *Mcl-1* (*Mcl-1*$^{\Delta/+}$*CreER*) resulted in elevated apoptosis, measured by flow cytometry, when directly compared to *Mcl-1*$^{fl/+}$*CreER* cells, treated with vehicle control (Figure 5.1 A) as well as a continuous decrease of viability over time (Figure 5.1 B). In *Mcl-1*$^{+/+}$*CreER* T-NHL cells, no change in viability was visible after Cre induction. (Figure 5.1 C). Heterozygous loss of *Mcl-1* reduced protein levels of MCL-1 to about 50%, accompanied by the cleavage of CASPASE 3 after 24h of treatment (Figure 5.1 D). To confirm if the impairment of T-NHL cell survival upon Cre induction with TMX was specifically due to *Mcl-1* deletion, human MCL-1 was ectopically expressed in *Mcl-1*$^{fl/+}$*CreER* T-NHL cells before endogenous *Mcl-1* deletion. Human MCL-1 expression rescued T-NHL cells from cell death (Figure 5.2 A) and prevented cleavage of CASPASE 3 (Figure 5.2 B), which was not the case upon transduction with the empty pMIG vector (Figure 5.2 A and C). Furthermore, ectopic expression of the other anti-apoptotic Bcl-2 proteins BCL-2, BCL-X_L and BCL-W also rescued T-NHL cells from cell death upon heterozygous *Mcl-1* deletion (Figure 5.2 D-F).

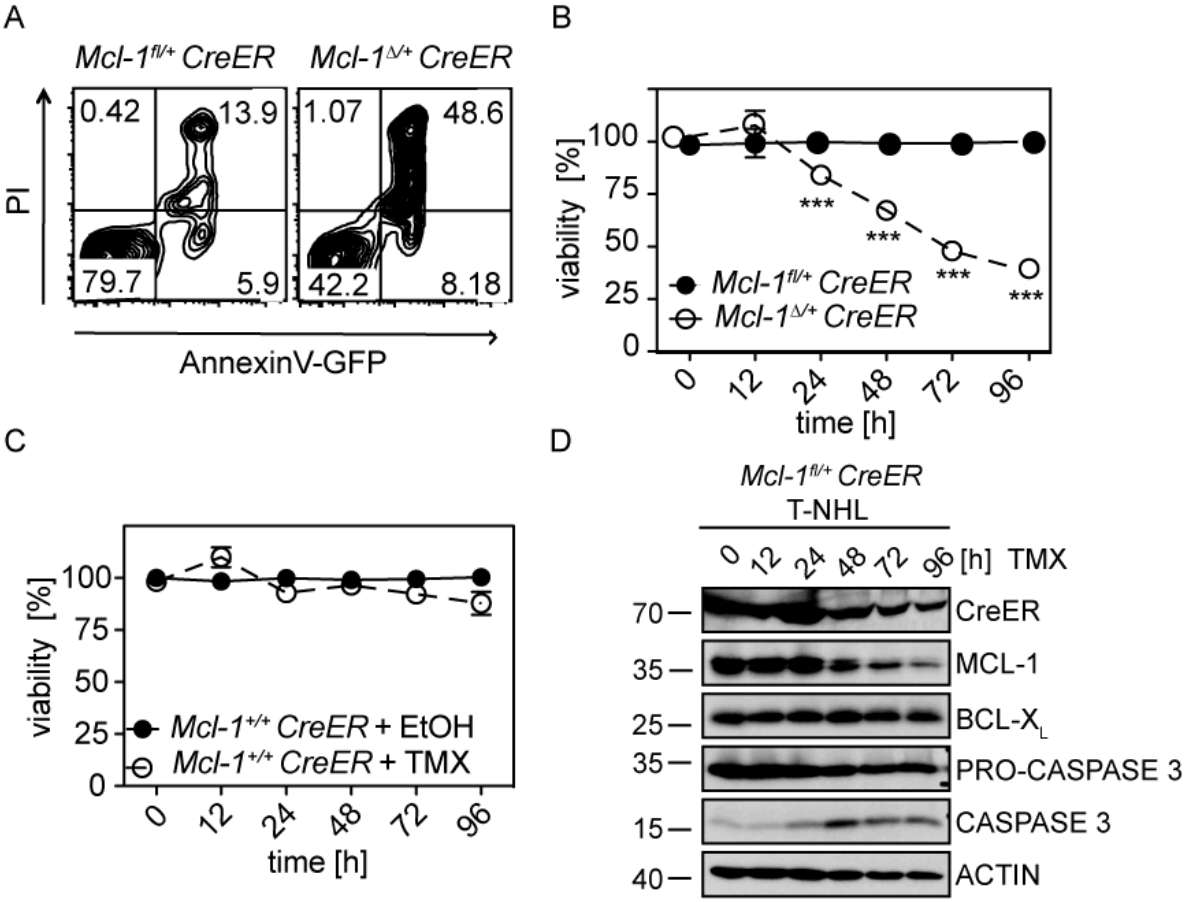

Figure 5.1 The effect of heterozygous *Mcl-1* deletion on viability of T-NHL cells *ex vivo*. (A) T-NHL cells, isolated from irradiated and diseased *Mcl-1$^{fl/+}$CreER* mice were treated with either 100 nM TMX (right panel) or EtOH (left panel) for 48 hours. (B) and (C) T-NHL cells, isolated from irradiated and diseased (B) *Mcl-1$^{fl/+}$CreER* or (C) *Mcl-1$^{+/+}$CreER* mice were treated with either 100 nM TMX (dashed line) or EtOH (continuous line) for 0, 12, 24, 48, 72 and 96 hours as indicated. (A)-(C) Viability was estimated by AnnexinV/PI staining and subsequent Flow Cytometry. Statistical analysis was done with unpaired t-test. Asterisks denote significant differences (*p< 0,05, ** p< 0,005; ***p< 0,0005). (D) *Mcl-1$^{fl/+}$CreER* T-NHL cells from (B) were lysed after 0, 12, 24, 48, 72 and 96 hours of TMX treatment and Western Blot analysis was performed on protein expression of MCL-1, BCL-XL, CreER and CASPASE 3 activation.

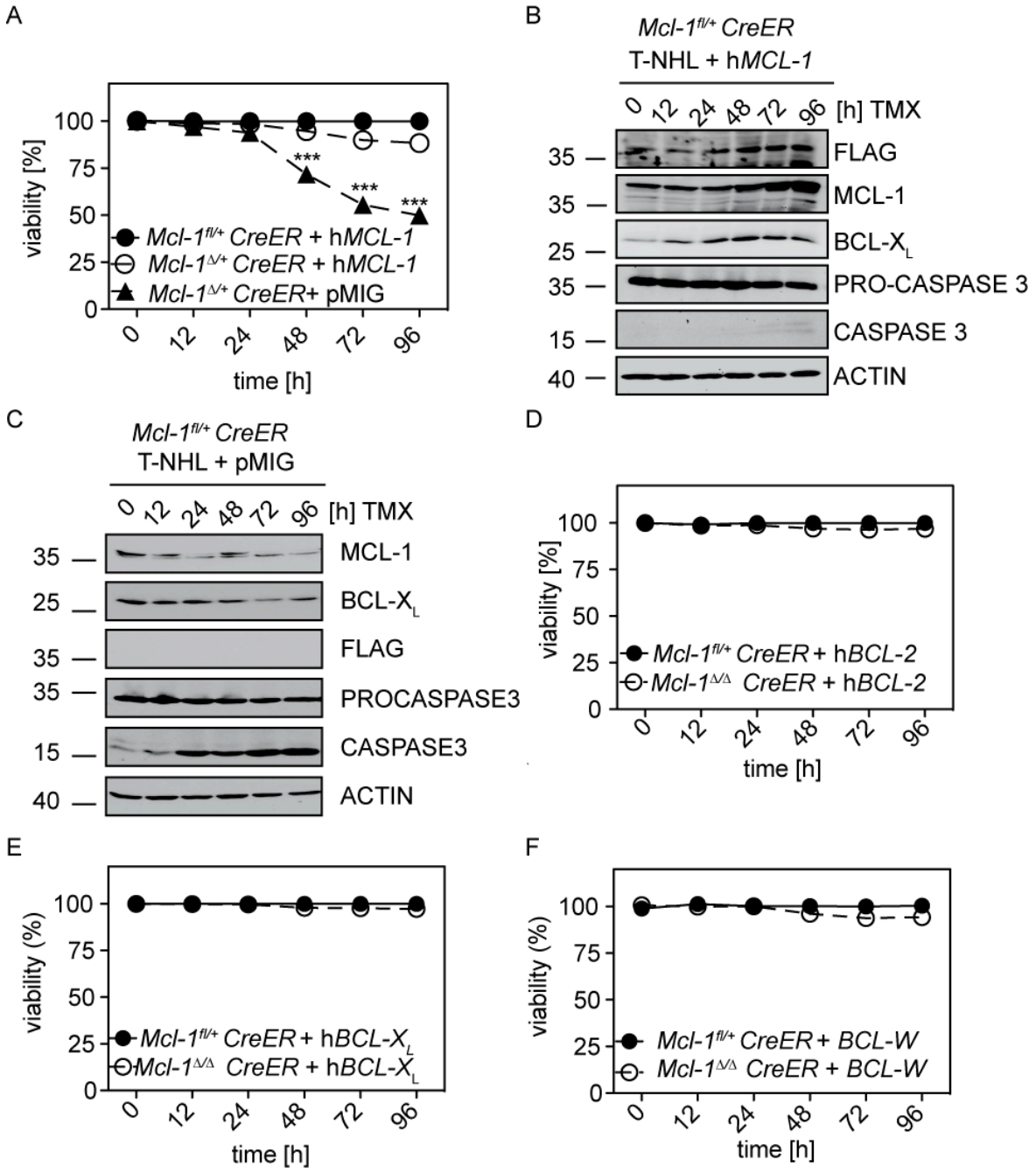

Figure 5.2 Ectopic expression of anti-apoptotic Bcl-2 proteins rescues T-NHL cells from cell death after heterozygous *Mcl-1* deletion. (A) *Mcl-1$^{fl/+}$CreER* T-NHL cells were retrovirally transduced with pMSCV-FLAG-*hsMCL-1*-IRES-GFP or pMSCV-IRES-GFP and sorted on GFP-positive cells. Subsequently, cells were treated with TMX as indicated and viability was measured by PI staining and Flow Cytometry. (B)-(C) Sorted *Mcl-1$^{fl/+}$CreER* T-NHL cells, transduced with (B) pMSCV-FLAG-*hsMCL-1*-IRES-GFP or (C) pMIG were treated with TMX for 0,12, 24, 48, 72 and 96 hours as indicated. Cells were lysed and Western Blot performed on protein expression of MCL-1, FLAG,

BCL-X_L, BCL-2 and CASPASE 3 activation. (D)-(F) *Mcl-1$^{fl/+}$CreER* T-NHL cells were transduced with (D) pMSCV-FLAG-*hBCL-2*-IRES-GFP, (E) pMSCV-FLAG-*hBCL-X$_L$*-IRES-GFP or (F) pMSCV-FLAG-*hsBCL-W*-IRES-GFP and sorted by FACS on GFP positive cells. Cells were treated with 100 nm TMX (dashed line) or EtOH respectively (continuous line). Viability was measured by PI staining and subsequent Flow Cytometry. Viability of TMX treated cells was normalized to EtOH treated cells. Asterisks denote significant differences (*p< 0,05, ** p< 0,005; ***p< 0,0005).

5.1.2 Inhibition of other anti-apoptotic Bcl-2 proteins has a minor effect on T-NHL cell survival

MCL-1 is not the only anti-apoptotic Bcl-2 protein that has been demonstrated to be important for normal T lymphocyte survival. BCL-X_L and BCL-2 have been shown to play a role for survival at several stages of T lymphocyte development. Furthermore, both these proteins are known to be involved in the development of B cell lymphoma (Section 1.2.2). Therefore, the effect of conditional *Bcl-x$_L$* deletion on T-NHL survival was investigated.

Loss of both alleles of *Bcl-x$_L$* showed a significant reduction of BCL-X_L protein levels, accompanied by an increase in cleaved CASPASE 3 levels (Figure 5.3 A). AnnexinV/PI staining depicted a decrease in overall survival of T-NHL cells upon loss of *Bcl-x$_L$* (Figure 5.4 B), which could be rescued by ectopic BCL-X_L, BCL-2, BCL-W or MCL-1 expression (Figure 5.3 C-F). Still, the effect of total *Bcl-x$_L$* deletion was less profound than the effect of mono-allelic *Mcl-1* deletion (Figure 5.1 B).

To further address the question whether the combination of BCL-X_L, BCL-2 and BCL-W is essential for T-NHL cell survival, lymphoma cells were treated with the BH3 mimetic ABT-737. It harbors chemical features that resemble BAD and therefore shows the same binding affinities (148). It is able to bind and neutralize BCL-2, BCL-X_L and BCL-W but cannot neutralize MCL-1 or A1, that both show features, distinct from the other Bcl-2 proteins. Treatment with different

concentrations of ABT-737 showed a minor effect on the viability of T-NHL cells. Heterozygous deletion of *Mcl-1* lead to significant reduction of viability, after 72 hours, also in the absence of ABT-737 (Figure 5.4 A). Combined deletion of *Mcl-1* and 1 µM ABT-737 treatment showed a synergistic effect on T-NHL cell survival (Figure 5.4 A and B). Combined *Bcl-x$_L$* deletion and ABT-737 treatment also had a synergistic effect on viability that was however less profound than that observed for *Mcl-1* deletion (Figure 5.4 C).

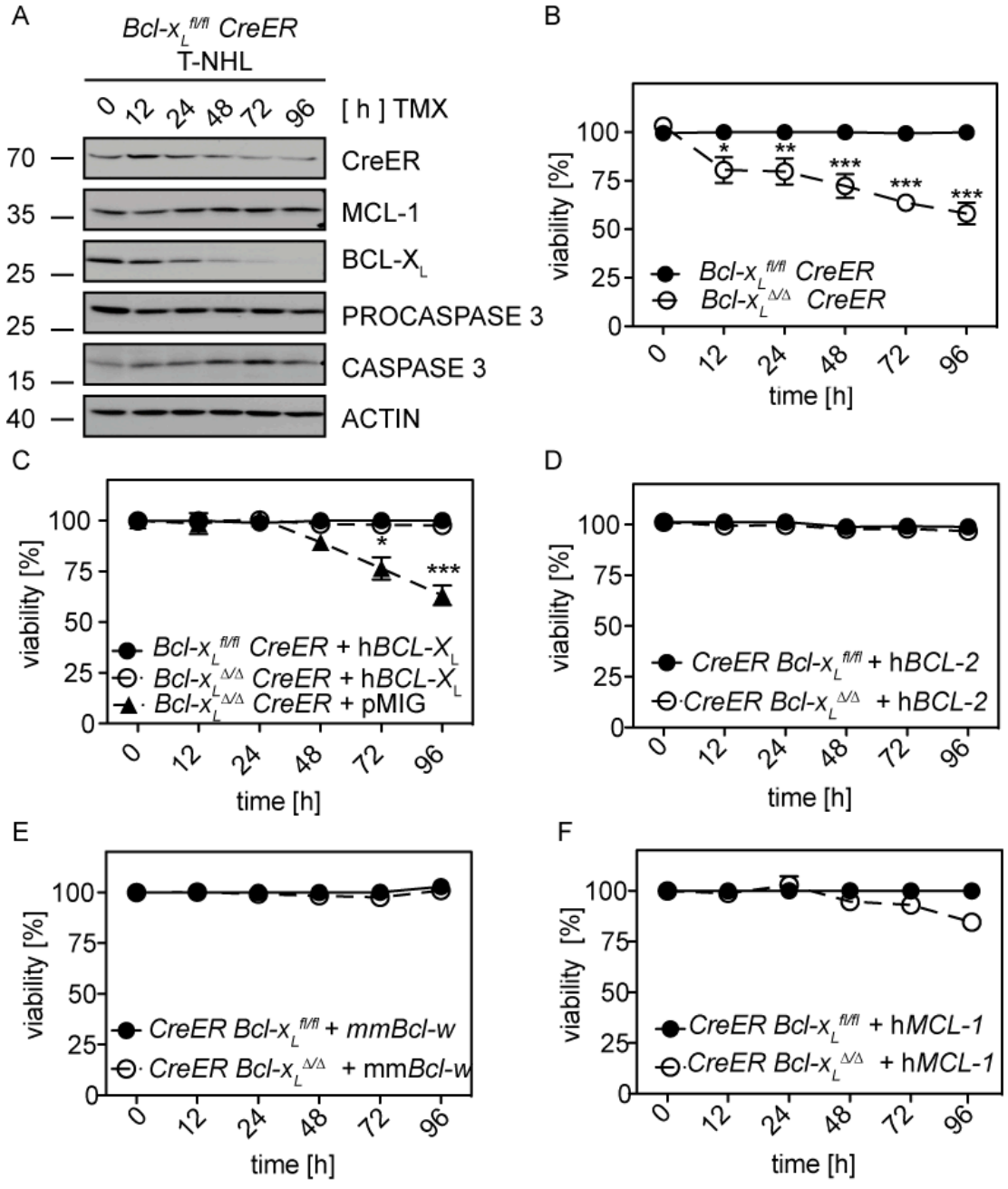

Figure 5.3 Complete *Bcl-x$_L$* deletion specifically leads to a moderate decrease in viability of T-NHL cells. (A) Western Blot with T-NHL cells isolated from irradiated, diseased *Bcl-x$_L^{fl/fl}$CreER* mice, treated with 100 nM TMX for indicated time (hours). (B) Viability of T-NHL cells isolated from irradiated, diseased *Bcl-x$_L^{fl/fl}$CreER* mice treated with either 100 nM TMX (dashed line) or EtOH (continuous line) for 0, 12, 24, 48, 72 and 96 hours as indicated. Viability was estimated by AnnexinV/PI staining and subsequent Flow Cytometry. (C) Viability of *Bcl-x$_L^{fl/fl}$CreER* T-NHL cells, retrovirally transduced with pMSCV-FLAG-hs*BCL-X$_L$*-IRES-GFP or pMSCV-IRES-GFP and sorted on GFP-positive cells. Cells were treated with TMX (dashed line) or vehicle control (continuous line) as indicated. (D)- (F) Viability of *Bcl-x$_L^{fl/fl}$CreER* T-NHL cells retrovirally transduced with (D) pMSCV-FLAG-*hsBCL-2*-IRES-GFP, (E) pMSCV-FLAG-*mmBcl-w*-IRES-GFP or (F) pMSCV-FLAG-*hsMCL-1*-IRES-GFP and treated with either TMX (dashed line) or vehicle control (continuous line) as indicated. (C)- (E) Viability was measured by PI staining and subsequent Flow Cytometry. Asterisks denote significant differences (*p< 0,05, ** p< 0,005; ***p< 0,0005).

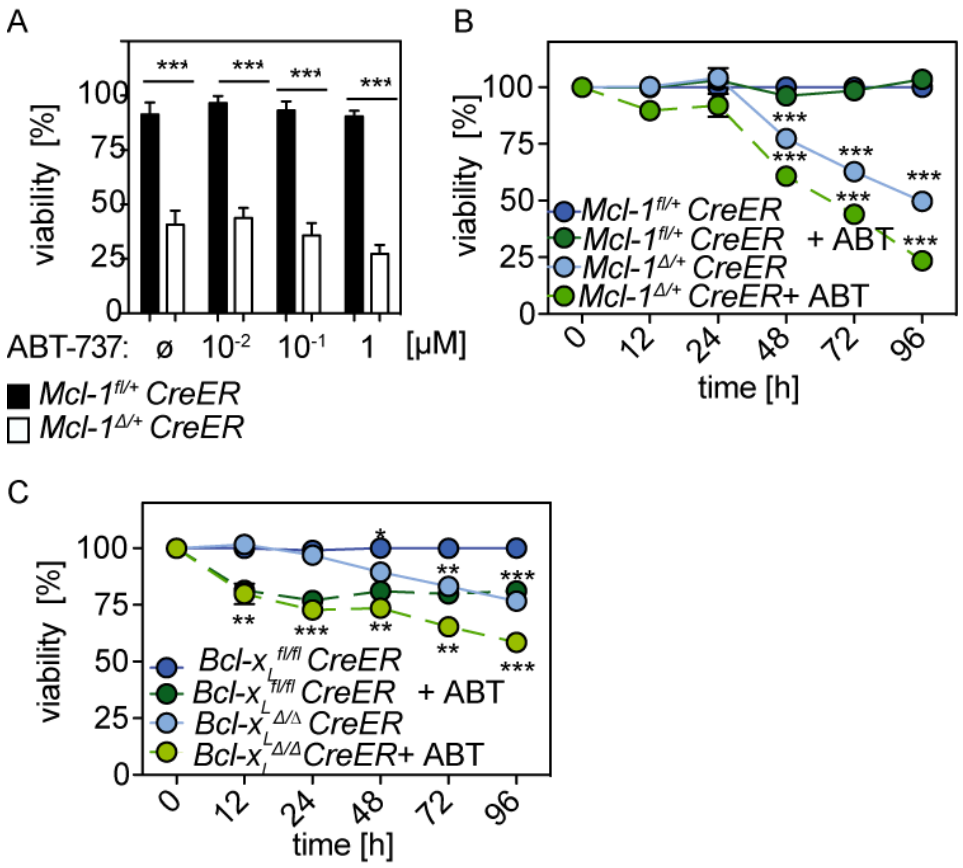

Figure 5.4 Synergistic effect on viability of T-HNL cells of *Mcl-1* deletion and ABT-737 treatment. (A) Viability of T-NHL cells isolated from irradiated, diseased *Mcl-1$^{fl/+}$CreER* mice, treated with different concentrations ABT-737 (0 − 1 µM) and co-treated with 100 nM TMX (white columns) or vehicle control (black columns) for 72 hours. (B) Viability of T-NHL cells isolated from irradiated, diseased *Mcl-1$^{fl/+}$CreER* mice treated with vehicle control (dark blue circles), 1 µM ABT-737 (dark green circles), 100 nM TMX (bright blue circles) or co-treated with 1 µM ABT-737 and 100 nM TMX (bright green circles) for the indicated time. (C) Viability of T-NHL cells isolated from irradiated, diseased *Bcl-x$_L^{fl/fl}$CreER* mice treated with vehicle control (dark blue circles), 1 µM ABT-737 (dark green circles), 100 nM TMX (bright blue circles) or co-treated with 1 µM ABT-737 and 100 nM TMX (bright green circles) for the indicated time. Viability was throughout measured using Cell Titer Glo Luminesecent Assay. Asterisks denote significant differences (*p< 0,05, ** p< 0,005; ***p< 0,0005).

5.2 The role of MCL-1 for murine T-NHL cell survival *in vivo*

5.2.1 Transplantation of irradiation-induced T-NHL causes lymphoma in recipient C57BL76 mice

To test if irradiation-induced lymphoma cells can reconsitute after transplantation in recipient mice, *Mcl-1$^{+/+}$CreER* lymphoma cells were injected into syngeneic and immuno-competent wild type (WT) C57BL/6 mice. About 20 days after transplantation mice diseased and presented with enlarged spleens in comparison to healthy control mice, that were not transplanted with lymphoma cells (Figure 5.5 A). Furthermore Flow Cytometry analysis of spleen, lymph node, bone marrow and blood showed infiltration with TCRβ positive cells (Figure 5.5 B). In some cases kidneys exhibited white spots, which showed to be caused by infiltrated CD3 positive cells (Figure 5.5 C). The cells isolated from the diseased mice showed expression of TCRβ and were mostly single positive for CD8 or CD4 but also double positive (DP) in some cases. Furthermore, the T-NHL cells showed to be

positive for the T cell activation markers CD69, CD62L, CD25 and CD44 (Figure 5.6).

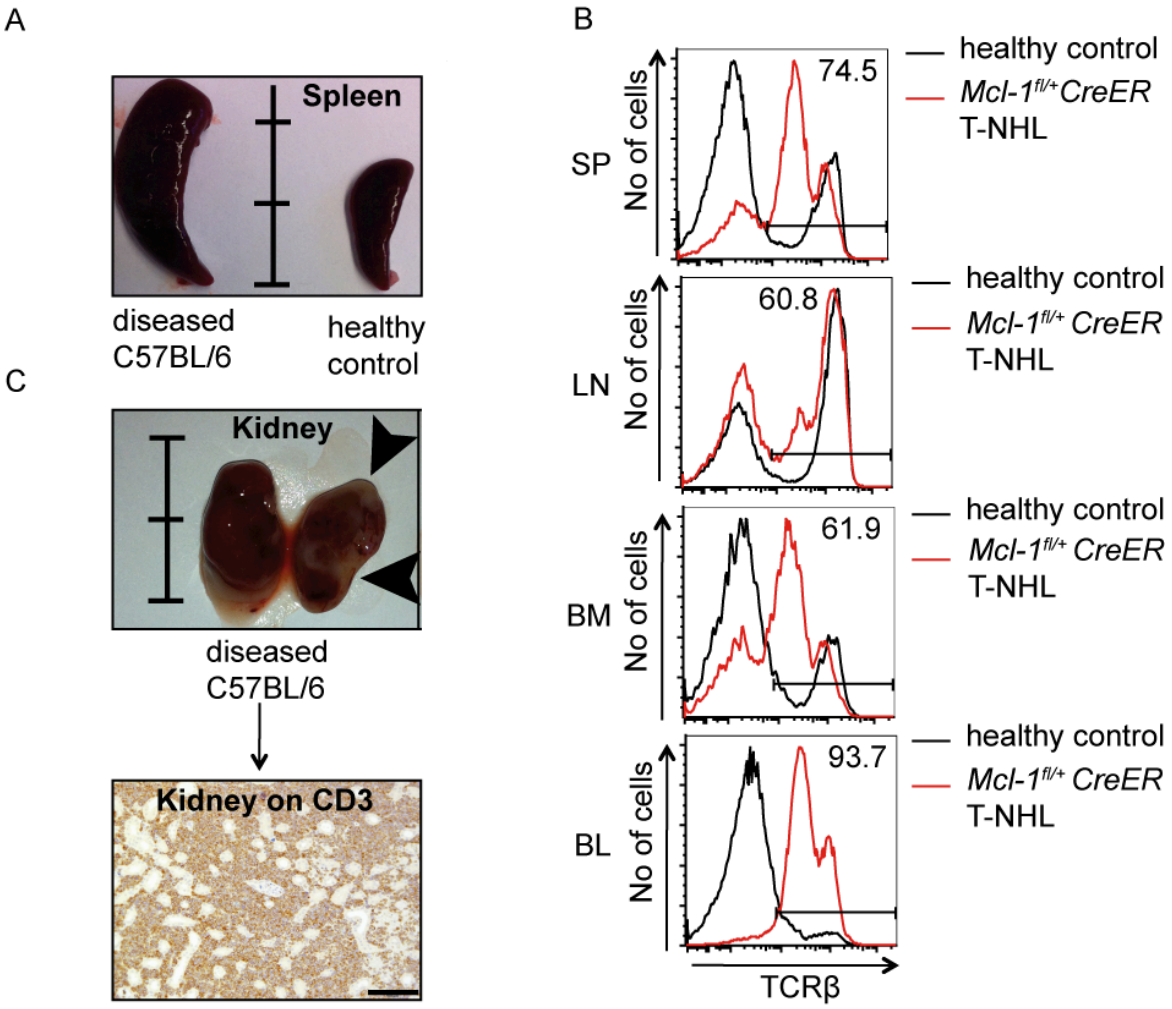

Figure 5.5 Phenotype of C57BL/6 mice, transplanted with T-NHL cells. (A) Spleens of C57BL/6 mice injected with 10^7 mouse T-NHL cells and diseased (on the left) and the age-matched healthy control (on the right). One bar segment represents 1 cm (B) Flow Cytometry on TCRβ expression in the spleen (SP), lymph nodes (LN), bone marrow (BM) and blood (BL) of C57BL/6 mice, injected with 10^7 T-NHL cells (red) and age-matched control mouse (black). The numbers indicate the percentage of TCRβ-positive cells in the transplanted, diseased mouse. (C) Kidneys of diseased C57BL/6 mice injected with 10^7 mouse T-NHL cells. The arrows indicate white areas, infiltrated with CD3 positive cells, shown as histology in the lower panel. The black bar represents 100 µm.

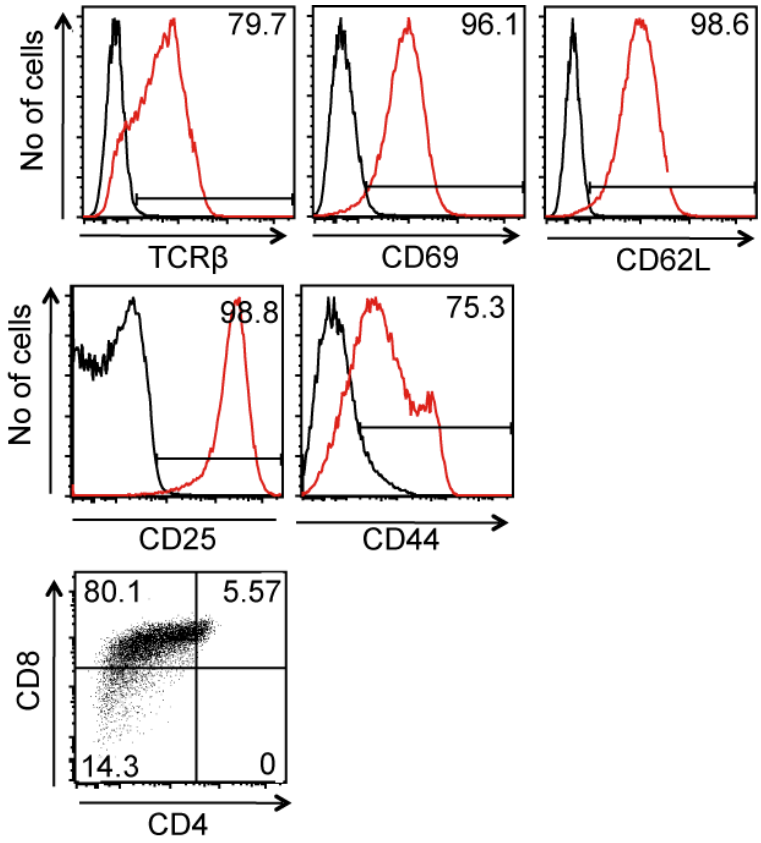

Figure 5.6 Phenotype of transplanted T-NHL cells isolated from lymphoma-burdened mouse. Flow Cytometry on cells isolated from the spleen of diseased C57BL/6 mice transplanted with 10^7 *Mcl-1*$^{fl/+}$*CreER* T-NHL cells on T cell (activation) markers TCRβ, CD69, CD62L, CD25, CD44 and the expression of CD8 and CD4. The numbers indicate the percentage of positive cells.

5.2.2 Heterozygous deletion of *Mcl-1* impaired T-NHL reconstitution after transplantation

To see whether lymphoma reconstitution, as observed above (5.2.1), was dependent on full MCL-1 expression, *Mcl-1$^{fl/+}$CreER* T-NHL cells were injected into WT recipient mice. 16 days after transplantation TMX or vehicle control was administered to the mice by i.p. injection, to activate CreER and induce target gene deletion (Figure 5.7). Alternatively, WT mice received *Mcl-1$^{+/+}$CreER* T-NHL cells in order to examine the effect of CreER activation in the absence of target gene deletion (Cre- toxicity).

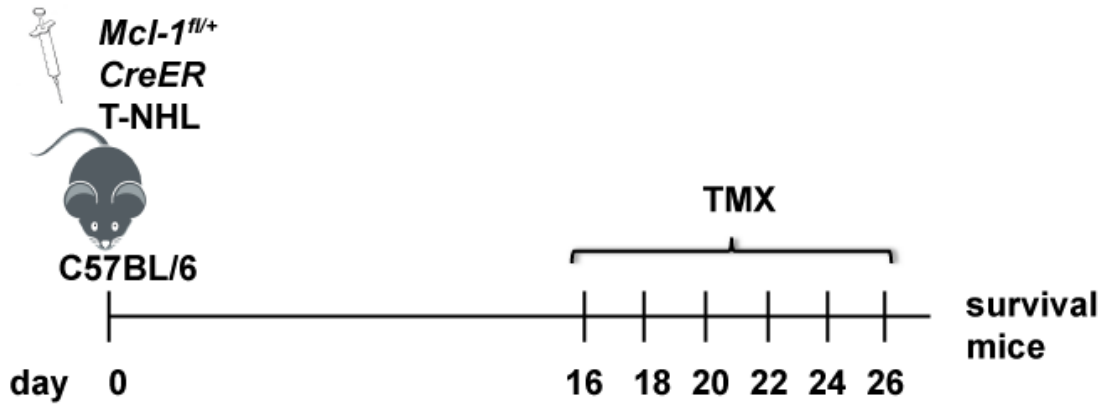

Figure 5.7 Schematic view of transplantation of T-NHL cells into WT recipients. 10^7 T-NHL cells were injected into the tail vein of C57BL/6 wild type recipient mice. On days 16, 18, 20, 22, 24 and 26 TMX was administered by i.p. injection.

PCR analysis confirmed that mice that received *Mcl-1$^{fl/+}$CreER* T-NHL cells and were treated with TMX (*Mcl-1$^{\Delta/+}$CreER*) showed effective deletion of one allele *Mcl-1,* in contrast to mice that received vehicle control (Figure 5.8 A). Furthermore, lymphoma cells from mice treated with TMX showed reduced *Mcl-1* mRNA expression compared to the controls (Figure 5.8. B).

Importantly, the mice that harbored *Mcl-1*$^{\Delta/+}$*CreER* T-NHL cells exhibited prolonged survival in comparison to mice with *Mcl-1*$^{fl/+}$*CreER* T-NHL cells (Figure 5.9 A). Activation of CreER, without target gene deletion, had no effect on survival of the mice. This was shown by TMX treatment of the mice harboring the *Mcl1*$^{+/+}$ *CreER* T-NHL cells, which succumbed to disease at the same rate as the vehicle treated controls (Figure 5.9 B). To see whether deletion of *Mcl-1* influenced the expression of other Bcl-2 proteins that usually play a role in the survival of T cells, their expression level in the T-NHL infiltrated spleens of diseased mice was measured. Quantitative PCR of *Bcl-x*$_L$ showed an increased mRNA expression in diseased *Mcl-1*$^{\Delta/+}$*CreER* mice (Figure 5.10 A). Also BCL-X$_L$ protein levels were increased upon reduction of MCL-1 levels (Figure 5.10 C). No significant changes in *Bcl-2* mRNA and protein levels were observed upon deletion of *Mcl-1* (Figure 5.10 B and C). Finally, distinct changes in the expression pattern of the key pro-apoptotic player BIM was observed in spleens from vehicle control compared to *Mcl-1*$^{\Delta/+}$*CreER* mice (Figure 5.10 C).

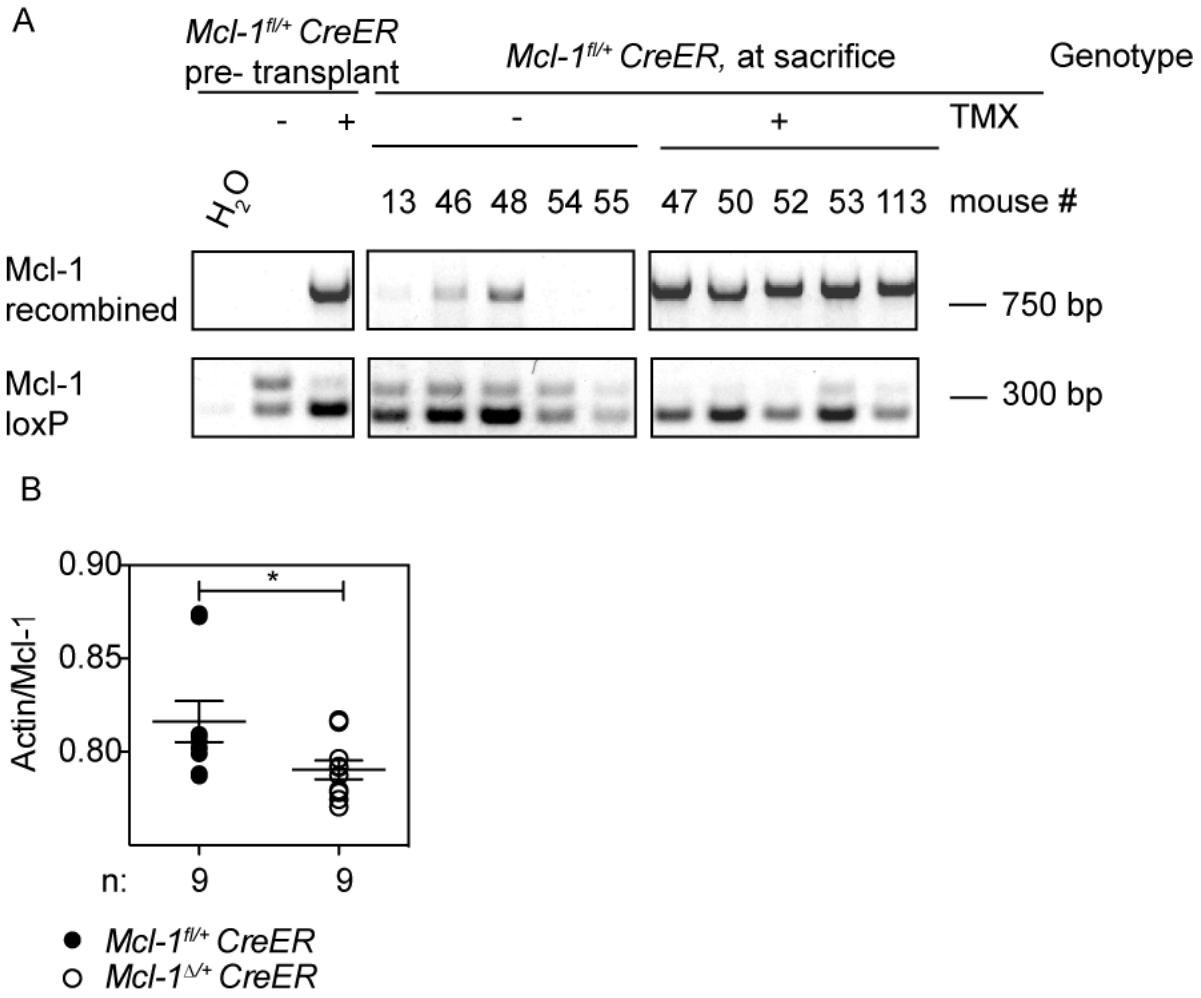

Figure 5.8 Target gene deletion of *Mcl-1* in lymphoma burdened, transplanted C57BL/6 mice. (A) PCR with DNA from lymphoma cells, isolated from diseased C57BL/6 mice that were transplanted with 10^7 *Mcl-1$^{fl/+}$CreER* T-NHL cells. The upper panel shows the recombined *Mcl-1* allele, the lower panel shows the floxed allele. The first segment on the left shows the T-NHL cells before being transplanted. (B) mRNA expression of *Mcl-1* in lymphoma cells of diseased C57BL/6 mice that were transplanted with *Mcl-1$^{fl/+}$CreER* T-NHL cells. Calculated was the CT value of Actin in relation to the CT value of *Mcl-1*. The black dots show cells from mice treated with vehicle (0,82 ± 0,01), the white dots represent mice that got TMX (0,79 ± 0,01). Each dot represents one mouse. Statistical analysis was done by unpaired t-test (p= 0,042).

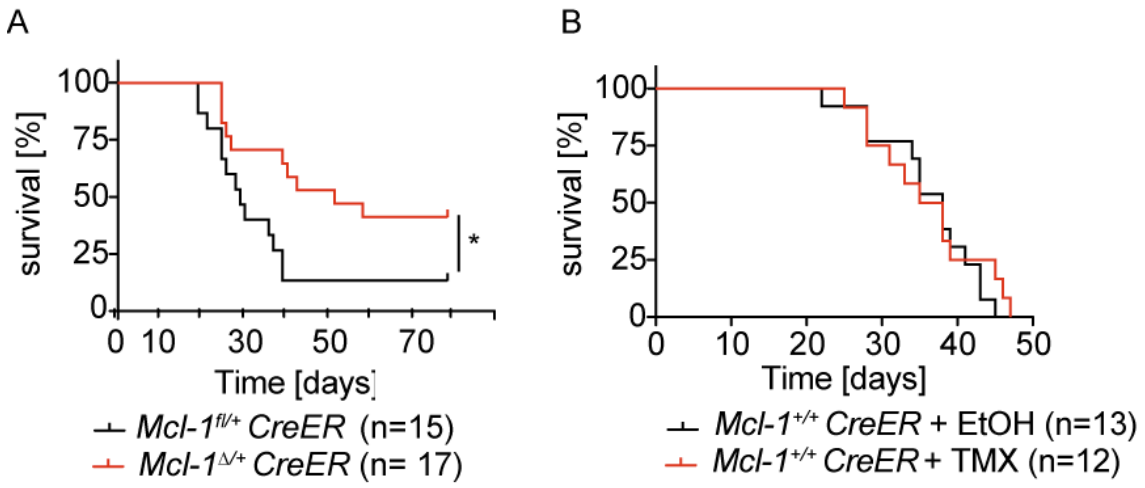

Figure 5.9 Survival of C57BL/6 mice transplanted with *Mcl-1$^{fl/+}$ CreER* and *Mcl-1$^{+/+}$ CreER* T-NHL cells. (A) Kaplan-Meier Curves of WT C57BL/6 mice transplanted with *Mcl-1$^{fl/+}$CreER* T-NHL cells and treated with vehicle control (median survival: 26 days) or TMX (median survival: 46 days). Analysis was done by Mantle-Cox test (p= 0,02). (B) Kaplan-Meier Curves of WT C57BL/6 mice transplanted with *Mcl-1$^{+/+}$CreER* T-NHL cells and treated with vehicle control (median survival: 38 days) or TMX (median survival: 36,5 days). Analysis was done by Mantle-Cox test (p= 0,30).

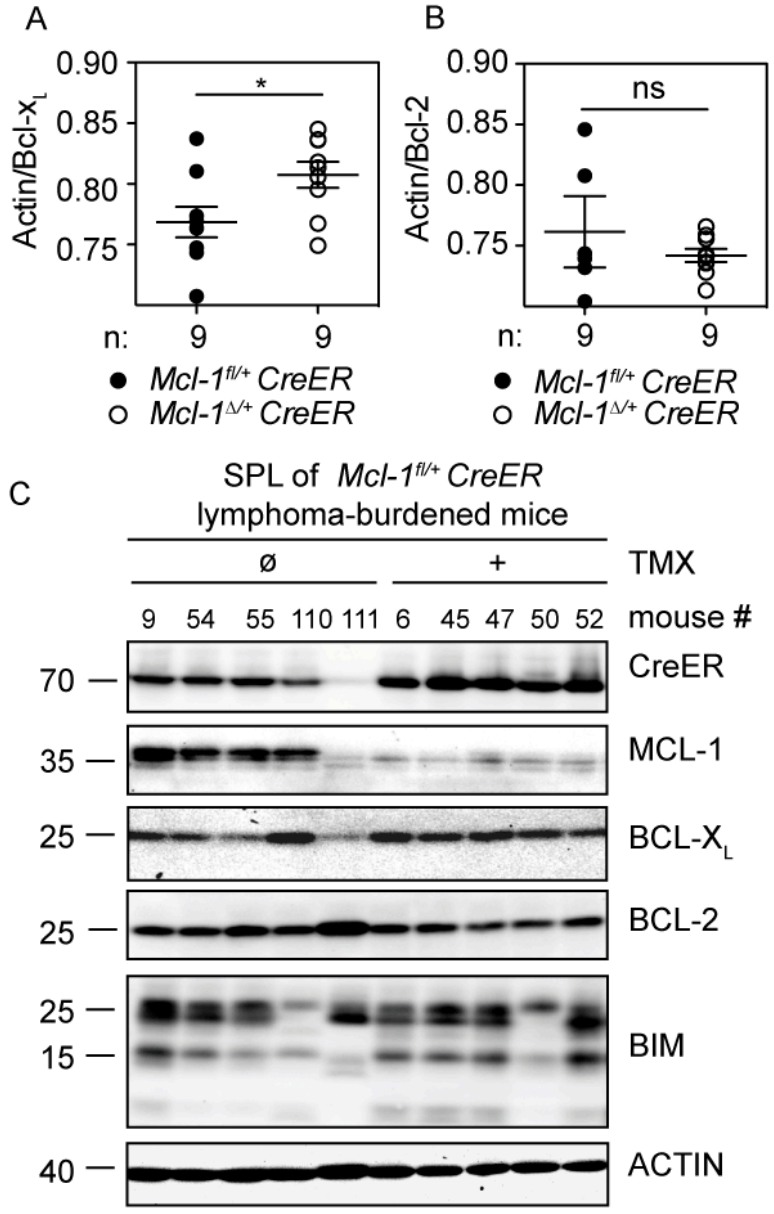

Figure 5.10 Expression of Bcl-2 proteins in diseased C57BL/6 mice transplanted with T-NHL cells. (A) mRNA expression of *Bcl-x$_L$* in lymphoma cells from diseased C57BL/6 mice that were transplanted with *Mcl-1$^{fl/+}$CreER* T-NHL cells. The black dots represent mice treated with vehicle (0,77 ± 0,01), the white dots mice that got TMX (0,81 ± 0,01). Calculated was the CT value of Actin in relation to the CT value of *Bcl-x$_L$*. Each dot represents one mouse. Statistical analysis was done by unpaired t-test (p= 0,040). (B) mRNA Expression of *Bcl-2* in lymphoma cells of diseased C57BL/6 mice that were transplanted with *Mcl-1$^{fl/+}$CreER* T-NHL cells. The black dots shows cells from mice treated with vehicle (0,76 ± 0,03), the white dots mice that got TMX (0,74 ± 0,01). Calculated was the CT value of Actin in relation to the CT value of *Bcl-2*. Each dot

represents one mouse. Statistical analysis was done by unpaired t-test (p= 0,521). (C) Western Blot Analysis of lymphoma cells from diseased C57BL/6 mice that were transplanted with *Mcl-1$^{fl/+}$CreER* T-NHL cells. The left panel shows vehicle treated mice (# 9, 54, 55, 110, 111), the right panel (# 6, 45, 47, 50, 52) TMX treated mice.

5.2.3 Deletion of *Mcl-1* delays lymphoma progression in an ITK-SYK induced T-NHL model

As shown in section 5.2.2, heterozygous *Mcl-1* deletion impaired maintenance of already established T-NHL cells *ex vivo* and *in vivo*. To test whether MCL-1 protects lymphoma cells also during the process of malignant transformation, an alternative mouse T-NHL model, based on the fusion kinase ITK-SYK, was used (5). In this model, CD4Cre-inducible expression of ITK-SYK from the Rosa26 locus drives the development of a GFP$^+$ mature peripheral T-NHL in *Rosa26-lox-STOP-loxITK-SYK$^{ki/+}$CD4Cre$^{+/-}$* mice (referred to as *IS$^{+/-}$CD4Cre*). To study the role of MCL-1 in this model, *IS+/-CD4Cre* mice were interbred with mice harboring floxed alleles of *Mcl-1* to obtain *Mcl-1$^{fl/+}$Rosa26-lsl-ITK-SYK$^{ki/+}$CD4Cre$^{+/-}$* (referred to as *Mcl-1$^{fl/+}$IS$^{+/-}$CD4Cre*), *Mcl-1$^{fl/fl}$Rosa26-lsl-ITK-SYK$^{ki/+}$CD4Cre$^{+/-}$* (referred to as *Mcl-1$^{fl/fl}$IS$^{+/-}$CD4Cre*) and respective control mice without the IS allele.

To determine whether *Mcl-1* deletion in double positive (DP) T cells in the thymus influences lymphoma development, *ITK-SYK* transgenic mice of the different genotypes described above were screened for T cell infiltration in the peripheral blood 4 and 16 weeks after birth. As previously reported, at 4 weeks, *IS$^{+/-}$CD4Cre* mice showed diminished numbers of T cells compared to control *CD4Cre* mice, due to increased negative selection of DP cells in the thymus (5) (Figure 5.11 A). Deletion of one allele of *Mcl-1* in *Mcl-1$^{fl/+}$IS$^{+/-}$CD4Cre* mice lead to a further reduction of T cell numbers that was exacerbated when both *Mcl-1* alleles were deleted in *Mcl-1$^{fl/fl}$IS$^{+/-}$CD4Cre* and *Mcl-1$^{fl/fl}$CD4Cre* mice (Figure 5.11 A). All the

other *CD4Cre* control mice showed no significant differences in T cell numbers in comparison to *Mcl-1*$^{fl/fl}$ mice (Figure 5.11 A).
16 weeks after birth, the *IS*$^{+/-}$*CD4Cre* mice showed a strong increase in TCRβ^{+} cells in the peripheral blood in comparison to *CD4Cre* mice (Figure 5.11 B). This IS driven infiltration with TCRβ+ cells was significantly reduced in both *Mcl-1*$^{fl/+}$*IS*$^{+/-}$*CD4Cre* and *Mcl-1*$^{fl/fl}$*IS*$^{+/-}$*CD4Cre* mice. While *Mcl-1*$^{fl/fl}$*CD4Cre* mice still exhibited a lack of T cells, *Mcl-1*$^{fl/fl}$*IS*$^{+/-}$*CD4Cre* mice showed approximately normal T cell numbers, comparable to *Mcl-1*$^{fl/fl}$ mice (Figure 5.11 B).

IS$^{+/-}$*CD4Cre* mice showed a median survival of 28,7 days, which was prolonged in *Mcl-1*$^{fl/+}$*IS*$^{+/-}$*CD4Cre* mice to 175 days. *Mcl-1*$^{fl/fl}$*IS*$^{+/-}$*CD4Cre* mice exhibited a medial survival of 206 days, which was not significant compared to *Mcl-1*$^{fl/+}$*IS*$^{+/-}$*CD4Cre* mice due to the small mouse numbers (Figure 5.11 C). All diseased *IS* transgenic mice exhibited infiltration of spleens, lymph nodes and bone marrow with GFP positive T cell lymphoma cells (Figure 5.12).

The lymphoma cells from diseased *Mcl-1*$^{fl/+}$*IS*$^{+/-}$*CD4Cre* mice showed recombination of the floxed *Mcl-1* allele, which was not seen in *IS*$^{+/-}$*CD4Cre* mice (Figure 5.13 A). Protein levels of MCL-1 in lymphoma cells from *Mcl-1*$^{fl/+}$*IS*$^{+/-}$*CD4Cre* mice were diminished compared to *IS*$^{+/-}$*CD4Cre* cells (Figure 5.13 B). To investigate whether alternative anti-apoptotic BCL-2 proteins were up-regulated upon MCL-1 reduction, the expression of BCL-X_L and BCL-2 in the lymphoma samples was analyzed. QPCR on *Bcl-x*$_L$ showed increased, although not significant, *Bcl-x*$_L$ mRNA in *Mcl-1*$^{fl/+}$*ISCD4Cre*, compared to *ISCD4Cre mice*, which was also observed in *Mcl-1*$^{fl/fl}$*IS*$^{+/-}$*CD4Cre* mice (Figure 5.13 C). This tendency also translated into increased protein levels of *Bcl-x*$_L$ (Figure 5.13 B). The mRNA level of *Bcl-2* was significant elevated in *Mcl-1*$^{fl/+}$*IS*$^{+/-}$*CD4Cre* as well as in *Mcl-1*$^{fl/fl}$*IS*$^{+/-}$*CD4Cre* mice (Figure 5.13 D). On protein level, BCL-2 showed heterogeneous expression within the lymphoma cells of the individual mice, which was also the case for BIM (Figure 5.13 B).

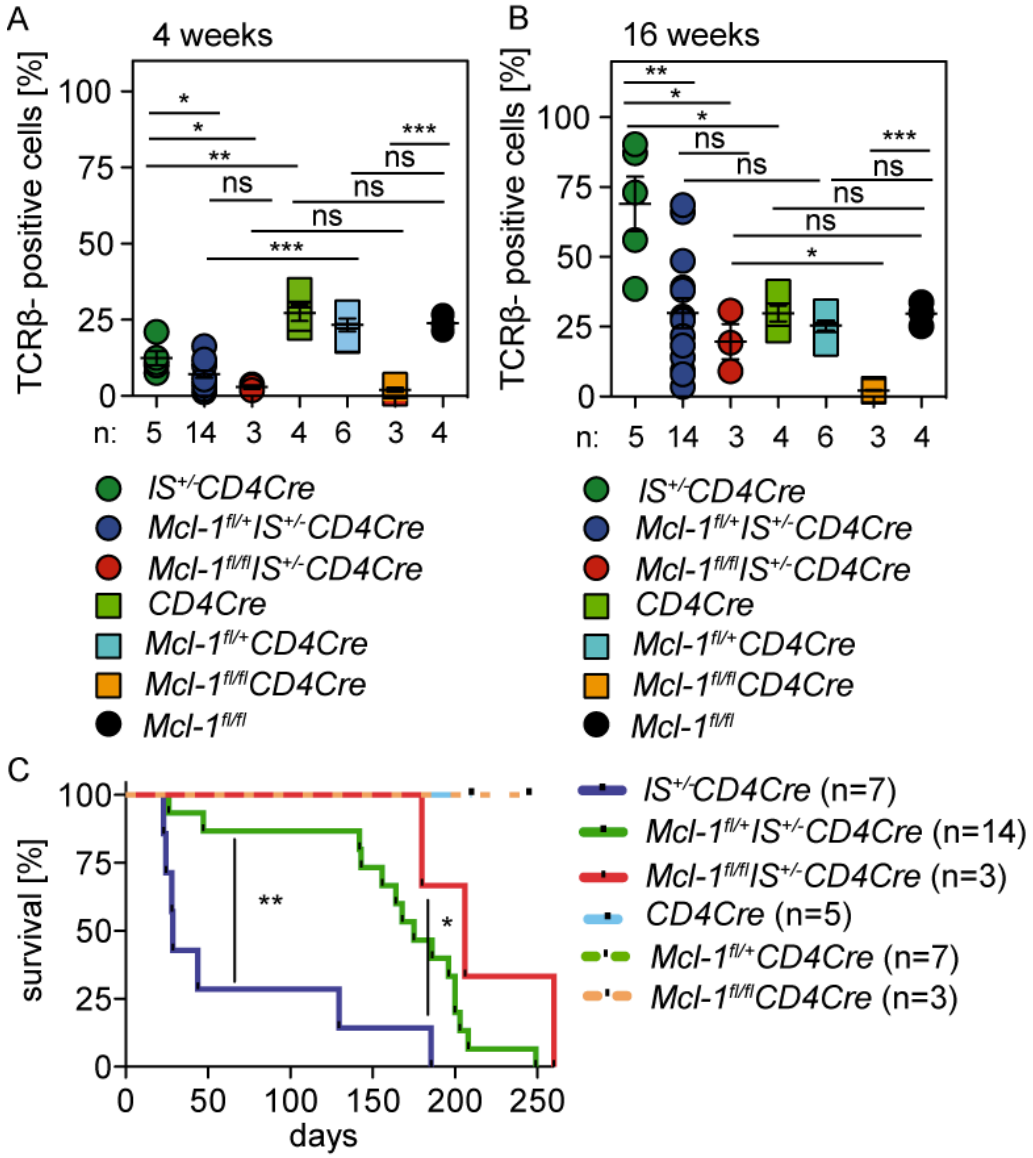

Figure 5.11 Progression of ITK-SYK induced T-NHL in mice with and without *Mcl-1* deletion. (A) and (B) Number (in %) of TCRβ-positive cells in (A) 4-weeks old and (B) 16 weeks old mice. Shown is the relative number of TCRβ+ cells in the peripheral blood of *IS$^{+/-}$CD4Cre* (n= 5), *Mcl-1$^{fl/+}$IS$^{+/-}$CD4Cre* (n=14), *Mcl-1$^{fl/fl}$IS$^{+/-}$CD4Cre* (n=3), *CD4Cre* (n=4), *Mcl-1$^{fl/+}$CD4Cre* (n=6), *Mcl-1$^{fl/fl}$IS$^{+/-}$CD4Cre* (n=3) and *Mcl-1$^{fl/fl}$* (n=4) mice. Graphs show mean ± SEM. Analysis was done with unpaired t-test and asterisks denote significant differences (*p< 0,05, ** p< 0,005; ***p< 0,0005). (C) Kaplan-Meier survival curves of *IS$^{+/-}$CD4Cre* (n= 7), *Mcl-1$^{fl/+}$IS$^{+/-}$CD4Cre* (n= 14), *Mcl-1$^{fl/fl}$IS$^{+/-}$CD4Cre* (n= 3), *CD4Cre* (n = 5), *Mcl-1$^{fl/+}$CD4Cre* (n= 7) and *Mcl-1$^{fl/fl}$CD4Cre* (n= 3). Analysis was done with Mantle-Cox test (p= 0,001; p= 0,028). The graph comprises male and female mice.

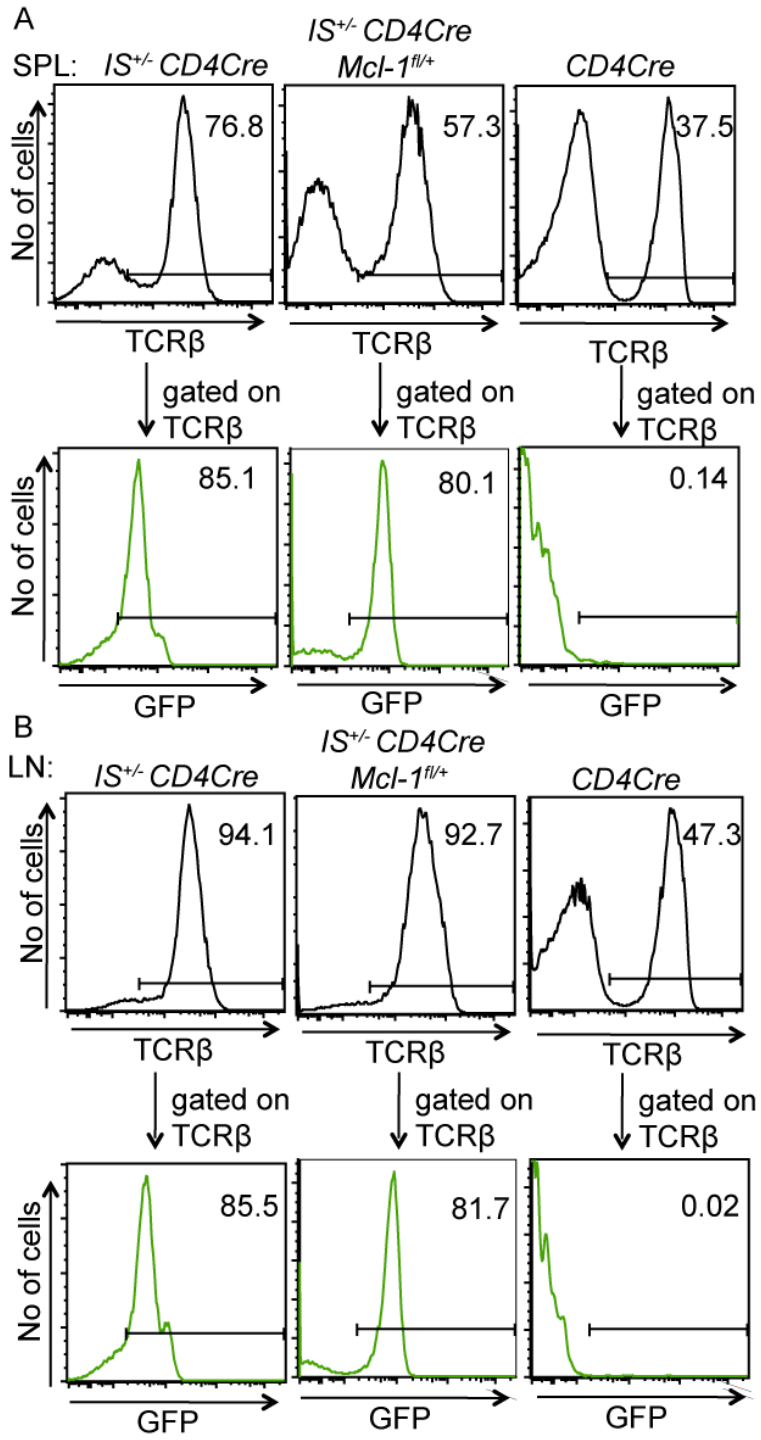

Figure 5.12 T cell infiltration in *ITK-SYK* transgenic, diseased mice. (A)-(C) Flow cytometric analysis on TCRβ and GFP expression of (A) splenocytes and (B) lymphocytes of diseased *IS$^{+/-}$CD4Cre* diseased after 185 days (on the left), *Mcl-1$^{fl/+}$IS$^{+/-}$ CD4Cre* diseased after 200 days (in the middle) or a healthy, age-matched *CD4Cre* mouse (on the right). Numbers indicate the percentage of positive cells. Each genotype is represented by one mouse.

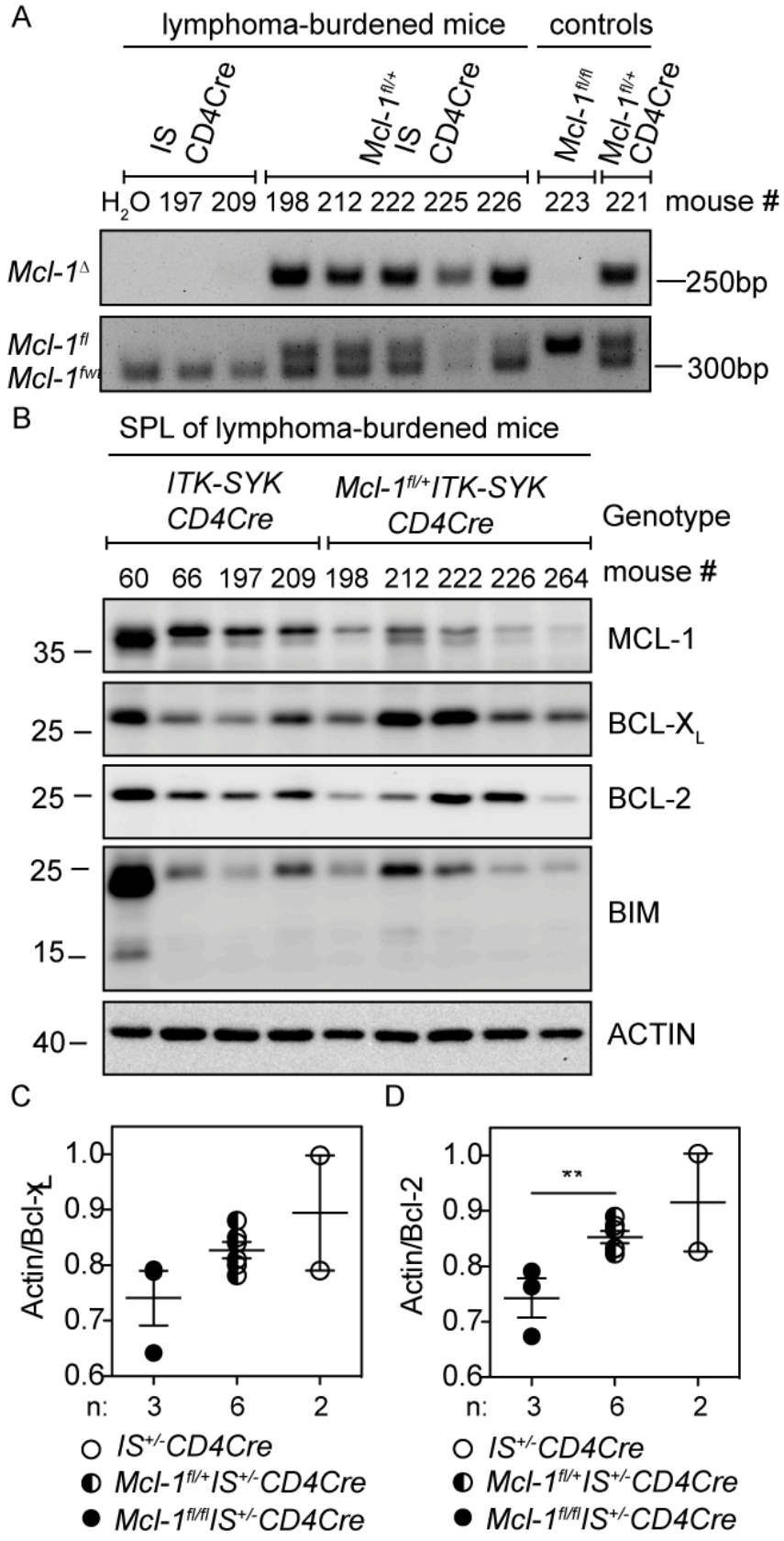
A
lymphoma-burdened mice
controls
IS CD4Cre
Mcl-1fl/+ IS CD4Cre
Mcl-1fl/fl
Mcl-1fl/+ CD4Cre
H2O 197 209 198 212 222 225 226 223 221 mouse #
Mcl-1Δ
Mcl-1fl
Mcl-1fw
250bp
300bp
B
SPL of lymphoma-burdened mice
ITK-SYK CD4Cre
Mcl-1fl/+ITK-SYK CD4Cre
Genotype
60 66 197 209 198 212 222 226 264 mouse #
35
25
25
25
15
40
MCL-1
BCL-XL
BCL-2
BIM
ACTIN
C
D
Actin/Bcl-xL
Actin/Bcl-2
1.0
0.9
0.8
0.7
0.6
n: 3 6 2
**
IS+/-CD4Cre
Mcl-1fl/+IS+/-CD4Cre
Mcl-1fl/flIS+/-CD4Cre

Figure 5.13 Expression of Bcl-2 proteins in lymphoma cells of *ITK-SYK* transgenic mice. (A) PCR on target gene deletion of *Mcl-1* in lymphoma cells. Shown are lymphoma cells from the infiltrated spleens of *IS$^{+/-}$CD4Cre* mice (197,209) and *Mcl-1$^{fl/+}$IS$^{+/-}$CD4Cre* mice (198,212,222,225,226) and splenocytes from Mcl-1$^{fl/fl}$ and *Mcl-1$^{fl/+}$CD4Cre* mice. The upper panel shows the deleted *Mcl-1* allele, the lower panel shows the *Mcl-1* WT and loxP alleles. (B) Western Blot on Bcl-2 proteins and BIM in lymphoma cells from diseased ITK-SYK transgenic mice. Shown are *IS$^{+/-}$CD4Cre* (60,66,197,209) and *Mcl-1$^{fl/+}$IS$^{+/-}$CD4Cre* (198,212,222,226,264) mice. (C) QPCR on *Bcl-x$_L$* mRNA in lymphoma cells of diseased *ISCD4Cre* (white dots, n=3), *Mcl-1$^{fl/+}$IS$^{+/-}$CD4Cre* (black and white dots, n=6) and *Mcl-1$^{fl/fl}$IS$^{+/-}$CD4Cre* (black dots, n=2) mice. (D) qPCR on *Bcl-2* mRNA in lymphoma cells of diseased *IS$^{+/-}$CD4Cre* (white dots, n=3), *Mcl-1$^{fl/+}$IS$^{+/-}$CD4Cre* (black and white dots, n=6) and *Mcl-1$^{fl/fl}$IS$^{+/-}$CD4Cre* (black dots, n=2) mice.

5.3 The role of *Mcl-1* for the chemosensitivity of T-NHL cells

5.3.1 Heterozygous deletion of *Mcl-1* sensitizes T-NHL cells to chemotherapeutic treatment *ex vivo*

To test the ability of MCL-1 and BCL-X_L to protect lymphoma cells from apoptosis induced by external stimulation, T-NHL cells were subjected to standard chemotherapeutic drugs used for the treatment of various subtypes of T-NHL. Cell survival was measured after 48 hours of treatment and the half maximal inhibitory concentration (IC50) was calcuated. *Mcl-1*$^{fl/+}$*CreER* T-NHL cells co-treated with tamoxifen (TMX) to induce MCl-1 deletion, showed reduced IC50 values for all chemotherapeutics used, in comparison to the mock treated cells (Table 5.1). Mock treated cells were resistant to cyclophosphamide and etoposide, which was overcome by deletion of one allele of *Mcl-1*. Deletion of *Bcl-x*$_L$ in addition to chemotherapeutical treatment lead to a reduced IC50 for doxorubicine. The remaining chemotherapeutics showed no enhanced effect upon *Bcl-x*$_L$ deletion. This was also the case for *CreER* T-NHL cells, where no target gene is deleted upon Cre induction. Within these cells, no chemotherapeutic drug showed significant changes of IC50 upon Cre induction.

Next was to see, whether chemotherapeutic induced death is affected by the expression of Cre over time. For this purpose, *CreER* T-NHL were treated with the chemotherapeutic drugs from table 5.1 and co-treated either with mock or TMX. Viability was measured 0, 12, 24, 48, 72 and 96 hours after administration. T-NHL cells were treated with the respective concentration of chemotherapeutic that showed the most significant difference between TMX and vehicle control in the titration experiments. Mock or TMX treatment had, consistent with the results from chemotherapeutic titration, no influence on sensitivity of *CreER* T-NHL cells to chemotherapy (Figure 5.14).

In contrast, *Mcl-1$^{fl/+}$CreER* T-NHL cells showed significantly reduced viability upon cyclophosphamide (CYCLO), doxorubicine (DOXO) and etoposide (ETO) treatment over time when *Mcl-1* deletion was induced (Figure 5.15). Treatment with dexamethasone (DEXA) and vincristine (VCR) efficiently killed the T-NHL cells independently of *Mcl-1* deletion. Complete deletion of *Bcl-x$_L$* in *Bcl-x$_L^{fl/fl}$CreER* T-NHL cells significantly increased the number of apoptotic cell compared to Mock treated cells, with the exception of dexamethasone, where deletion of *Bcl-x$_L$* did not affect the rate of cell death (Figure 5.16).

T-NHL Genotype	Treatment (48 h)	EtOH (in nM)	TMX (in nM)
Mcl-1$^{fl/+}$CreER	**Dexamethasone**	1,4	0,9
	Vincristine	4,3	1,5
	Cyclophosphamide	> 100	0,01
	Doxorubicine	3,2	0,2
	Etoposide	43,6	1,0
Bcl-x$_L^{fl/fl}$ CreER	**Dexamethasone**	1,6	1,4
	Vincristine	1,5	1,3
	Cyclophosphamide	> 100	> 100
	Doxorubicine	30,4	10,2
	Etoposide	43,9	45,7
CreER	**Dexamethasone**	13,0	18,0
	Vincristine	0,8	1,5
	Cyclophosphamide	> 100	> 100
	Doxorubicine	2,0	1,7
	Etoposide	34,2	32,9

Table 5.1 IC50 of chemotherapeutics after 48 hours of treatment. The table shows the half maximal inhibitory concentrations of different chemotherapeutic drugs in nM. The first row indicates the genotype of the treated T-NHL cells, the second row the chemotherapeutics used, the last two rows show the IC50 value in cells, co-treated with Ethanol (mock; third row) or with 4`OH-Tamxifen (TMX, forth row).

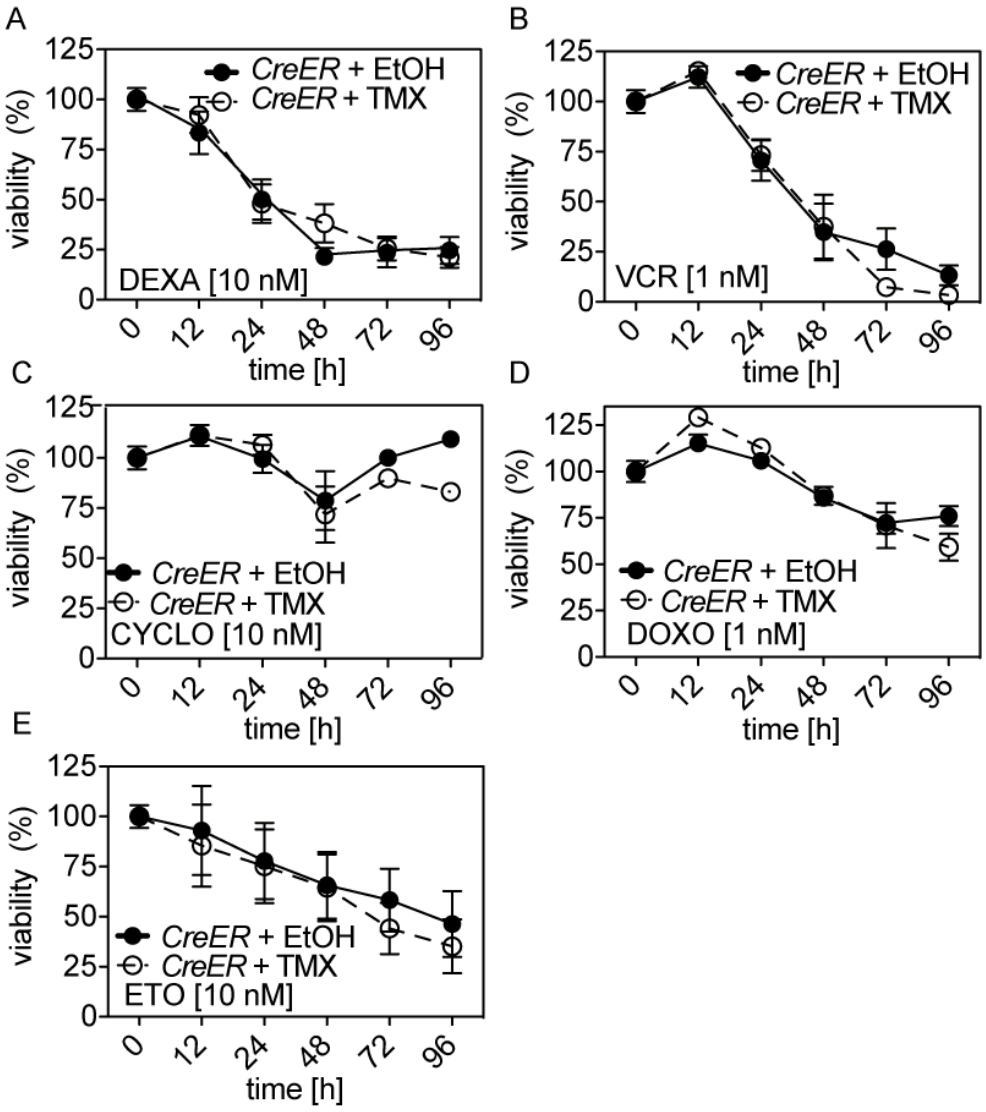

Figure 5.14 Viability of T-NHL cells after exposure to chemotherapeutic drugs without additional target gene deletion. *CreER* T-NHL cells were treated with (A) 1 nM dexamethasone (DEXA), (B) 1 nM vincristine (VCR), (C) 10 nM cyclophosphamide (CYCLO), (D) 1 nM doxorubicine (DOXO) or (E) 10 nM etoposide (ETO). The black dots represent T-NHL cells co-treated with Ethanol (mock), the white dots depict co-treatment with 4´OH-tamoxifen (TMX). Shown are mean ± SEM of three independent experiments with three replicates each. Analysis was done with unpaired t-test and asterisks denote significant differences (*p< 0,05, ** p< 0,005; ***p< 0,0005).

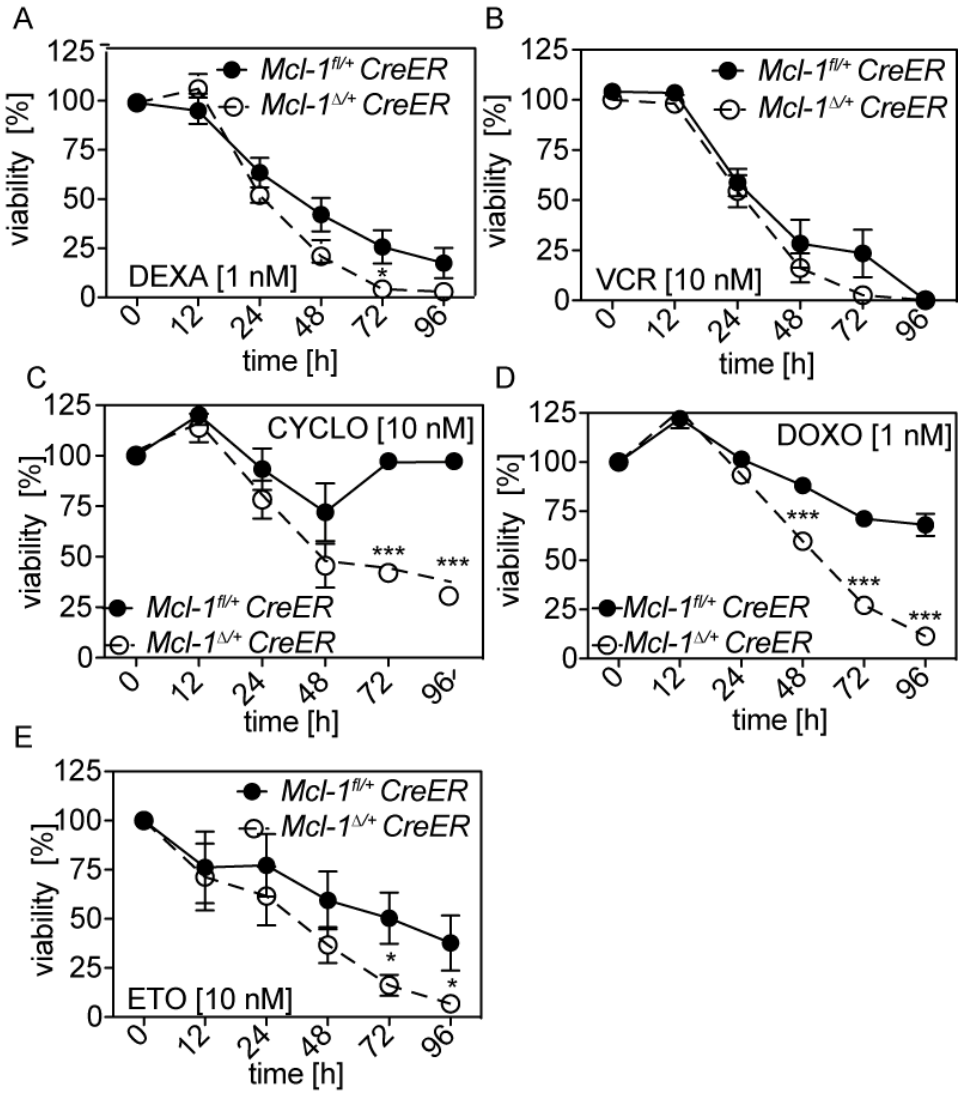

Figure 5.15 Viability of T-NHL cells after exposure to chemotherapeutic drugs and heterozygous deletion of *Mcl-1*. *Mcl-1$^{fl/+}$CreER* T-NHL cells were treated with (A) 1 nM dexamethasone (DEXA), (B) 1 nM vincristine (VCR), (C) 10 nM cyclophosphamide (CYCLO), (D) 1 nM doxorubicine (DOXO) or (E) 10 nM etoposide (ETO). The black dots represent T-NHL cells co-treated with Ethanol (mock). The white dots depict co-treatment with 4´OH-tamoxifen (TMX). Shown are mean ± SEM of three independent experiments with three replicates each; statistical analysis was done with unpaired t-test (*p < 0,05, **p < 0,005, ***p < 0,0005).

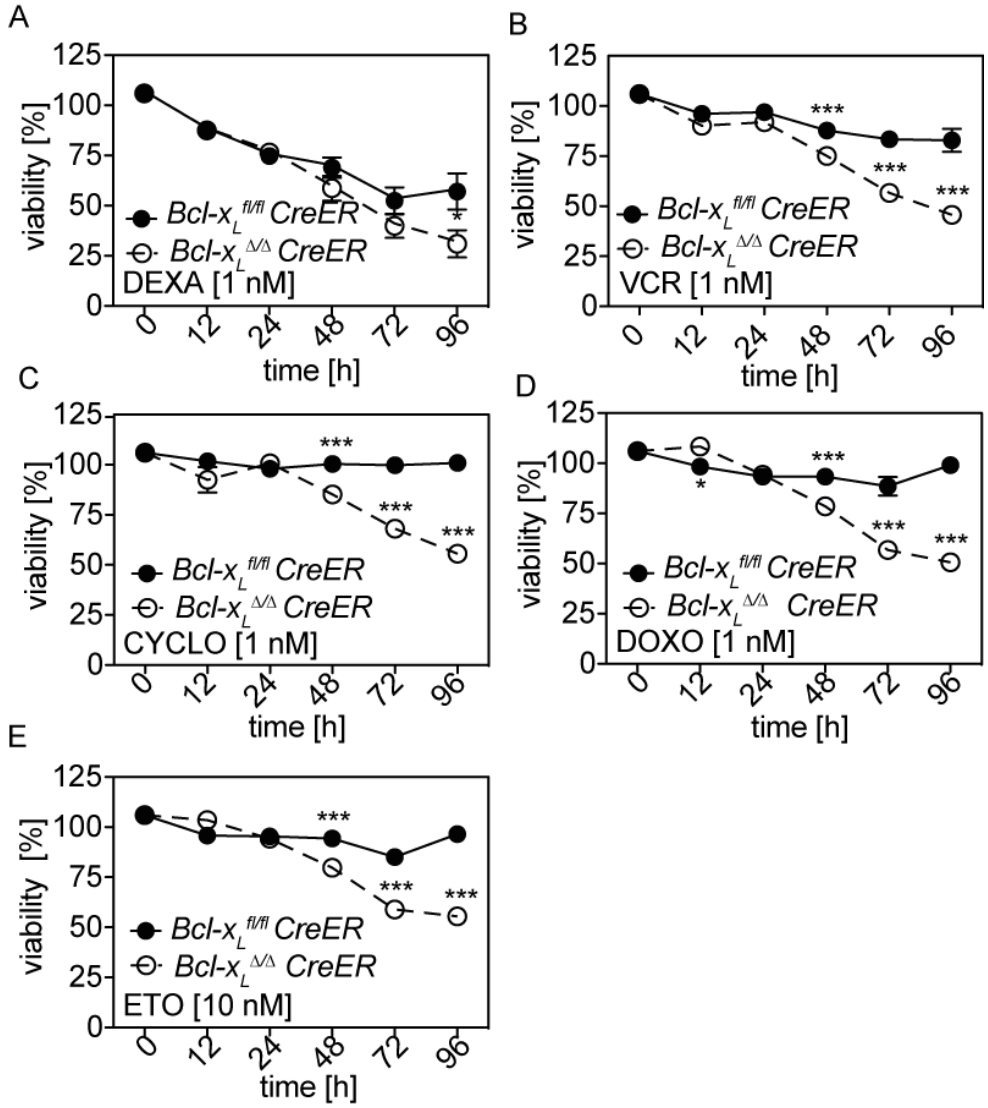

Figure 5.16 Viability of T-NHL cells with and without *Bcl-x$_L$* deletion after exposure to chemotherapeutic drugs. *Bcl-x$_L^{fl/fl}$CreER* T-NHL cells were treated with (A) 1 nM dexamethasone (DEXA), (B) 1 nM vincristine (VCR), (C) 10 nM cyclophosphamide (CYCLO), (D) 1 nM doxorubicine (DOXO) or (E) 10 nM etoposide (ETO). The black dots represent T-NHL cells co-treated with Ethanol (mock). The white dots depict co-treatment with 4´OH-tamoxifen (TMX). Shown are mean ± SEM of three independent experiments with three replicates each; statistical analysis was done with unpaired t-test (*p < 0,05, **p < 0,005, ***p < 0,0005).

5.3.2 Heterozygous deletion of *Mcl-1* sensitizes T-NHL cells to chemotherapeutic treatment *in vivo*

As shown in Figure 5.15, the heterozygous deletion of *Mcl-1* in T-NHL cells significantly increased their sensitivity to doxorubicine (DOXO) treatment *ex vivo*. So next was to investigate the *in vivo* effect of *Mcl-1* deletion on the clinical outcome of T-NHL burdened mice treated with DOXO. To this end, C57BL/6 mice were transplanted with *Mcl-1*$^{fl/+}$*CreER* T-NHL cells and treated as illustrated in Figure 5.17. To monitor the effect of DOXO and *Mcl-1* deletion, PET-CT was performed before and after TMX and DOXO administration. *Mcl-1*$^{fl/+}$*CreER* T-NHL burdened mice showed strong infiltration of tumor cells in the spleens, lymph nodes and bone marrow 16 days after transplantation of T-NHL cells, measured by PET-CT on FDG-uptake (Figure 5.18). When treated with TMX and DOXO, FDG uptake was extenuated in some areas (Figure 5.18 A). This reduction was absent in T-NHL-burdened mice that were co-treated with mock instead of TMX. Here the signal intensities of FDG showed no regression after chemotherapeutic treatment (Figure 5.18 B). The fold change of FDG uptake before and after DOXO treatment showed a significant difference between mice that received only DOXO and mice that were co-treated with TMX and therefore harbored *Mcl-1*$^{\Delta/+}$*CreER* T-NHL cells (Figure 5.18 C). Mice with *Mcl-1*$^{fl/+}$*CreER* T-NHL cells showed an increased PET signal after DOXO treatment (1,4 ± 0,16) whereas mice with *Mcl-1*$^{\Delta/+}$*CreER* T-NHL cells showed a reduction of FDG-uptake (0,8 ± 0,16), which was a significant difference (p= 0,03) (Figure 5.18 C).

At day 18 after PET-CT analysis, all DOXO treated mice were sacrificed to see if FDG-uptake was linked to infiltration of lymphoid organs by T-NHL cells. Histological analysis of the spleens, livers, kidneys and bone marrow of the mice showed infiltration with CD3 positive cells (Figure 5.19 A). Mice that were treated with TMX (*Mcl-1*$^{\Delta/+}$*CreER*) showed less CD3 positive cells in all organs in comparison to mice treated with DOXO only (*Mcl-1*$^{fl/+}$*CreER*). Furthermore, TMX treated mice showed reduced splenomegaly (Figure 5.19 B), caused by a reduced infiltration of T cells, as confirmed by Flow Cytometry (Figure 5.19 C).

Flow Cytometry on TCRβ expression could furthermore substantiate a reduction of T cell infiltration in the lymph nodes and bone marrow (Figure 5.19 D and E). Kidneys from TMX treated mice also showed less infiltration with T cells, which was reflected by reduced kidney weight (Figure 5.19 F) and reduced numbers of TCRβ-positive cells (Figure 5.19 G). Lastly, T cell infiltration was also reduced in the liver (Figure 5.19 H).

To determine whether *Mcl-1* deletion in the T-NHL cells also influenced survival of T-NHL burdened mice, male C57BL/6 mice, transplanted with *Mcl-1*$^{fl/+}$*CreER* T-NHL cells were treated with DOXO and TMX or mock as described in Figure 5.17. Untreated mice (*Mcl-1*$^{fl/+}$*CreER*) died with a median survival of 22 days, which could be prolonged by TMX treatment (*Mcl-1*$^{\Delta/+}$*CreER*) to 23,5 days (Figure 5.20 A). When mice were treated with DOXO only (*Mcl-1*$^{fl/+}$*CreER*), median survival was 28 days. Upon co-treatment with TMX (*Mcl-1*$^{\Delta/+}$*CreER*) median survival was raised to 32,5 days with one mouse not succumbing to disease at all (Figure 5.20 B).

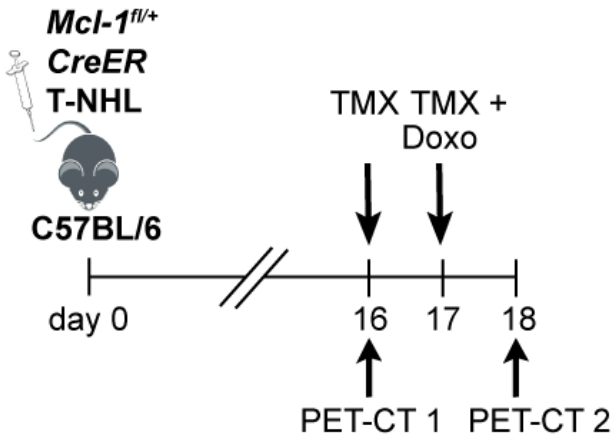

Figure 5.17 Schematic view of doxorubicine treatment and *Mcl-1* deletion *in vivo*. C57BL/6 mice were transplanted with 10^7 *Mcl-1*$^{fl/+}$*CreER* T-NHL cells. 16 days after transplantation, the first PET-CT was performed and mice were treated with 4 mg tamoxifen (TMX) by oral gavage. On day 17, mice received another dosage of TMX and 100 µg doxorubicine (DOXO) by i.p. Injection. On day 18 the second PET-CT was performed.

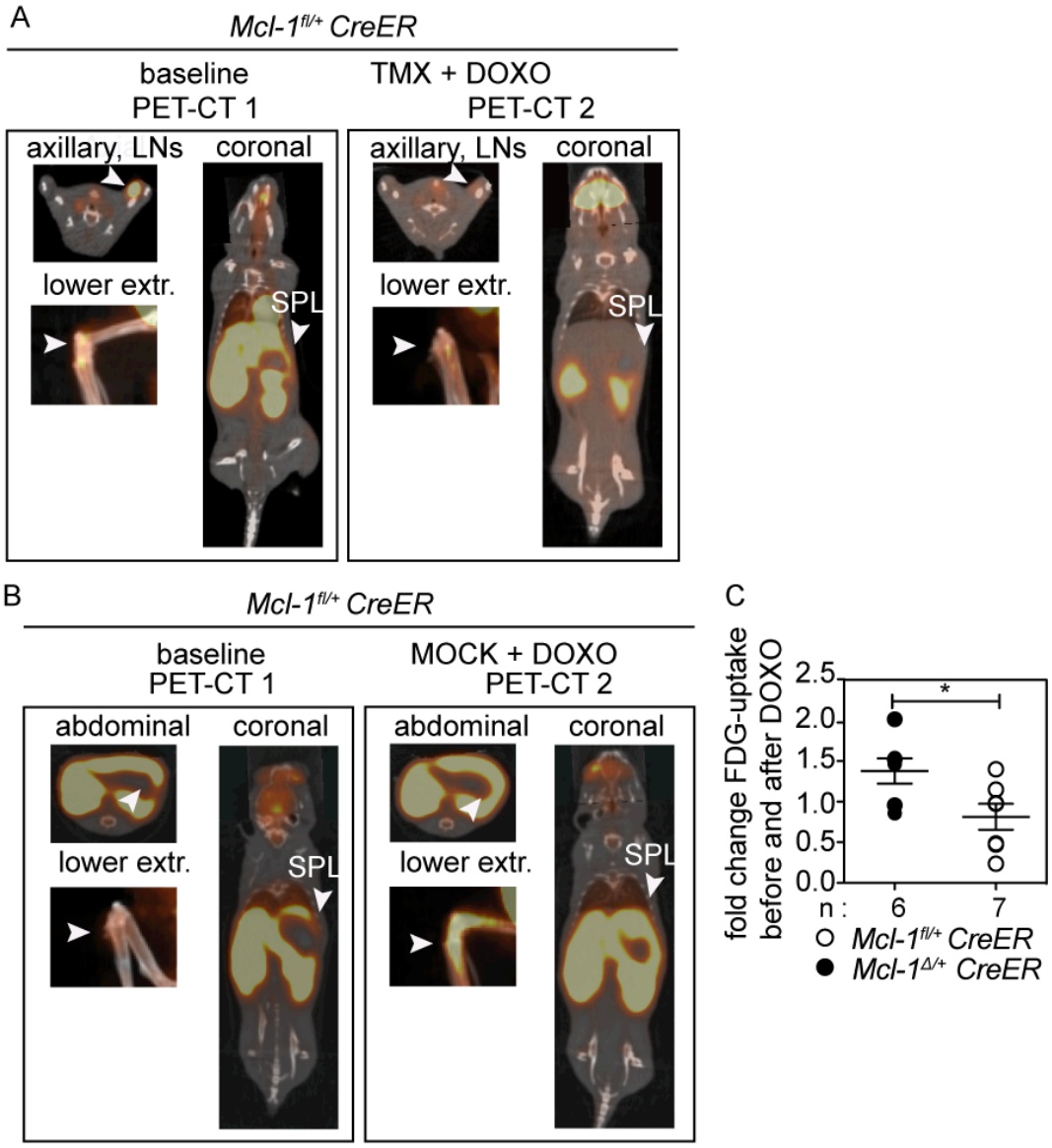

Figure 5.18 PET-CT of doxorubicine treated T-NHL burdened mice. (A) PET-CT of mice transplanted with 10^7 *Mcl-1$^{fl/+}$CreER* T-NHL cells. The left panel shows baseline PET-CT before treatment and the right panel shows the PET-CT of the same mouse after treatment with tamoxifen (TMX) and doxorubicine (DOXO). (B) PET-CT of mice transplanted with 10^7 *Mcl-1$^{fl/+}$CreER* T-NHL cells. The left panel shows baseline PET-CT before treatment and the right panel shows the PET-CT of the same mouse after treatment with mock and doxorubicine. (A) and (B) Shown are different organic systems, as described. White arrows indicate areas of interest. (C) Quantification of PET-CT signal intensities. Shown is the fold change of FDG-uptake before and after DOXO treatment. Black dots represent mice that received DOXO and mock (n = 6) and white dots represent

mice treated with DOXO and TMX (n = 7). Statistical analysis was done using unpaired t-test (p= 0,03).

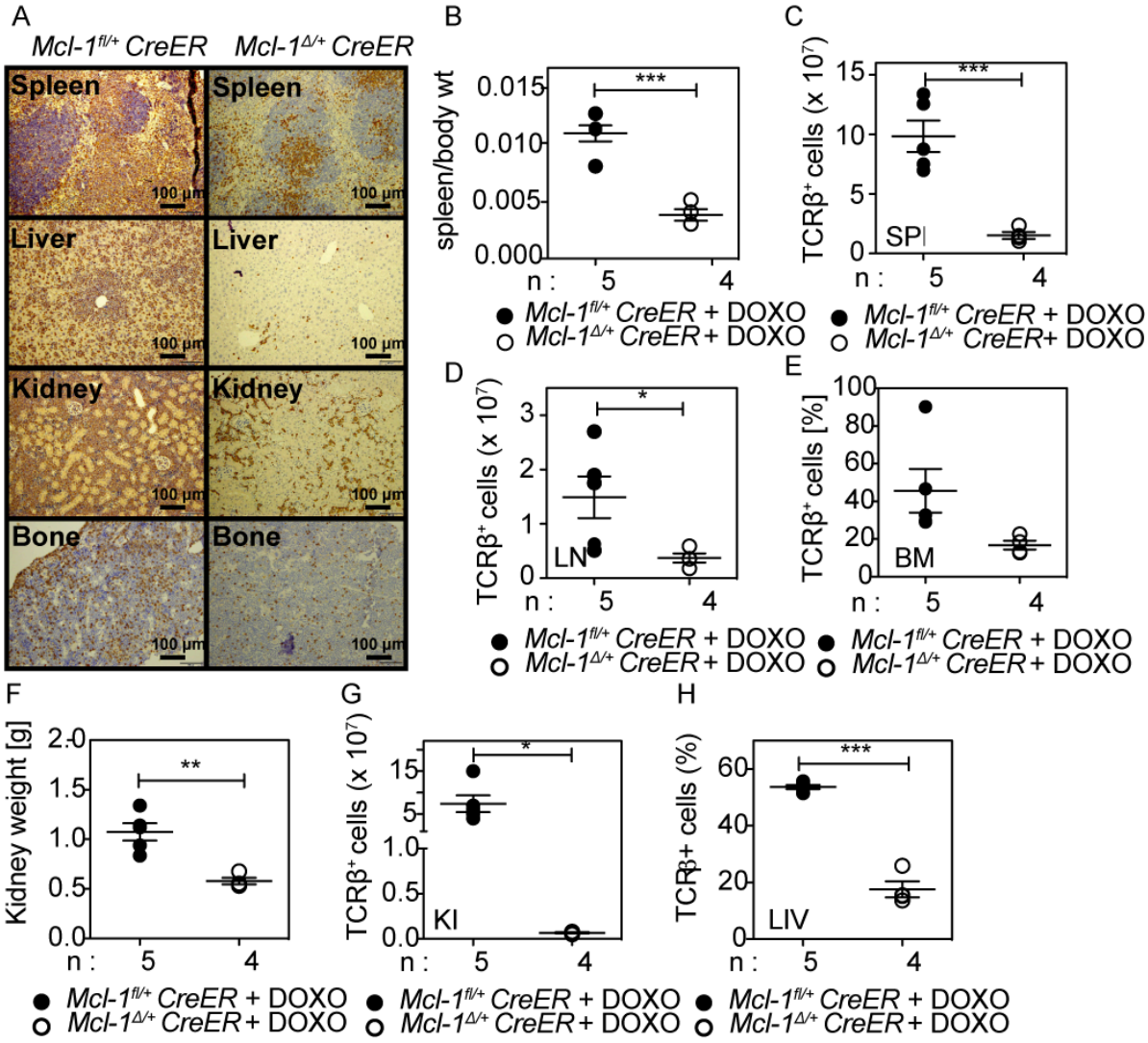

Figure 5.19 T cell infiltration of T-NHL burdened mice after Doxorubicine treatment. C57BL/6 mice, transplanted with *Mcl-1$^{fl/+}$CreER* T-NHL cells and either treated with doxorubicine (DOXO) alone or co-treated with tamoxifen (TMX), were sacrificed on day 18 after transplantation and the organs were screened for T cell infiltration. (A) Histological analysis of CD3 expression (brown dots) in the spleen, liver, kidney and bone marrow. The left panel shows one representative mouse that was only treated with DOXO (*Mcl-1$^{fl/+}$CreER*) and the right panel shows one representative mouse that received DOXO and TMX (*Mcl-1$^{\Delta/+}$CreER*) (B)-(H): analysis of mice, transplanted with *Mcl-1$^{fl/+}$CreER* T-NHL cells. Black dots represent mice that received only DOXO (*Mcl-1$^{fl/+}$CreER*) and white

dots represent mice that got DOXO and TMX (*Mcl-1*$^{\Delta/+}$*CreER*). Statistical analysis was done with unpaired t-test. Asterisks denote significant differences (*p< 0,05, ** p< 0,005; ***p< 0,0005). (*p < 0,05, **p < 0,005, ***p < 0,0005). B) Spleen to body weight ratio (C) Absolute number of T cells in the spleen (SPL), (D) Absolute T cell numbers in the lymph nodes (LN), (E) Relative T cell numbers in the bone marrow (BM), (F) Kidney weight (G) Absolute T cell numbers in the kidney (KI), (H) Relative T cell numbers in the liver (LIV)

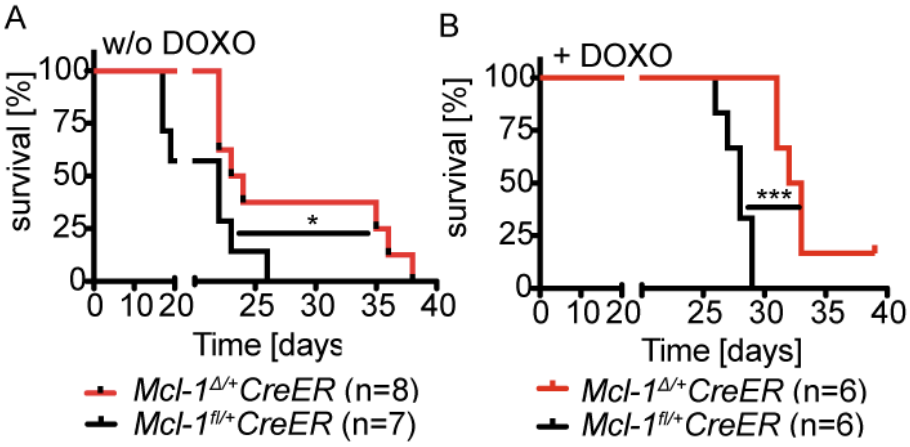

Figure 5.20 Survival of T-NHL burdened mice after doxorubicine treatment. (A) Kaplan-Meier survival curves of male C57BL/6 mice, transplanted with *Mcl-1*$^{fl/+}$*CreER* T-NHL cells and treated with tamoxifen (TMX) (red, n=8; median survival 23,5 days) or mock (black; n=7; median survival: 22 days). Statistical analysis was done with Mantle-Cox test (p=0,04). (B) Kaplan-Meier survival curves of male C57BL/6 mice, transplanted with *Mcl-1*$^{fl/+}$*CreER* T-NHL cells and treated with doxorubicine (DOXO) and co-treated with TMX (red; n=6; median survival: 32,5 days) or mock (black; n=6; median survival: 28 days). Statistical analysis was done with Mantle-Cox test (p=0,0008).

5.4 *Mcl-1* deletion in normal lymphocytes

5.4.1 Complete *Mcl-1* deletion leads to disrupted spleen structure

To examine whether *Mcl-1* inhibition would provoke severe toxicity for normal lymphocytes, *Mcl-1*$^{fl/+}$*CreER* and *Mcl-1*$^{fl/fl}$*CreER* mice were treated with tamoxifen (TMX) to induce target gene deletion in all kinds of tissues. Deletion of both alleles of *Mcl-1* lead to a substantial clinical deterioration of *Mcl-1*$^{fl/fl}$*CreER* mice, which had to be sacrificed three days after TMX treatment whereas *Mcl-1*$^{fl/+}$*CreER* mice remained unaffected. When analyzed, *Mcl-1*$^{\Delta/\Delta}$*CreER* mice exhibited reduced spleen sizes, a tendency also observed in *Mcl-1*$^{\Delta/+}$*CreER* mice that was, however, less profound (Figure 5.21 A and B). Histological analysis of the spleens showed no structural abnormalities by H&E staining in *Mcl-1*$^{\Delta/+}$*CreER* mice whereas full genetic deletion of *Mcl-1* caused substantial structural spleen damage (Figure 5.21 C). Furthermore there was an increase of cleaved CASPASE 3 upon complete *Mcl-1* deletion. CD3 staining showed no reduction of signal upon *Mcl-1* deletion (Figure 5.21 C).

.

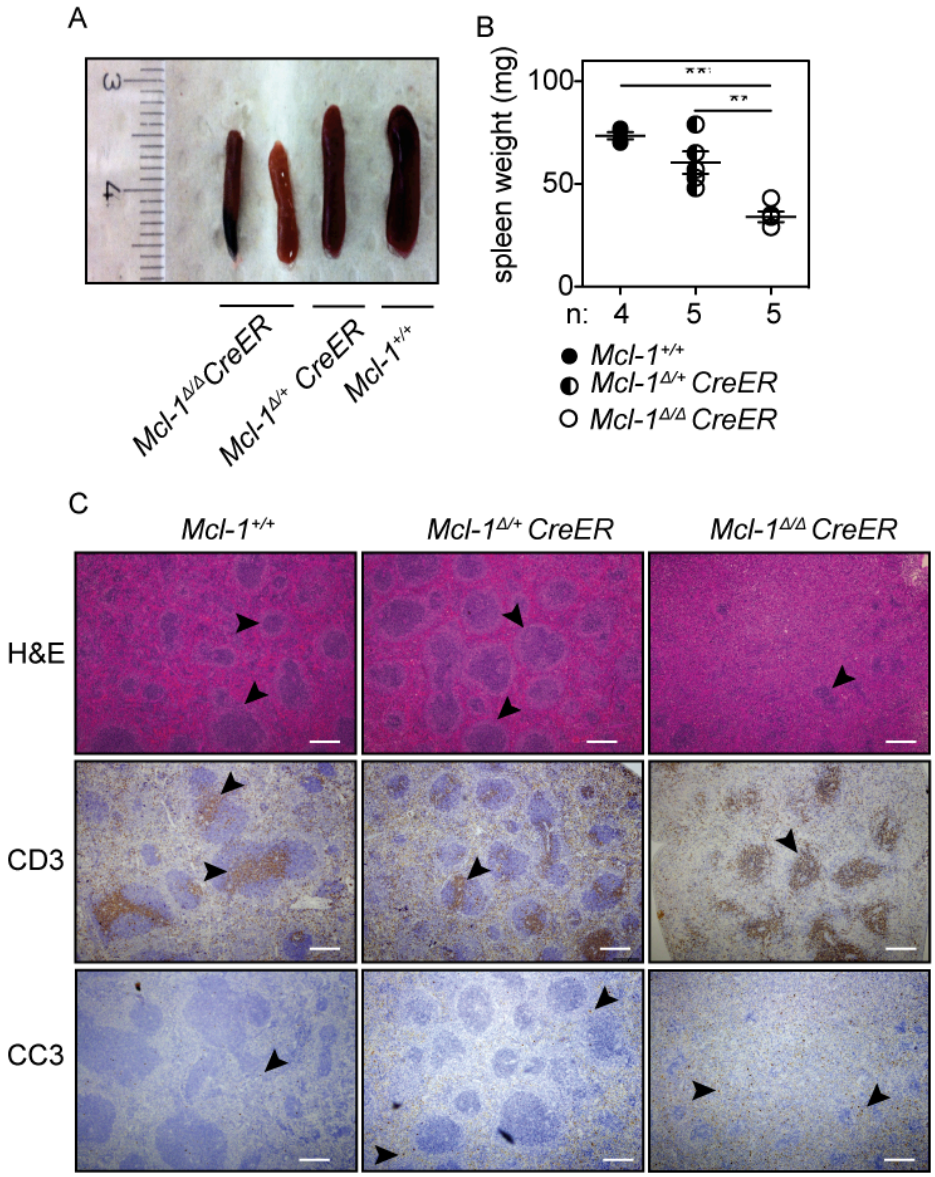

Figure 5.21 Effect of homo- and heterozygous *Mcl-1* deletion on the spleen structure. (A) Spleens of *Mcl-1*$^{fl/fl}$*CreER*, *Mcl-1*$^{fl/+}$*CreER* and wild type mice, treated with tamoxifen (TMX) and sacrificed on day 3 after treatment. (B) Spleen weight of TMX treated mice. Shown are *Mcl-1*$^{+/+}$ mice (black dots, n = 4), *Mcl-1*$^{fl/+}$*CreER* (*Mcl-1*$^{\Delta/+}$*CreER*, black/white dots, n = 5) and *Mcl-1*$^{fl/fl}$*CreER* mice (*Mcl-1*$^{\Delta/\Delta}$*CreER*, white dots, n =5). Statistical analysis was done with unpaired t-test and asterisks denote significant differences (*p< 0,05, ** p< 0,005; ***p< 0,0005). (C) Histological analysis of spleens of three representative mice with the indicated genotypes after TMX treatment. The upper panel shows H & E staining, the medial panel shows CD3 staining and the lower panel cleaved Caspase 3. White bars represent 200 µm.

5.4.2 Heterozygous *Mcl-1* deletion does not influence T cell numbers *in vivo*

MCL-1 plays an important role for the development and survival of normal lymphocytes (2,28). Complete deletion of *Mcl-1* leads to a massive loss of thymocytes as well as mature T cells in the lymph nodes and spleen (28). Therefore the effect of heterozygous deletion of *Mcl-1* on T cell numbers was examined. T cell numbers of *Mcl-1*$^{\Delta/\Delta}$*CreER* mice were significantly reduced in comparison to *Mcl-1*$^{+/+}$ and *Mcl-1*$^{\Delta/+}$*CreER* mice, whereas the later did not show significant differences in comparison to the wild type control (Figure 5.22 A). The lymph nodes also showed a decrease in T cell numbers of *Mcl-1*$^{\Delta/\Delta}$*CreER* mice and an increase in *Mcl-1*$^{\Delta/+}$*CreER* mice, compared to *Mcl-1*$^{+/+}$ mice (Figure 5.22 B). T cell numbers in the thymus showed to be heterogeneous, but again there was a significant reduction of T cell numbers in *Mcl-1*$^{\Delta/\Delta}$*CreER* mice, which was not seen in *Mcl-1*$^{\Delta/+}$*CreER* mice (Figure 5.22 C). Analysis of peripheral blood (PB) did not show any differences in relative T cell numbers between the different genotypes (Figure 5.22 D). The bone marrow (BM), in contrast, showed a significant increase in relative T cell numbers in *Mcl-1*$^{\Delta/\Delta}$*CreER* mice, compared to *Mcl-1*$^{+/+}$ and *Mcl-1*$^{\Delta/+}$*CreER* mice (Figure 5.22 E). To exclude that there might be any more severe long-term effects on T cells when one allele of *Mcl-1* is deleted, *Mcl-1*$^{\Delta/+}$*CreER* mice were analyzed four weeks after TMX treatment. T cell numbers in the spleens of *Mcl-1*$^{\Delta/+}$*CreER* mice were significantly reduced in comparison to *Mcl-1*$^{+/+}$ mice (Figure 5.23 A). In contrast, lymph nodes (LN; Figure 5.23 B), thymus (THY; Figure 5.23 C), blood (PB; Figure 5.23 D) and bone marrow (BM Figure 5.23 E) showed no differences in T cell numbers.

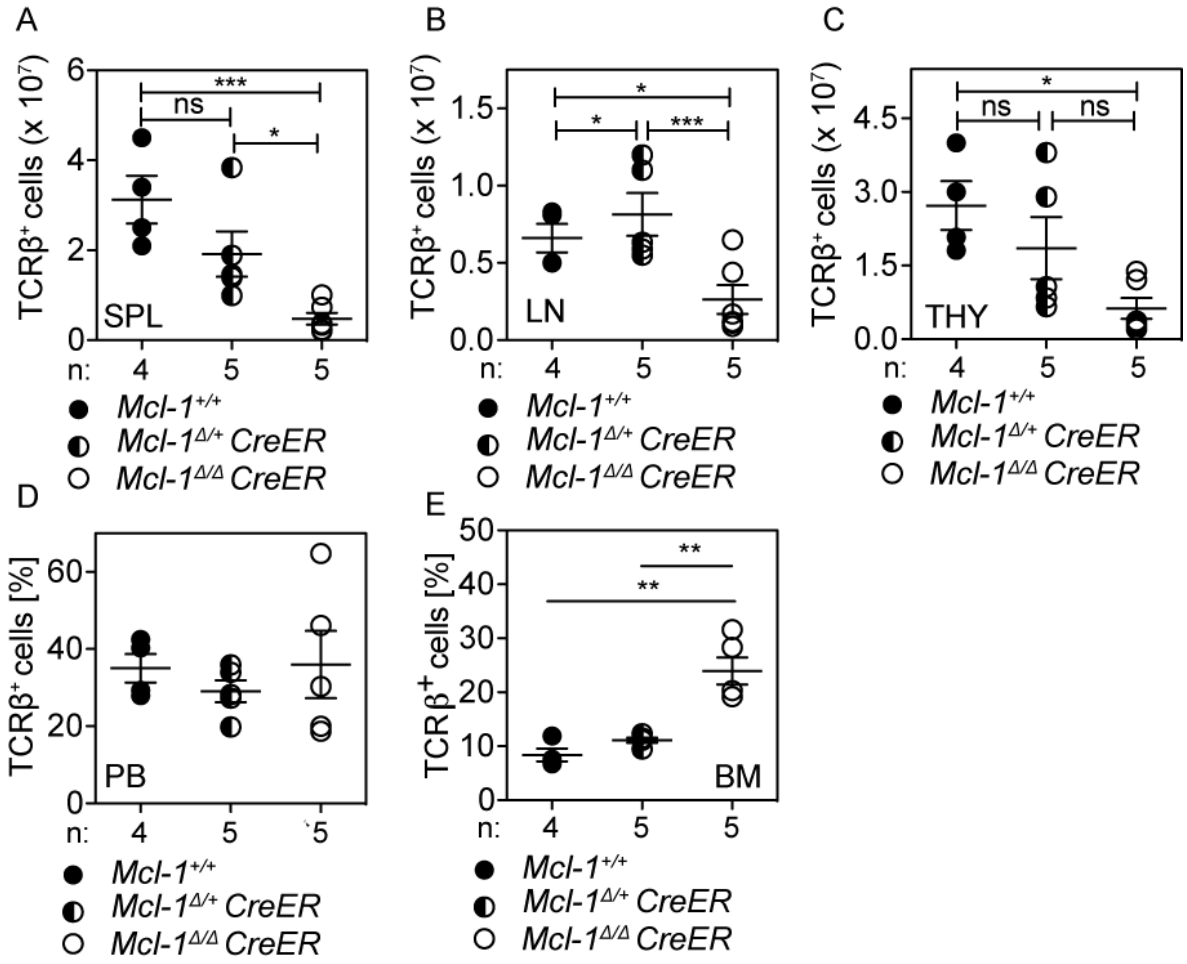

Figure 5.22 Effect of homo- and heterozygous *Mcl-1* deletion on T cell numbers. (A)-(E) T cell numbers of tamoxifen (TMX) treated mice after 3 days of treatment. The black dots show wild type (*Mcl-1*$^{+/+}$), the black-white dots show *Mcl-1*$^{fl/+}$*Cre* (*Mcl-1*$^{\Delta/+}$*CreER*) and the white dots *Mcl-1*$^{fl/fl}$*CreER* (*Mcl-1*$^{\Delta/\Delta}$*CreER*) mice treated with TMX. Statistical analysis was done by unpaired t-test and asterisks denote significant differences (*p < 0,05, **p < 0,005, ***p < 0,0005). (A) Absolute T numbers of the spleen (SPL) (B) Absolute T cell numbers in the lymph nodes (LN) (C) Absolute T cell numbers in the thymus (THY) (D) Relative T cell numbers in the blood (PB) (E) Relative T cell numbers in the bone marrow (BM).

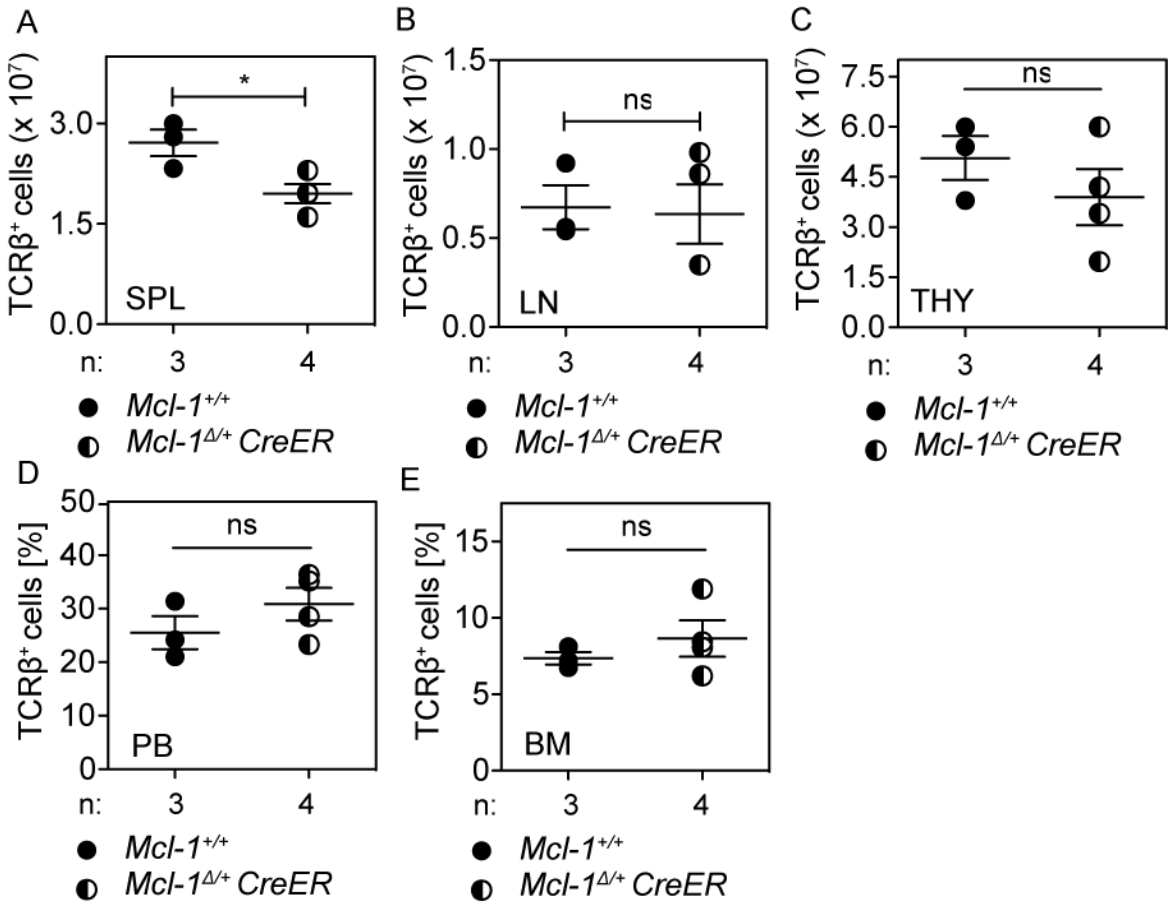

Figure 5.23 Long-term effect of heterozygous *Mcl-1* deletion on T cell numbers. (A)-(E) T cell numbers in different organs of tamoxifen (TMX) treated mice. Black dots show Wild type (*Mcl-1*$^{+/+}$) mice and black-white dots show *Mcl-1*$^{fl/+}$*CreER* (*Mcl-1*$^{\Delta/+}$*CreER*) mice. Statistical analysis was done with unpaired t-test and asterisks denote significant differences (*p < 0,05, **p < 0,005, ***p < 0,0005). (A) Absolute T cell numbers in the spleen (SPL) (B) Absolute T cell numbers in the lymph nodes (LN) (C) Absolute T cell numbers in the thymus (THY) (D) Relative T cell numbers in the blood (PB) (E) Relative T cell numbers in the bone marrow (BM).

5.4.3 Heterozygous *Mcl-1* deletion leads to reduction of B cells *in vivo*

The spleens of *Mcl-1*$^{\Delta/\Delta}$*CreER* mice showed disrupted structure and decreased size (Figure 5.21), which was not primarily due to the reduction of T cell numbers (Section 5.4.2). As mentioned before, homozygous deletion of *Mcl-1* impairs also B cell maintenance (28). To compare the effect of heterozygous *Mcl-1* deletion on B cells, *Mcl-1*$^{+/+}$, *Mcl-1*$^{fl/fl}$*Cre* and *Mcl-1*$^{fl/+}$*CreER* mice were treated with tamoxifen (TMX) and analyzed for B cells numbers. The spleens of *Mcl-1*$^{\Delta/\Delta}$*CreER* mice showed a complete loss of B cells whereas *Mcl-1*$^{\Delta/+}$*CreER* had reduced B cell numbers in comparison to wild type mice (Figure 5.24 A). B cell numbers of lymph nodes (LN; Figure 5.24 B), blood (PB; Figure 5.24 C) and bone marrow (BM; Figure 5.24 D) from *Mcl-1*$^{\Delta/+}$*CreER* mice showed no significant difference in comparison to *Mcl-1*$^{+/+}$ mice. B cells from *Mcl-1*$^{\Delta/\Delta}$*CreER* mice instead, were significantly reduced in all organs (Figure 5.24).

To determine the long-term effect of heterozygous *Mcl-1* deletion on B cell survival, mice were analyzed 4 weeks after TMX administration and B cell numbers collected. *Mcl-1*$^{\Delta/+}$*CreER* mice still exhibited a reduction of B cells in the spleen (SPL; Figure 5.25 A), whereas lymph nodes (LN; Figure 5.25 B), blood (PB; Figure 5.25 C) and bone marrow (BM; Figure 5.25 D) showed no reduction in B cell numbers.

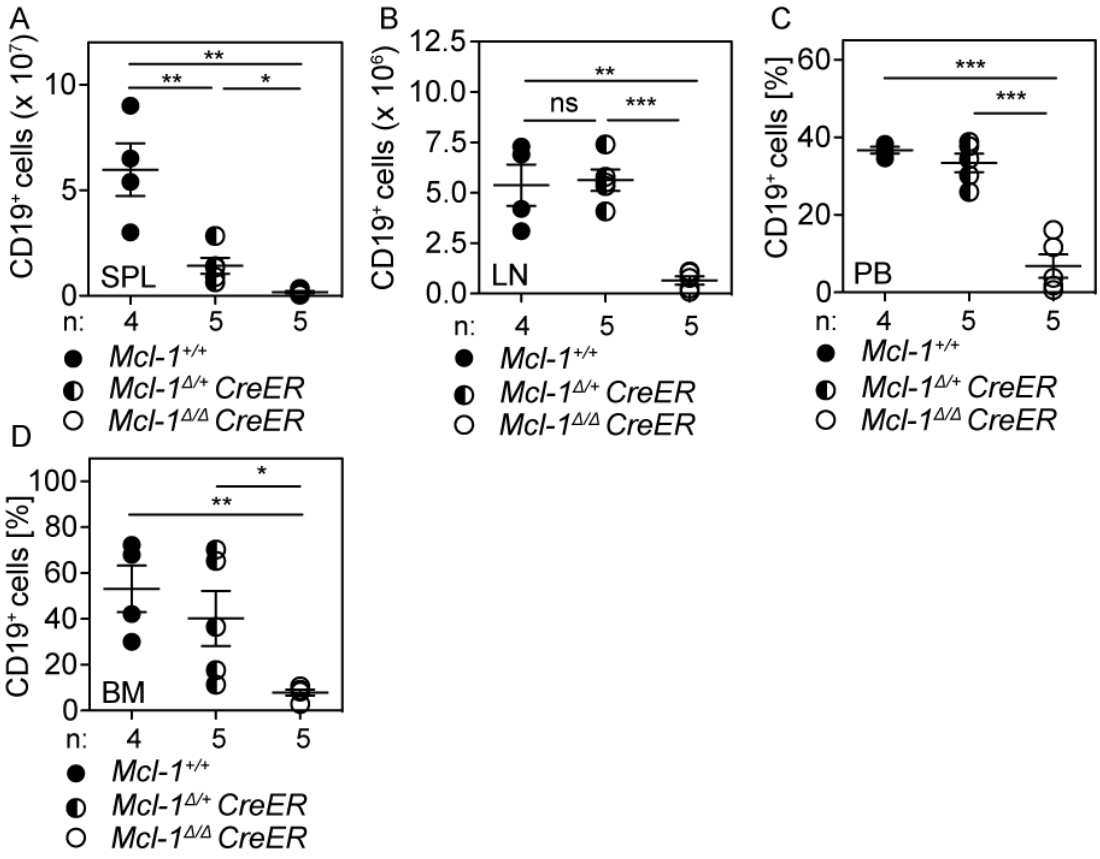

Figure 5.24 Effect of *Mcl-1* deletion on B cell numbers. (A)- (D) B cell ($CD19^+$) numbers in tamoxifen (TMX) treated mice after 3 days of treatment. The black dots show wild type (*Mcl-1*$^{+/+}$) the black-white dots show *Mcl-1*$^{fl/+}$*Cre* (*Mcl-1*$^{\Delta/+}$*CreER*) and the white dots *Mcl-1*$^{fl/lf}$*CreER* (*Mcl-1*$^{\Delta/\Delta}$*CreER*) mice treated with TMX. Statistical analysis was done with unpaired t-test (*p < 0,05, **p < 0,005, ***p < 0,0005). (A) Absolute B cell numbers in the spleen (SPL) (B) absolute B cell numbers in the lymph nodes (LN) (C) relative B cell numbers in the blood (PB) (D) relative B cell number in the bone marrow (BM).

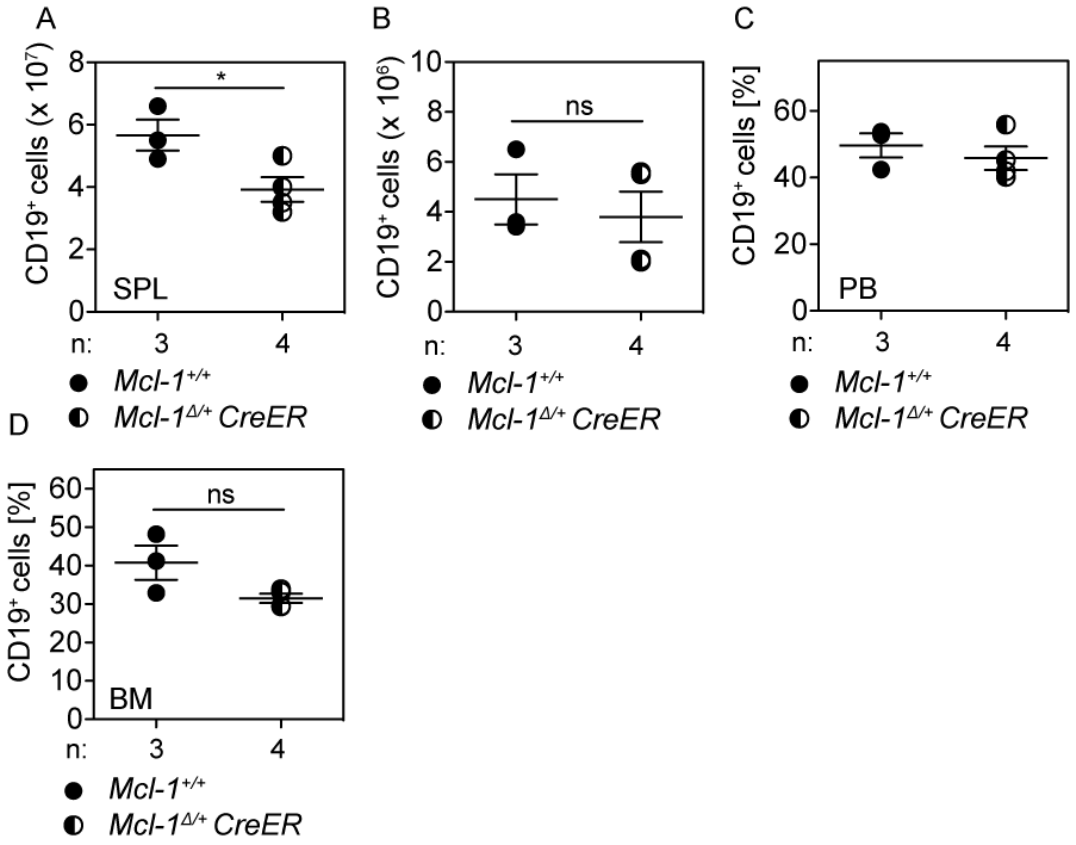

Figure 5.25 Long-term effect of heterozygous *Mcl-1* deletion on B cell numbers. (A)-(D) B cell numbers ($CD19^+$) in different organs of tamoxifen (TMX) treated mice, 4 weeks after treatment. Black dots show wild type (*Mcl-1*$^{+/+}$) mice and black-white dots show *Mcl-1*$^{fl/+}$*CreER* (*Mcl-1*$^{\Delta/+}$*CreER*) mice treated with TMX. Statistical analysis was done with unpaired t-test and asterisks denote significant differences (*p < 0,05, **p < 0,005, ***p < 0,0005). (A) Absolute B cell numbers in the spleen (SPL (B) Absolute B cell numbers in the lymph nodes (LN) (C) Relative B cell numbers in the blood (PB) (D) Relative B cell numbers in the bone marrow (BM)**.**

5.5 The role of MCL-1 in human T-NHL cell lines

5.5.1 The effect of BIM_S-constructs on the viability of human T-NHL cell lines

As shown in sections 5.1 to 5.3, reduction of MCL-1 levels was able to impair the viability of murine T-NHL cells *in vitro* and *in vivo*. To test whether MCL-1 has the same impact on human T-NHL cells, three human cutaneous T cell lymphoma (CTCL) cell lines (HH, Hut-78 and MyLa) and one T cell leukemia cell line (Jurkat) were transduced with doxycycline (DOX)-inducible BIM_S-constructs. These constructs exhibit different binding affinities for the individual Bcl-2 proteins due to modified BH3-regions (149). BIM_SWT is able to bind to all anti-apoptotic Bcl-2 proteins, whereas BIM_S2A selectively binds to MCL-1 and BIM_SBAD captures BCL-2, BCL-W and BCL-X_L. BIM_S4E functions as mock control because it does not bind any of the Bcl-2 proteins (Figure 5.26 A).

The different CTCL cell lines exhibited distinct expression patterns of anti-apoptotic Bcl-2 proteins with MCL-1 being most highly expressed in Hut-78, whereas BCL-X_L was highly expressed in HH and Hut-78. BCL-W, in contrast, was weakly expressed in HH and Hut-78 and BCL-2 was high in the T cell leukemia cell line Jurkat, intermediate in HH and Hut-78 and low in MyLa cells (Figure 5.26 B). After the cells were transduced with the BIM_S constructs, DOX treatment lead to induced BIM expression, shown in HUT-78 CTCL cells (Figure 5.26 C).

To test the impact of MCL-1 in comparison to the other BCL-2 proteins, the four human cell lines were transduced with the BIM_S constructs and treated with DOX to induce ectopic BIM_S-expression. Viability was measured after 48 hours, normalized to mock treated cells and depicted as percentage.
After DOX treatment for 48 hours, Hut-78 showed a significant loss of viability when the cells were transduced with BIM_SWT (60,8 ± 3,5%) BIM_S2A (62,6 ± 2,5%) or BIM_SBAD (63,9 ± 4,1%) whereas BIM_S4E had no impact on viability (95,8 ± 4,0%)

(Figure 5.27 A). The reduction of viability was similar for all constructs, resulting in about 60% viability compared to untreated cells.

MyLa were highly sensitive to induction of BIM_SWT by DOX treatment (45,3 ± 4,5%), which was significant different to BIM_S2A (90,3 ± 2,8%; p < 00001) and BIM_SBAD (65,4 ± 5,0%; p = 0,006). Furthermore viability showed to be more impaired by BIM_SBAD than by BIM_S2A (p = 0,0002) (Figure 5.27 B).

HH exhibited reduced viability upon treatment with DOX for all BIM_S constructs, also BIM_S4E (67,4 ± 1,4%) (Figure 5.27 C). Only BIM_S2A lead to a significant decrease in comparison to BIM_S4E (63,0 ± 1,4% vs 67,4 ± 1,4%; p= 0,04) and the effect on viability was furthermore stronger than that of BIM_SBAD (73,0 ± 3,0% vs 63,0 ± 1,4%; p = 0,006) (Figure 5.27 C) but not BIM_SWT (65.0 ± 2,7%; p = 0,5).

The sensitivity of Jurkat cells to BIM_SBAD induction (24,2 ± 3,0%) was comparable to BIM_SWT (19,6 ± 1,9%; p=0,2) and both showed a significant reduction compared to BIM_S4E transduced cells (109 ± 1,8%; p< 0,0001 for both). The effect of BIM_S2A was significantly less than BIM_SBAD (83,4 ± 0,9% vs 24,2 ± 3,0%; p<0,0001), but remained significant in comparison to BIM_S4E control (83,4 ± 0,9% vs 109,4 ± 1,8%; p< 0,0001) (Figure 5.27 D).

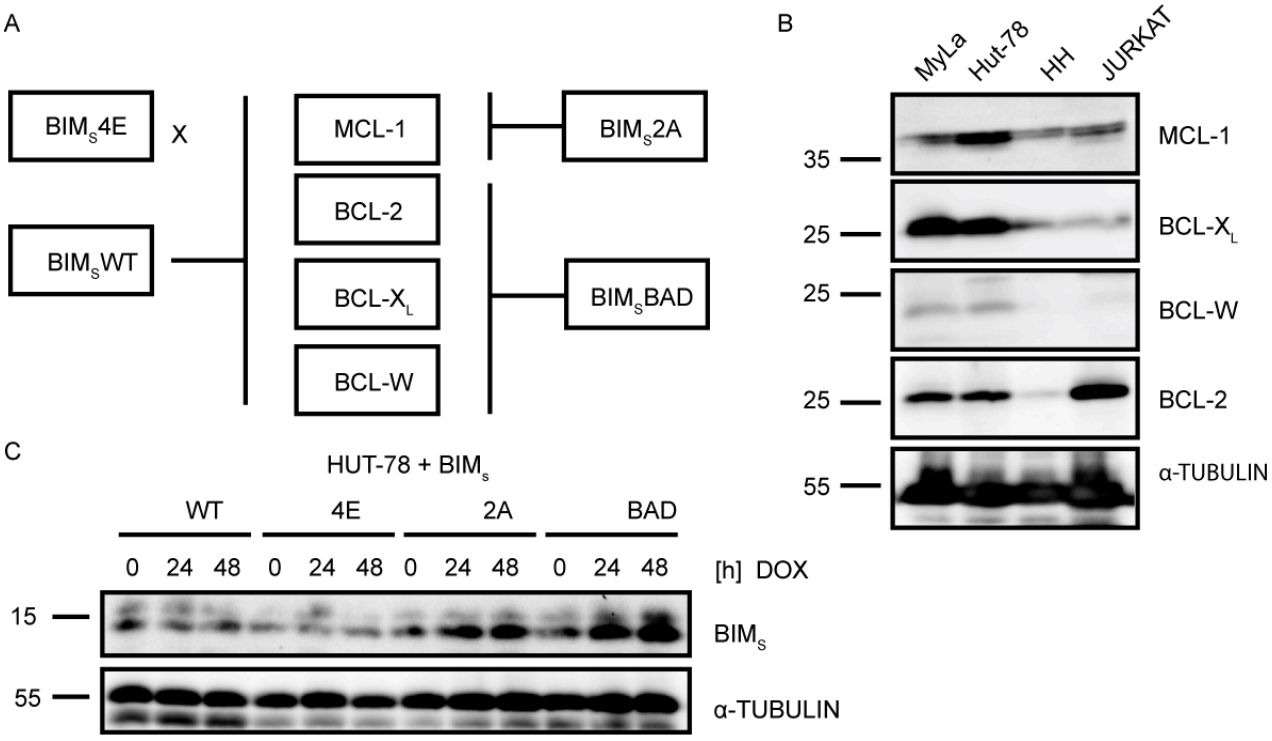

Figure 5.26 Exogenous expression of BIM$_S$ constructs in human T-NHL cell lines. (A) Schematic view of the affinities of the BIM$_S$ constructs to the different Bcl-2 proteins. (B) Western Blot with human T-NHL cell lines MyLa, Hut-78, HH and the leukemia cell line Jurkat. Cells were screened for protein expression of anti-apoptotic Bcl-2 proteins. (C) Western Blot analysis of HUT-78 PTCL cells, transduced with BIM$_S$ constructs. The cells were treated with 1 µg/ml DOX for 0, 24 and 48 hours, lysed and screened for BIM$_S$ expression.

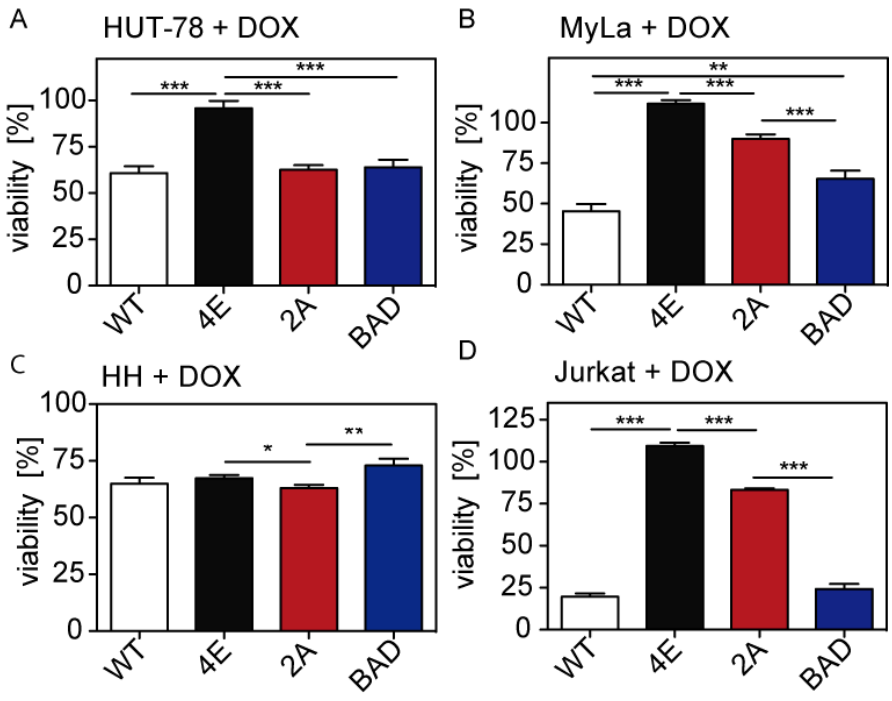

Figure 5.27 Effect of exogenous expression of BIM_S constructs on human T-NHL cell survival. (A)-(D) Viability, defined as PI negative and GFP positive cells, normalized to vehicle control, 48 hours after induction of BIM_S-constructs. Bars represent mean ± SEM of three individual experiments, each consisting of triplicates. White bars = BIM_SWT, black bars = BIM_S4E, red bars = BIM_S2A, blue bars = BIM_SBAD. Statistical analysis was done with unpaired t-test and asterisks denote significant differences (*p < 0,05, **p < 0,005, ***p < 0,0005). (A) Hut-78 (B) MyLa (C) HH (D) Jurkats

5.5.2 The effect of BIM_S-constructs on the sensitivity of human T-NHL cell lines to apoptotic stimulators

As shown in section 5.3, heterozygous *Mcl-1* deletion was able to sensitize murine T-NHL cells to several apoptotic stimuli (Figure 5.4; Figure 5.15). To test whether this was also the case in human T-NHL cells, BIM_S transduced cell lines were co-treated with doxycycline (DOX) and either etoposide (ETO), doxorubicine (DOXO) or ABT-737 for 48 hours.

Etoposide (ETO):

BIM_S induction by DOX treatment lead to a decrease of viability comparable to what was shown in the section before (see table 5.2 column 1). Upon single-agent treatment with ETO, all transduced Hut-78 cells showed reduced viability to between 52 and 60 % (Table 5.2 column 2 and Figure 5.28 A, middle). Upon co-treatment with ETO and DOX, only BIM_S2A transduced Hut-78 cells showed a synergistic effect, resulting in 40,8 ± 7,0% viability. In contrast, cells transduced with BIM_S4E, BIM_SBAD and also BIM_SWT showed no further reduction of viability upon ETO treatment when BIM_S was induced by DOX treatment (Table 5.2 column 3 and Figure 5.28 A, right panel).

Column	**1**	**2**	**3**
BIM_S construct	**DOX (1µg/ml)**	**ETO (100 nM)**	**DOX + ETO**
WT	75,02 ± 1,9	59,7 ± 2,1	64,3 ± 3,3 (*)(ns)
4E	110,0 ± 4,4	52,2 ± 5,9	95,8 ± 3,2 (ns)(***)
2A	67, 6 ± 1,7	53,7 ± 7,2	40,8 ± 7,0 (**)(ns)
BAD	71,9 ± 2,8	60,1 ± 2,2	67,4 ± 3,9

Table 5.2 Viability of HUT-78 cells upon etoposide treatment and BIM_S induction. Viability of Hut-78 treated either with 1 µg/ml doxycycline (DOX), or 100 nM etoposide (ETO) or both, was normalized to mock treated cells and is depicted as %. The

asterisks in brackets within the last column indicate whether differences to the single agent treated cells were significant. Analysis was done with unpaired t-test (*p < 0,05, **p < 0,005, ***p < 0,0005).

MyLa showed a response to ETO treatment by means of a 50 to 60 % reduction of viability (Table 5.3 column 2 and Figure 5.28 B, middle). Co-treatment with DOX significantly further reduced viability of cells positive for BIM_SWT to 22 % (Table 5.3 column 3 and Figure 5.28 B, right panel). BIM_SBAD transduced cells also showed less viability upon co-treatment with ETO and DOX than with single-agent treatment. Still, the difference between ETO treatment and additional induction of BIM_SBAD was not significant (Table 5.3 column 3). BIM_S2A transduced MyLa cells showed less sensitivity to DOX and ETO co-treatment in comparison to BIM_SWT$^+$ cells and no synergistic effect of DOX and ETO (Table 5.3 column 3 and Figure 5.28 B, right panel).

Column	**1**	**2**	**3**
BIM_S construct	**DOX (1µg/ml)**	**ETO (100 nM)**	**DOX + ETO**
WT	45,9 ± 2,1	45,9 ± 8,4	22,0 ± 3,9 (**)(*)
4E	107,5 ± 1,8	41,2 ± 5,1	69,6 ± 4,2 (***) (***)
2A	91,6 ± 2,3	33,0 ± 6,8	42,4 ± 4,1 (***)(ns)
BAD	56,4 ± 2,3	46,8 ± 8,1	28,9 ± 7,7 (*)(ns)

Table 5.3 Viability of MyLa cells upon etoposide treatment and BIM_S induction. Viability of MyLa treated either with 1 µg/ml doxycycline (DOX), or 100 nM etoposide (ETO) or both, was normalized to mock treated cells and is depicted as %. The asterisks in brackets within the last column indicate whether differences to the single agent treated cells were significant. Analysis was done with unpaired t-test (*p < 0,05, **p < 0,005, ***p < 0,0005).

HH again showed reduced viability after induction of all BIM_S constructs (Table 5.4 column 1 and Figure 5.28 C, left panel). Upon treatment with ETO viability was reduced to 67 – 87% (Table 5.4 column 2 and Figure 5.28, middle). Whereas DOX

treated, BIM_S4E^+ and BIM_SBAD^+ cells showed comparable viabilities upon co-treatment with ETO and DOX, BIM_SWT^+ and BIM_S2A^+ cells showed a synergistic effect and further reduction of viability (Table 5.4 column 3 and Figure 5.28 C, right panel).

Column	**1**	**2**	**3**
BIM_S construct	**DOX (1µg/ml)**	**ETO (100 nM)**	**DOX + ETO**
WT	66,2 ± 2,6	78,4 ± 4,9	56,9 ± 2,4 (*)(***)
4E	68,5 ± 1,6	87,0 ± 6,0	71,7 ± 4,7 (ns)(ns)
2A	64,3 ± 2,4	86,5 ± 5,2	56,7 ± 5,0 (ns)(***)
BAD	73,0 ± 4,6	66,5 ± 10,0	64,2 ± 4,3 (ns)(ns)

Table 5.4 Viability of HH cells upon etoposide treatment and BIM_S induction. Viability of HH treated either with 1 µg/ml doxycycline (DOX), or 100 nM etoposide (ETO) or both, was normalized to mock treated cells and is depicted as %. The asterisks in brackets within the last column indicate whether differences to the single agent treated cells were significant. Analysis was done with unpaired t-test (*p < 0,05, **p < 0,005, ***p < 0,0005).

Upon single-agent treatment with ETO, Jurkats showed a moderate reduction of viability to approx. 70% (Table 5.5 column 2 and Figure 5.28 D, middle). Co-treatment with DOX lead to a decrease in viability comparable to DOX-only treated cells (Table 5.5 column 1 and 3), with BIM_SWT and BIM_SBAD transduced cells showing a significant reduced viability in comparison to BIM_S2A^+ cells (Figure 5.28 D right and left panels). There was no further reduction of viability when the BIM_S-constructs were induced in addition to ETO treatment (Table 5.5 column 3 and Figure 28 D, right panel).

Column	1	2	3
BIM_S construct	**DOX (1µg/ml)**	**ETO (100 nM)**	**DOX + ETO**
WT	14,0 ± 1,6	64,9 ± 8,7	14,3 ± 3,1 (ns)(***)
4E	112,8 ± 2,9	69,8 ± 6,3	87,1 ± 3,3 (***)(*)
2A	83,0 ± 1,1	73,5 ± 4,4	65,1 ± 0,8 (***)(ns)
BAD	20,1 ± 1,0	70,8 ± 8,7	26,0 ± 3,9 (ns)(***)

Table 5.5 Viability of Jurkat cells upon etoposide treatment and BIM_S induction. Viability of Jurkats treated either with 1 µg/ml doxycycline (DOX), or 100 nM etoposide (ETO) or both, was normalized to mock treated cells and is depicted as %. The asterisks in brackets within the last column indicate whether differences to the single agent treated cells were significant. Analysis was done with unpaired t-test (*p < 0,05, **p < 0,005, ***p < 0,0005).

Doxorubicine (DOXO):

When treated with doxorubicine (DOXO), Hut-78 cells showed impaired viability of less than 10% with no significant differences between the diverse BIM_S-constructs (Table 5.6 column 2 and Figure 5.29 A, middle). Upon additional induction of BIM_S by DOX treatment, no further reduction of viability, for none of the BIM_S-constructs, was observed (Table 5.6 column 3 and Figure 5.29 A, right panel).

Column	1	2	3
BIM_S construct	**DOX (1µg/ml)**	**DOXO (10 nM)**	**DOX + DOXO**
WT	74,9 ± 1,7	8,1 ± 0,8	6,3 ± 0,8 (***)(ns)
4E	109,4 ± 4,0	5,8 ± 1,5	8,2 ± 2,8 (***)(ns)
2A	67,4 ± 1,5	5,3 ± 1,1	4,4 ± 0,6 (***)(ns)
BAD	70,9 ± 2,7	4,6 ± 0,8	2,9 ± 0,4 (***)(ns)

Table 5.6 Viability of Hut-78 cells upon doxorubicine treatment and BIM_S induction. Viability of Hut-78 treated either with 1 µg/ml doxycycline (DOX), or 10 nM doxorubicine (DOXO) or both, was normalized to mock treated cells and is depicted as %.

The asterisks in brackets within the last column indicate whether differences to the single agent treated cells were significant. Analysis was done with unpaired t-test (*p < 0,05, **p < 0,005, ***p < 0,0005).

MyLa were also sensitive to DOXO treatment with a maximum reduction of viability to 32,4 % (Table 5.7 column 2 and Figure 5.29 B, middle). Co-treatment with DOX showed a synergistic effect in BIM_SWT positive cells, resulting in 19,3% viability (Table 5.7 column 3 and Figure 5.29 B, right panel). BIM_SBAD and BIM_S2A cells instead exhibited no further decrease of viability compared to single-agent treatment with DOXO. (Table 5.7 column 3 and Figure 5.29 B, right panel).

Column	**1**	**2**	**3**
BIM_S construct	**DOX (1µg/ml)**	**DOXO (10 nM)**	**DOX + DOXO**
WT	45,9 ± 2,1	42,6 ± 6,9	19,3 ± 5,2 (***)(*)
4E	107,5 ± 1,8	38,6 ± 5,1	52,3 ± 10,0 (***)(ns)
2A	91,6 ± 2,3	32,4 ± 3,9	31,5 ± 6,1 (***)(ns)
BAD	56,4 ± 2,3	40,0 ± 7,3	30,7 ± 9,5 (*)(ns)

Table 5.7 Viability of MyLa cells upon doxorubicine treatment and BIM_S induction. Viability of MyLa treated either with 1 µg/ml doxycycline (DOX), or 10 nM doxorubicine (DOXO) or both, was normalized to mock treated cells and is depicted as %. The asterisks in brackets within the last column indicate whether differences to the single agent treated cells were significant. Analysis was done with unpaired t-test (*p < 0,05, **p < 0,005, ***p < 0,0005).

Single-agent treatment of HH with DOXO lead to a reduction of viability to 18 – 28% (Table 5.8 column 2 and Figure 5.29 C, middle), which was comparable to cells co-treated with DOX (Table 5.8 column 3 and Figure 5.29 C, right panel). None of the BIM_S constructs sensitized the cells to DOXO treatment.

Column	1	2	3
BIM_S construct	**DOX (1µg/ml)**	**DOXO (10 nM)**	**DOX + DOXO**
WT	67,5 ± 2,3	18,0 ± 2,7	16,2 ± 2,7 (***)(ns)
4E	73,3 ± 3,5	27,9 ± 8,9	26,8 ± 6,5 (***)(ns)
2A	64,8 ± 2,0	28,5 ± 9,3	27,9 ± 7,9 (***)(ns)
BAD	71,0 ± 4,0	19,9 ± 5,9	16,6 ± 5,3 (***)(ns)

Table 5.8 Viability of HH cells upon doxorubicine treatment and BIM_S induction. Viability of HH treated either with 1 µg/ml doxycycline (DOX), or 10 nM doxorubicine (DOXO) or both, was normalized to mock treated cells and is depicted as %. The asterisks in brackets within the last column indicate whether differences to the single agent treated cells were significant. Analysis was done with unpaired t-test (*p < 0,05, **p < 0,005, ***p < 0,0005).

The viability of Jurkats upon DOXO-treatment was diminished to approximately 40% (Table 5.9, column 2 and Figure 5.19 D, middle). DOX co-treatment further decreased viability in BIM_SWT^+ and BIM_SBAD^+ cells compared to single agent treated cells. Still, there were no significant differences to cells, treated with DOXO only (Tabe 5.9 column 3 and Figure 5.29 D, right panel). Cells transduced with BIM_S4E^+ and BIM_S2A^+ also showed no synergistic effect in cell death upon co-treatment with DOX and DOXO (Table 5.9. column 3 and Figure 5.29 D, right panel) compared to single-agent treatment (Table 5.9 column 1 + 2 and Figure 5.29 D, left and middle panel).

Column	1	2	3
BIM_S construct	**DOX (1µg/ml)**	**DOXO (10 nM)**	**DOX + ETO**
WT	18,6 ± 2,7	28,1 ± 11,4	7,1 ± 2,9 (**)(ns)
4E	109,9 ± 2,7	64,5 ± 10,1	48,4 ± 8,2 (***)(ns)
2A	82,5 ± 1,1	38,7 ± 10,5	32,5 ± 6,9 (***)(ns)
BAD	27,9 ± 4,1	33,3 ± 12,3	17,4 ± 5,6 (ns)(ns)

Table 5.9 Viability of Jurkat cells upon doxorubicine treatment and BIM_S induction. Viability of Jurkats treated either with 1 µg/ml doxycycline (DOX), or 10 nM doxorubicine (DOXO) or both, was normalized to mock treated cells and is depicted as %. The asterisks in brackets within the last column indicate whether differences to the single agent treated cells were significant. Analysis was done with unpaired t-test (*p < 0,05, ** p < 0,005, ***p < 0,0005).

ABT-737:

The BH3 mimetic ABT-737 showed a synergistic effect with heterozygous *Mcl-1* deletion in murine T-NHL cells (Figure 5.4). In Hut-78, single-agent treatment of BIM_S^-transduced cells with ABT-737 lead to an approximately 50% decrease of viability (Table 5.10 column 2 and Figure 5.30 A, middle). Only BIM_S2A transduced cells showed a further reduction of viability when co-treated with DOX (Table 5.10 column 3 and Figure 5.30 A right panel).

Column	**1**	**2**	**3**
BIM_S construct	**DOX (1µg/ml)**	**ABT-737 (100 nM)**	**DOX + ABT-737**
WT	74,9 ± 1,7	63,4 ± 1,9	63,1 ± 2,1 (***)(ns)
4E	109,4 ± 4,2	51,3 ± 0,7	86,5 ± 1,6 (***)(***)
2A	67,4 ± 1,5	41,8 ± 8,7	26,1 ± 3,8 (***)(**)
BAD	70,9 ± 2,7	47,9 ± 2,4	53,6 ± 1,6 (***)(ns)

Table 5.10 Viability of Hut-78 cells upon ABT-737 treatment and BIM_S induction. Viability of Hut-78 treated either with 1 µg/ml doxycycline (DOX), or 100 nM ABT-737 or both, was normalized to mock treated cells and is depicted as %. The asterisks in brackets within the last column indicate whether differences to the single agent treated cells were significant. Analysis was done with unpaired t-test (*p < 0,05, **p < 0,005, ***p < 0,0005).

MyLa exhibited reduced viability upon ABT-737 treatment to about 40% (Table 5.11 column 2 and Figure 5.30 B, middle). The viability upon ABT-737 treatment alone

was comparable to when the cells were co-treated with DOX, resulting in additional BIM_S-induction (Table 5.11 column 3 and Figure 5.30 B, right panel). Although BIM_S-induction alone showed significant more cell death in cells positive for BIM_SWT (46% viability) and BIM_SBAD (56% viability) compared to BIM_S2A (92% viability) (Table 5.11 column 1; Figure 5.30 B, left panel), these differences were gone in ABT-737 co-treated cells, with all transduced cells showing approximately 30% viability (Table 5.11. column 3 and Figure 5.30 B, right panel). Only BIM_S4E transduced cells exhibited no further reduction of viability upon induction by DOX (Table 5.11 column 3 and Figure 5.30 B, right panel).

Column	**1**	**2**	**3**
BIM_S construct	**DOX (1µg/ml)**	**ABT-737 (100 nM)**	**DOX + ABT-737**
WT	45,8 ± 2,1	39,9 ± 2,4	31,5 ± 3,4 (**)(ns)
4E	107,5 ± 2,3	53,8 ± 1,4	52,4 ± 2,0 (***)(ns)
2A	91,6 ± 2,3	33,1 ± 3,6	29,4 ± 3,8 (***)(ns)
BAD	56,4 ± 2,3	35,5 ± 7,8	31,5 ± 7,6 (**)(ns)

Table 5.11 Viability of MyLa cells upon ABT-737 treatment and BIM_S induction. Viability of MyLa treated either with 1 µg/ml doxycycline (DOX), or 100 nM ABT-737 or both, was normalized to mock treated cells and is depicted as %. The asterisks in brackets within the last column indicate whether differences to the single agent treated cells were significant. Analysis was done with unpaired t-test (*p < 0,05, **p < 0,005, ***p < 0,0005).

The viability of HH cells was reduced to 64 – 83% upon ABT-737 treatment (Table 5.12 column 2 and Figure 5.30 C middle). Co-treatment with ABT-737 and DOX resulted in significant decreased viability of BIM_S2A transduced cells only (Table 5.12 column 3 and Figure 5.30 C, right panel). Mere ABT-737 treatment lead to significant more cell death than DOX treatment alone in BIM_SWT and BIM_SBAD positive cells (Table 5.12 column 1 and 2). Still, there was no significant difference after combined treatment, compared to cells treated with ABT-737 alone (Table 5.12 column 3 and Figure 5.30 C, right panel).

Column	1	2	3
BIM_S construct	**DOX (1µg/ml)**	**ABT-737 (100 nM)**	**DOX + ABT-737**
WT	67,9 ± 2,1	68,8 ± 6,3	57,1 ± 4,1 (*)(ns)
4E	74,9 ± 3,6	82, 6 ± 6,1	71,7 ± 3,3 (ns)(ns)
2A	64,9 ± 1,8	76,6 ± 5,6	53,6 ± 4,0 (*)(**)
BAD	70,0 ± 3,8	63 ± 6,2	57,0 ± 3,7 (*)(ns)

Table 5.12 Viability of HH cells upon ABT-737 treatment and BIM_S induction. Viability of HH treated either with 1 µg/ml doxycycline (DOX), or 100 nM ABT-737 or both, was normalized to mock treated cells and is depicted as %. The asterisks in brackets within the last column indicate whether differences to the single agent treated cells were significant. Analysis was done with unpaired t-test (*p < 0,05, **p < 0,005, ***p < 0,0005).

Jurkats treated with ABT-737, showed a reduction of viability to about 80- 90% (Table 5.13 column 2 and Figure 5.30 D, middle). Upon additional induction of BIM_S by DOX treatment, there was less viability in all transduced cells, except BIM_S4E (Table 5.13 column 3 and Figure 5.30 D, right pane). Compared to cells treated with DOX alone, only BIM_S2A^+ cells showed a significant reduced viability in double-treated cells (Table 5.13 column 1 and 3). In contrast, BIM_SWT and BIM_SBAD both showed higher viability when co-treated with ABT-737 than upon single-agent treatment with DOX (Table 5.13 column 1 and 3 and Figure 5.30 D).

Column	1	2	3
BIM_S construct	**DOX (1µg/ml)**	**ABT-737 (100 nM)**	**DOX + ABT-737**
WT	14,0 ± 1,6	74,7 ± 4,6	20,8 ± 2,1 (*)(***)
4E	112,8 ± 2,9	86,3 ± 2,8	104,0 ± 2,1 (*)(***)
2A	83,0 ± 1,1	85,3 ± 2,3	74,0 ± 1,1 (***)(***)
BAD	20,1 ± 1,0	91,8 ± 3,2	30,6 ± 2,9 (**)(**)

Table 5.13 Viability of Jurkat cells upon ABT-737 treatment and BIM_S induction. Viability of Jurkats treated either with 1 µg/ml doxycycline (DOX), or 100 nM ABT-737 or both was normalized to mock treated cells and is depicted as %. The asterisks

in brackets within the last column indicate whether differences to the single agent treated cells were significant. Analysis was done with unpaired t-test (*p < 0,05, **p < 0,005, ***p < 0,0005).

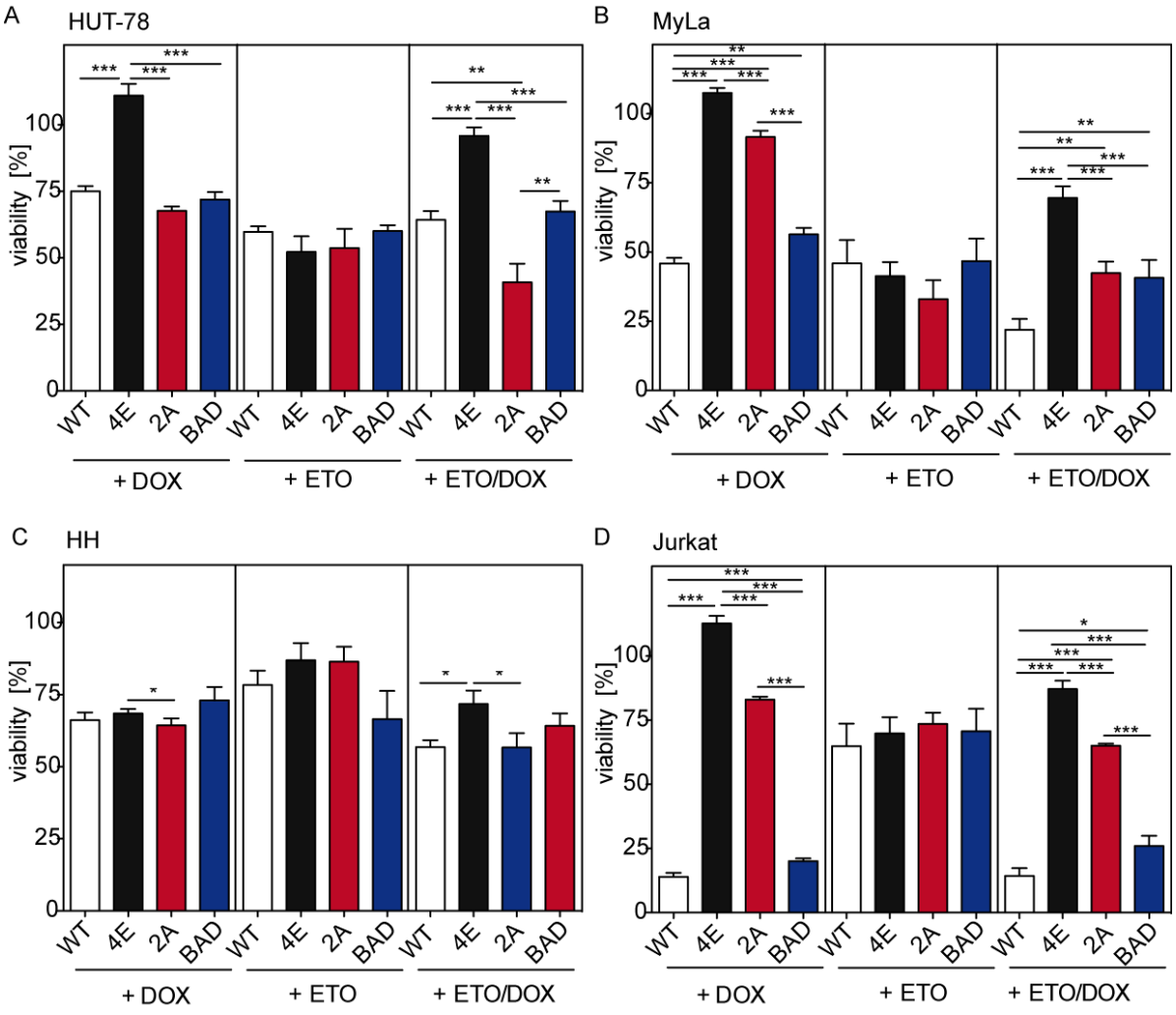

Figure 5.28 Effect of exogenous expression of BIM_S constructs on sensitivity of human T-NHL cells to etoposide treatment. (A)-(D) Viability of human T-NHL cells, defined as GFP^+/PI^- cells, normalized to mock control. Cells were treated 48 hours with etoposide and co-treated with mock or doxycyline (DOX). Bars represent mean ± SEM of three individual experiments, each consisting of triplicates. White bars = BIM_SWT, black bars = BIM_S4E, red bars = BIM_S2A, blue bars = BIM_SBAD. Statistical analysis was done with unpaired t-test (*p < 0,05, **p < 0,005, ***p < 0,0005). (A) Hut-78 (B) MyLa (C) HH (D) Jurkat

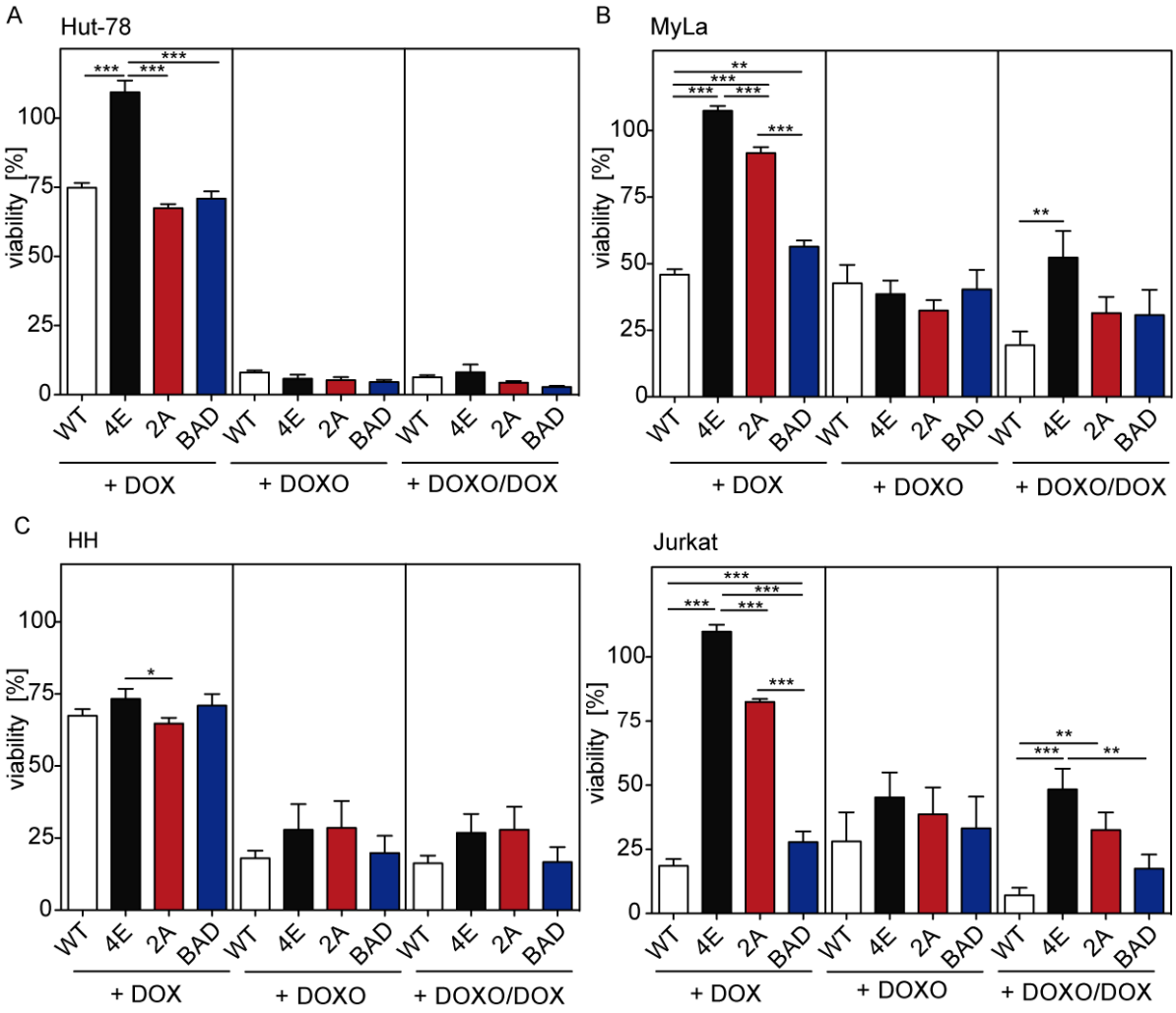

Figure 5.29 Effect of exogenous expression of BIM_S constructs on sensitivity of human T-NHL cells to doxorubicine (DOXO) treatment. (A)-(D) Viability of human T-NHL cells, defined as GFP^+/PI^- cells, normalized to mock control. Cells were treated 48 hours with 10 nM doxorubicine and co-treated with mock or 1µg/ml doxycycline (DOX). Bars represent mean ± SEM of three individual experiments, each consisting of triplicates. White bars = BIM_SWT, black bars = BIM_S4E, red bars = BIM_S2A, blue bars = BIM_SBAD. Statistical analysis was done with unpaired t-test (*p < 0,05, **p < 0,005, ***p < 0,0005). (A) Hut-78 (B) MyLa (C) HH (D) Jurkat

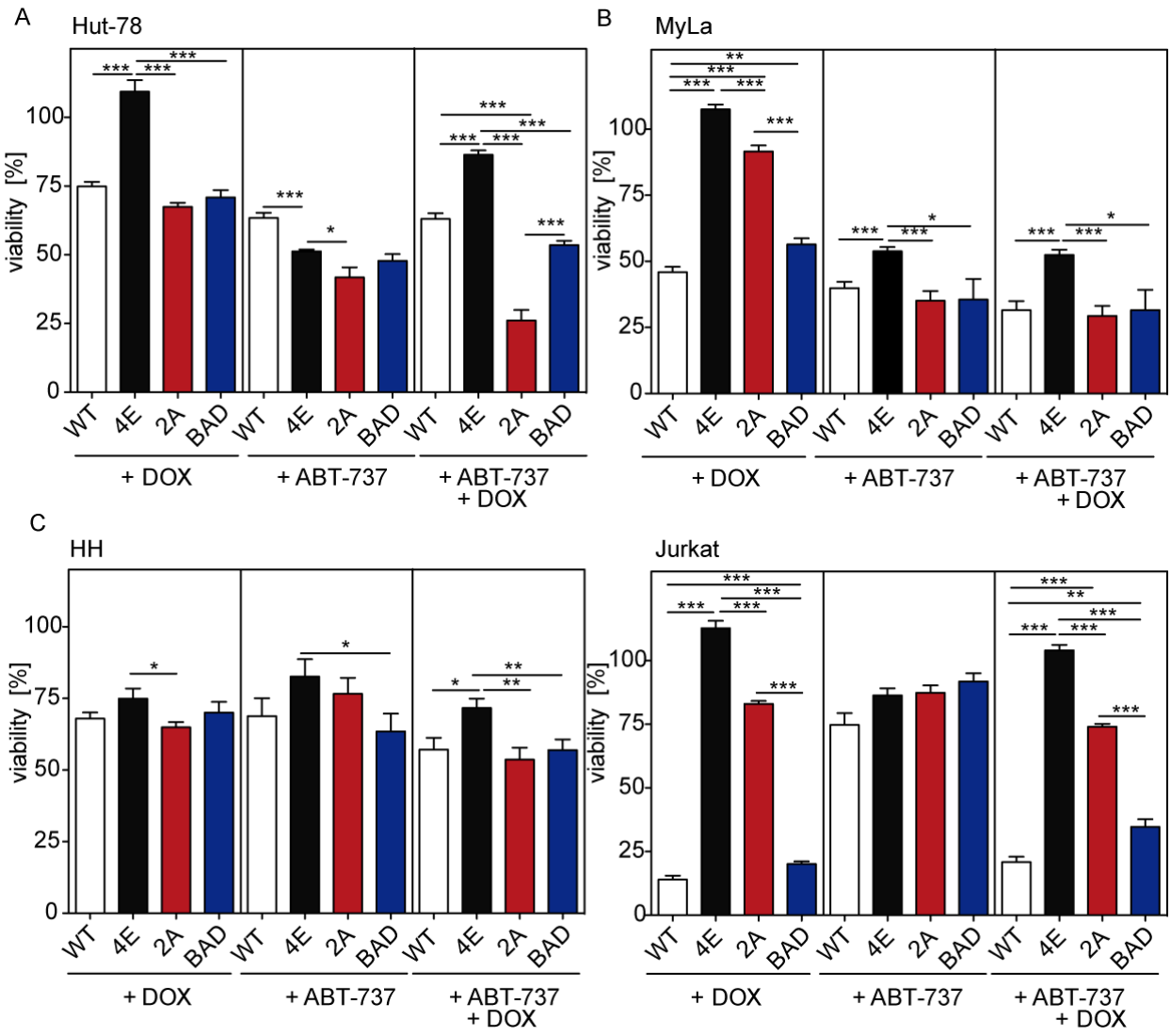

Figure 5.30 Effect of exogenous expression of BIM$_S$ constructs on sensitivity of human T-NHL cells to ABT-737 treatment. (A)-(D) Viability of human T-NHL cells, defined as GFP$^+$/PI$^-$ cells, normalized to mock control. Cells were treated 48 hours with 100 nM ABT-737 and co-treated with vehicle control or 1 µg/ml DOX. Bars represent mean ± SEM of three individual experiments, each consisting of triplicates. White bars = BIM$_S$WT, black bars = BIM$_S$4E, red bars = BIM$_S$2A, blue bars = BIM$_S$BAD. Statistical analysis was done with unpaired t-test (*p < 0,05, **p < 0,005, ***p < 0,0005). (A) Hut-78 (B) MyLa (C) HH (D) Jurkat.

5.6. Expression of apoptotic regulators in human T-NHL

5.6.1 High expression of *MCL-1* mRNA in various human T-NHL entities

Sections 5.1 to 5.3 showed that mono-allelic deletion of *Mcl-1* is sufficient to kill T-NHL cells from mouse origin. The effect of mere MCL-1 inhibition on human T-NHL cell lines was heterogeneous and less clear (Section 5.5). To gain more insights in the possible role of MCL-1 and the other Bcl-2 proteins in primary human lymphoma, biopsies from different human lymphoma entities were screened for Bcl-2 protein expression.

For that purpose, in collaboration with Marco Herling and Giuliano Crispatzu from the university of cologne, array-based mRNA expression profiles from 15 technical comparable, publicly available *in silico* data sets on primary human T cell lymphoma (henceforth simplified as T-NHL) were integrated. The dataset comprised various T-NHL subtypes (including T lymphoblastic leukemia), constituting the largest T-NHL data set available (96)(Table 5.14). The data were summarized in a heat map showing differential mRNA expression as depicted by the color-code histogram (white defined as low expression; red defined as high expression in comparison to the mean transcriptome; Figure 5.31). The focus was on pro- and anti-apoptotic proteins from the BCL-2 family to understand which individual anti-apoptotic BCL-2 family member might be essential for T-NHL cell survival and therefore serve as a possible target for therapy.

MCL-1 showed higher expression intensities than the transcriptome median in 36 out of 39 datasets on human T-NHL. Also T-NHL subtypes originating from NKT cells, hepatosplenic T cell lymphoma (often caused by transformation of γδ T cells) and angioimmunoblastic T cell lymphoma exhibited high expression levels of *MCL-1*. Furthermore, only the anti-apoptotic splice variant of *MCL-1*, namely

MCL-1long (*MCL-1l*), but not the short, pro-apoptotic form of *MCL-1* (*MCL-1short, MCL-1s*) was highly expressed. Besides anti-apoptotic *MCL-1*, A1 showed high expression intensities in 23 of the 39 T-NHL datasets, with highest intensity in ALK+ ALCL samples. *BCL-X_L* and *BCL-2* showed lower expression intensities and were never expressed above the transcriptome median. One dataset of CTCL samples showed high expression of BCL-W but all other T-NHL samples provided low expression intensities.

Reference	***NBCI GEO* or *EBI ArrayExpress* dataset ID**	**Platform abbreviation**
(1) Iqbal et al. 2010	GSE190679	HG-U133_Plus_2
(2) Piccaluga et al. 2007	GSE6338	HG-U133_Plus_2
(3) Iqbal et al. 2011	GSE19067	HG-U133_Plus_2
(4) van Doorn et al. 2009	GSE12902	HG-U133_Plus_2
(5) Travert et al. 2012	E-MTAB-638	HG-U133_Plus_2
(6) de Leval et al. 2007	E_TABM_783	HG-U133_Plus_2
(7) Duerig et al. 2007	GSE5788	HG-U133A
(8) Shin et al., 2007	GSE9479	HG-U133A
(9) Lamant et al. 2007	E-TABM-117	HG-U113A
(10) Nakahata et al. 2013	GSE43017	HG-U133_Plus_2
(11) Tan et al. 2011	GSE20874	HG-U133_Plus_2
(12) Huang et al. 2010	E-TABM-791	HG-U133_Plus_2
(13) Lukk et al. 2010	E-MTAB-62	HG-U133A
(14) Shah et al. 2008	GPL96	HG-U133A
(15) Rodriguez-Cabarello et al. 2008	GPL570	HG-U133_Plus_2

Table 5.14 Primary data references used for gene expression profiling. Publications considered for the heat map on expression of apoptotic regulators in human T-NHL subsets. Those publications comprise array-based expression profiles of human T-NHL subtypes. The table furthermore shows the dataset ID and the used Affymetrix chip.

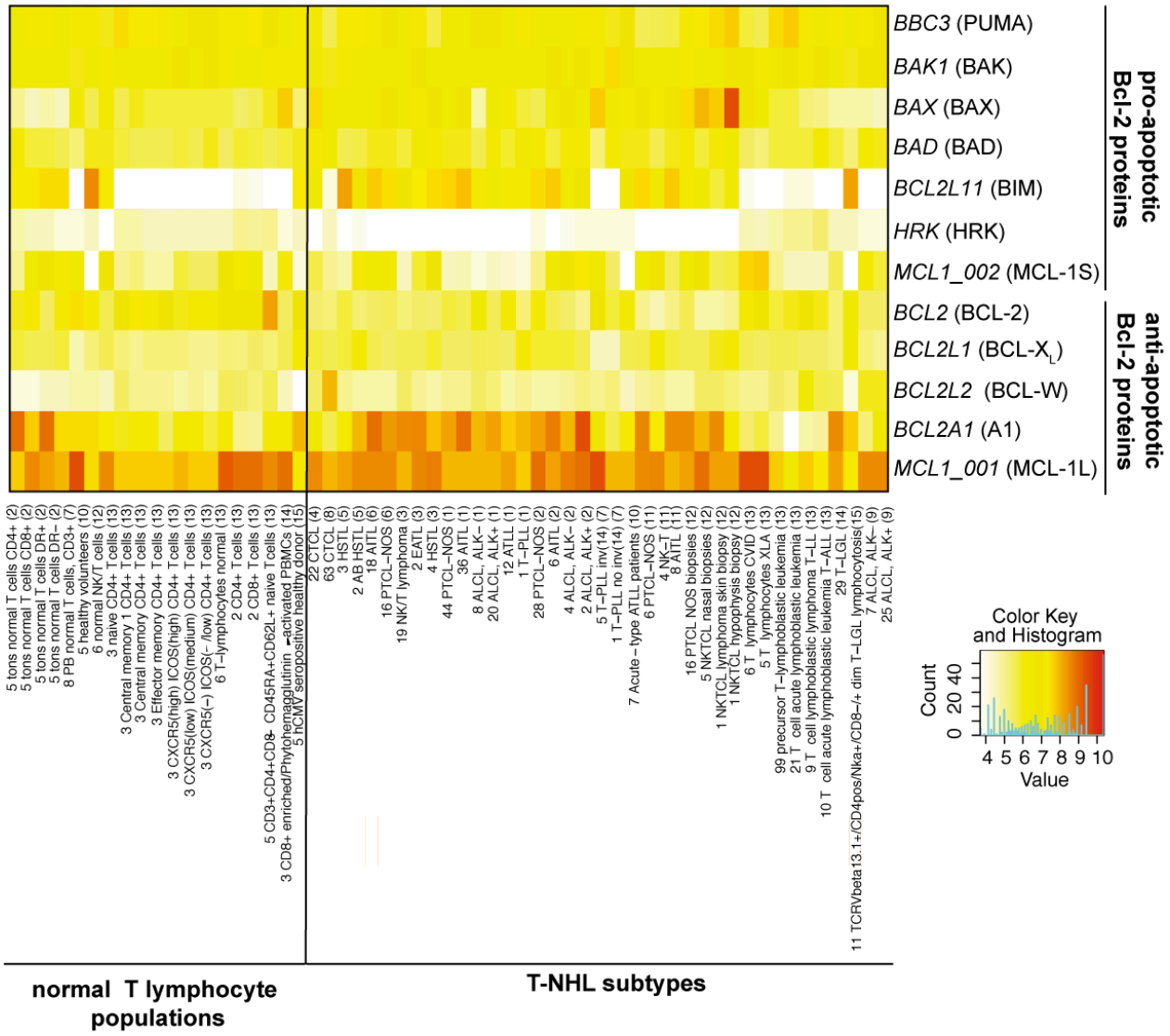

Figure 5.31 Heat-MAP on mRNA expression of Bcl-2 proteins in human T-NHL subtypes. Array-based gene expression data, retrieved from publically available primary *in-silico* data sets of whole-genome profilings were summarized in a heatmap showing mRNA expression across various human T cell lymphoma subsets and subtypes of normal T cells. High expression intensity, compared to the transcriptome median is depicted in red and low expression in white (see color-code histogram). On the X-axis, the first digit(s) indicate(s) the number of samples per entity per dataset; the second field abbreviates the entity followed by the primary data reference (see table 5.2). The molecular regulators of apoptosis, that were analyzed, are listed on the Y-Axis.

5.6.2 High expression of positive MCL-1 regulators

MCL-1 mRNA is highly expressed in human T-NHL and normal T cell subsets. Whether this also translates into protein expression is unclear. To get better insights into this, mRNA expression of MCL-1 regulators was screened. The positive MCL-1 regulators *USP9X* and *KU70* were highly expressed, whereas negative MCL-1 regulators *GSK3* and *MULE* showed lower expression intensities compared to the transcriptome median (Figure 5.32). To get an idea whether this also translates into protein expression, histological analysis of biopsies of patients with AITL, ALCL or PTL-NOS, was performed in collaboration with Dr. Sylvia Hartmann (Dr. Senckenberg Institute of Pathology, Goethe Universität, Frankfurt am Main). Almost all samples showed high MCL-1 protein expression, mostly accompanied by USP9X expression (Figure 5.33). Out of 21 PTCL-NOS patient 16 showed USP9X and 14 MCL-1 expression, for AITL and ALCL every tested biopsy showed to be positive for those two proteins (Table 5.15).

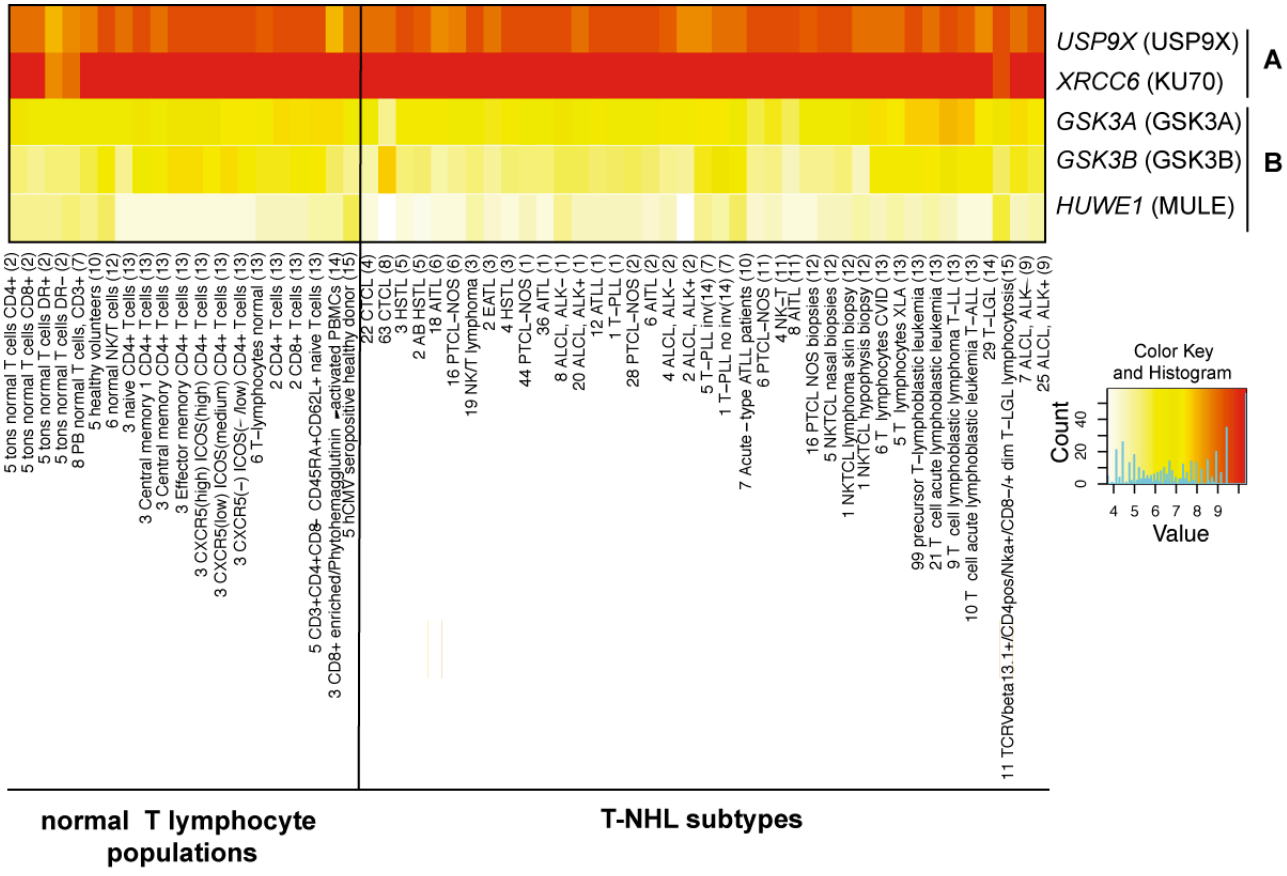

Figure 5.32 Expression of MCL-1 regulators in human T-NHL subtypes. Array-based gene expression data, retrieved from publically available primary *in-silico* data sets of whole-genome profilings were summarized in a heatmap showing mRNA expression across various human T cell lymphoma subsets and subtypes of normal T cells. High expression intensity in comparison to the transcriptome median is depicted in red and low expression in white (see color-code histogram). On the X-axis, the first digit(s) indicate(s) the number of samples per entity per dataset; the second field abbreviates the entity followed by the primary data reference (see Table 5.1). MCL-1 regulators, that were analyzed, are listed on the Y-Axis with A) positive MC-1 regulators and B) negative MCL-1 regulators.

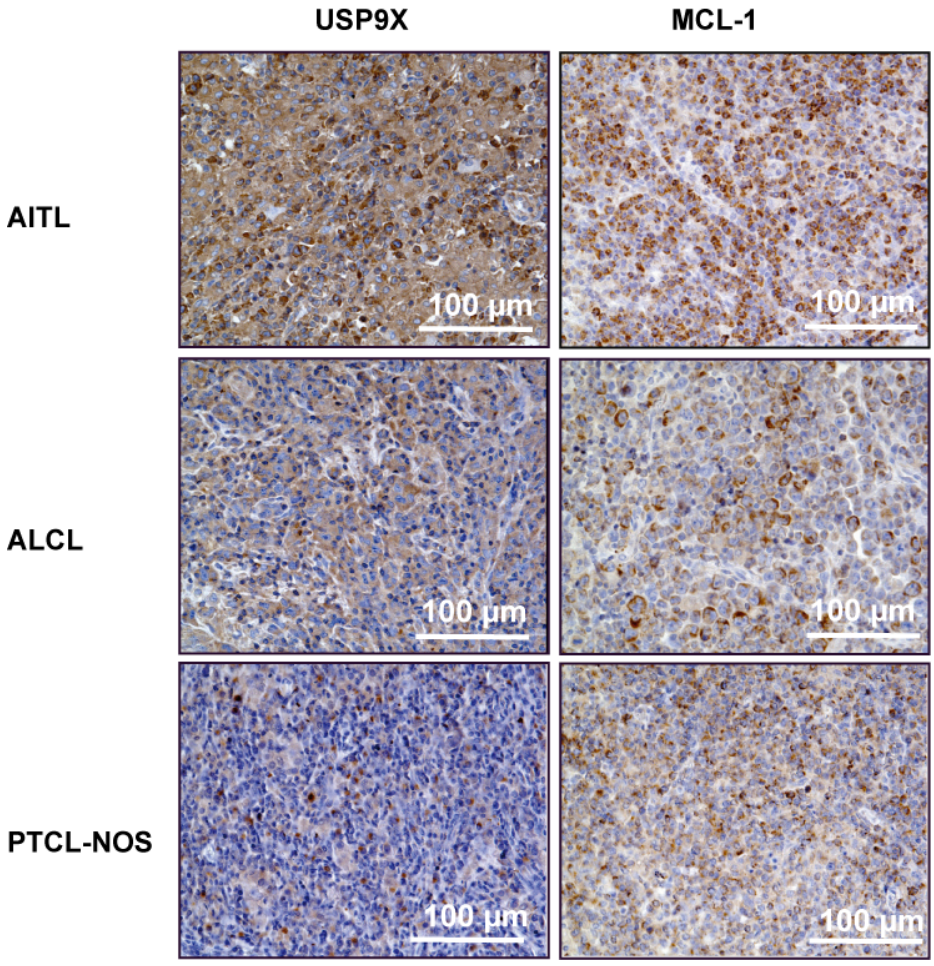

Figure 5.33 MCL-1 protein expression in human PTCL biopsies. Histological analysis of biopsies from patients with AITL, ALCL and PTCL-NOS on expression of MCL-1 (left panel) and USP9X (right panel).

Case Nr	Diagnosis	(Alias)	USP9X	MCL -1
1	PTCL-NOS	K6 -07	+	+
2		K1181 -02	-	+
3		K360 -07	+	+
4		4852 -08	-	-
5		K439 -07	+	+
6		K674 -08	-	-
7		K562 -07	-	+
8		K1184 -04	+	+
9		K353 -07	-	-
10		K562 -07	+	+
11		K872 -06	+	+
12		K171 -03	+	+
13		K151 -04	+	+
14		H19648 -08	+	-
15		K1022 -08	+	+
16		K568 -04	+	-
17		H20792 -04	+	-
18		K564 -07	+	-
19		K859 -05	+	+
20		K1216 -04	+	+
21		K1181 -02	+	+
			16/21	**14/21**
1	ALCL	K316 -08	+	+
2		K79 -12	+	+
3		K1386 -11	+	+
4		K1256 -08	+	+
5		K22 -13	+	+
6		K1199 -12	+	+
7		K99 -13	+	+
8		12003 -12	+	+
			8/8	**8/8**
1	AITL	K251 -13	+	+
2		K417 -14	+	+
3		K1322 -13	+	+
4		K220 -13	+	+
5		K363 -14	+	+
6		25351 -13	+	+
7		K1320 -13	+	+
			7/7	**7/7**

Table 5.15 Expression of MCL-1 and USP9X in human T-NHL subsets. Shown is the positivity (+) of individual human biopsies for immunhistochemical staining on USP9X (left panel) and MCL-1 (right panel). The samples were obtained from patients with PTCL-NOS, ALCL or AITL. Bold numbers at the end of the particular section show the number of positive cases and the total number of samples.

6 Discussion

6.1 MCL-1 critically determines the survival of mouse T-NHL cells *ex vivo*

Bcl-2 proteins are often deregulated in various kinds of cancers (150) and high expression of anti-apoptotic Bcl-2 proteins has been shown to be associated with tumor progression (21,44,67,70,73,76,151-153). Targeting of anti-apoptotic Bcl-2 proteins has also proved to be a promising tool for fighting different kinds of cancers (154,155). However, so far, little is known about the suitability of anti-apoptotic Bcl-2 proteins as therapeutic targets for the therapy of T-NHL.

Previous publications demonstrated, that anti-apoptotic Bcl-2 proteins are expressed in human PTCL samples and cell lines (156) and that BCL-X_L and MCL-1 expression correlate with apoptotic rates and proliferation (79). Recently, it was shown that MCL-1 is critical for the development of thymic lymphoma in p53 deficient mice (157), supporting the hypothesis that it might be essential for survival of T-NHL cells in general. To test the impact of anti-apoptotic Bcl-2 proteins on survival of T-NHL cells, we used an irradiation induced T-NHL mouse model. The used mice harbored loxP sites and expressed an inducible Cre recombinase ($CreER^{T2}$), to enable conditional knockout of the target gene.

Conditional knockout of one allele of *Mcl-1* resulted in significant cell death of T-NHL cells, which was not due to Cre toxicity. The decrease of viability was due to apoptosis, caused by *Mcl-1* deletion. This was shown by enhanced AnnexinV staining and CASPASE 3 cleavage. Furthermore cell death could be prevented by ectopic expression of any of the anti-apoptotic Bcl-2 proteins (Section 5.1.1). Complete *Bcl-x_L* deletion also caused apoptosis in T-NHL cells that could be rescued by ectopic Bcl-2 protein expression. Still, the effect of the complete loss of *Bcl-x_L* was not as potent as mono-allelic *Mcl-1* deletion, supporting the hypothesis

that *Mcl-1* is a more important key player in T-NHL cells (Section 5.1.2). This is consistent with the finding of Grabow et al. (157) who showed that MCL-1, but not BCL-X_L is critical for thymic lymphoma development in p53 KO mice.

Furthermore the T-NHL cells were resistant to treatment with the BH3-mimetic ABT-737, which selectively binds to BCL-2, BCL-X_L and BCL-W but not to MCL-1 and A1. Whereas co-deletion of *Bcl-x$_L$* had only a minor effect on ABT-737 sensitivity, mono-allelic deletion of *Mcl-1* showed a synergistic effect and significantly sensitized T-NHL cells to ABT-737 treatment (Section 5.1.2). This was consistent with previous findings that *Mcl-1* is a critical factor for ABT-737 resistance (158-161). The data support the notion that *Mcl-1* is the most critical anti-apoptotic Bcl-2 protein for the survival of T-NHL cells *ex vivo*.

6.2 MCL-1 is an important survival factor for T-NHL cells *in vivo*

To test the functional relevance of MCL-1 for the sustained survival of T-NHL cells *in vivo*, *Mcl-1$^{fl/+}$CreER* lymphoma cells or controls were injected into syngeneic and immuno-competent wild type (WT) C57BL/6 recipient mice. Transplantation of T-NHL cells lead to lymphoma in recipient mice within 20 to 40 days and showed to be caused by reconstitution of the donor-cells (Section 5.2.1). Deletion of one allele of *Mcl-1* was sufficient to prolong the survival of recipient mice (Section 5.2.2) demonstrating the critical role of sufficient MCL-1 levels for maintaining lymphoma cell survival.

To test whether MCL-1 also protected lymphoma cells during the process of malignant transformation, a mouse model based on the inducible expression of the patient-derived fusion kinase ITK-SYK was used (Section 5.2.3) (5). Here, *Mcl-1* was deleted heterozygously or homozygously at the same time as the expression of the oncogene ITK-SYK started- in the double positive stage of T cell development.

Consistent with Pechloff et al., *ITK-SYK* transgenic mice showed reduced numbers of T cells in the peripheral blood, four weeks after birth (5). This is caused by the constitutive ITK-SYK-dependent signaling and subsequent negative selection of double positive (DP) thymocytes during thymic development. The loss of peripheral T cells was aggravated in *Mcl-1$^{fl/+}$IS$^{+/-}$CD4Cre* and *Mcl-1$^{fl/fl}$IS$^{+/-}$CD4Cre* mice. In those mice, *Mcl-1* deletion further impaired survival of DP T-lymphocytes. This is consistent with previous findings that the process of thymic negative selection is antagonized by MCL-1 (44,162).

16 weeks after birth, the *IS$^{+/-}$CD4Cre* mice showed a strong increase in TCRβ$^+$ cells in the peripheral blood consistent with the rise of aberrant T cell populations and GFP$^+$ lymphoma development (5). In contrast, experimental mice deficient for one allele of *Mcl-1* (*Mcl-1$^{fl/+}$IS$^{+/-}$CD4Cre* mice) did not show this markedly elevation of T cell numbers. This finding was even more profound in *Mcl-1$^{fl/fl}$IS$^{+/-}$CD4Cre* mice, which lost both alleles of *Mcl-1*. They still showed rather diminished T cell numbers in the blood, compared to the control mice. Altogether, MCL-1 targeted mice exhibited TCRβ$^+$ cells in the peripheral blood comparable to that of control mice, effectively counterbalancing the oncogenic signaling emanating from ITK-SYK. This reduction in aberrant T cell numbers was consistent with a significantly delayed lymphoma onset and prolonged survival in *Mcl-1$^{fl/+}$IS$^{+/-}$CD4Cre* and *Mcl-1$^{fl/fl}$IS$^{+/-}$CD4Cre* mice.

Although there was a significant protective effect of targeting *Mcl-1*, mice in both T-NHL models diseased at some point and *Mcl-1$^{fl/+}$IS$^{+/-}$CD4Cre* mice showed infiltration of lymphoid organs by GFP positive T cells comparable to *IS$^{+/-}$CD4Cre* mice. The affection of mice with *Mcl-1$^{\Delta/+}$ CreER* T-NHL cells or *Mcl-1$^{fl/+}$IS$^{+/-}$CD4Cre* mice respectively was, in contrary to other models, not due to mutant loxP sites or mutations in CreER (163). PCR analysis showed successful recombination of the loxP-targeted *Mcl-1* allele in lymphoma cells from all *Mcl-1$^{fl/+}$* mice and was accompanied by reduction of MCL-1 protein levels.
Strikingly, *Mcl-1$^{\Delta/+}$CreER* as well as *Mcl-1$^{\Delta/+}$IS$^{+/-}$CD4Cre* lymphoma cells from diseased mice showed higher *Bcl-x$_L$* mRNA expression than control lymphoma cells

from diseased mice, as well as elevated protein levels. In *Mcl-1*$^{\Delta/+}$*IS*$^{+/-}$*CD4Cre* T-NHL cells there was furthermore a significant increase in *Bcl-2* mRNA levels which did not translate into higher protein levels and was missing in transplanted *Mcl-1*$^{\Delta/+}$*CreER* T-NHL cells. *Ex vivo*, irradiation-induced T-NHL cells were rescued from *Mcl-1* deletion-mediated cell death by ectopic expression of BCL-X_L, BCL-2 and BCL-W (Section 5.1.1). There are more studies that support the notion that loss of MCL-1 can be compensated by the other anti-apoptotic Bcl-2 proteins. It has been shown for example, that conditional deletion of *Mcl-1* in macrophages *in vivo* leads to higher expression of BCL-2 and BCL-X_L which rescues the cells from apoptosis (43). A similar effect was also observed in cardiomyocytes, where deletion of *Mcl-1* also results in higher BCL-2 and BCL-X_L expression (164). In normal T cells it was shown, that BCL-X_L and MCL-1 can compensate for each other in the DP thymocytes compartment (2).

Together, these data support the critical function of MCL-1 in protecting T cells during the process of malignant transformation and indicate that compensatory expression of alternative pro-survival BCL-2 proteins is capable of causing lymphoma relapse despite the genetic deletion of one allele of *Mcl-1*. This problem of compensation by other anti-apoptotic proteins could be solved if MCL-1 inhibition is combined with administration of pan-Bcl-2 inhibitors, as these data showed that MCL-1 reduction together with ABT-737 was very efficient to kill lymphoma cells (Section 5.2.2).

6.3 MCL-1 inhibition as a chemotherapeutic sensitizer

Although targeting of *Mcl-1* cannot totally abrogate the development of lymphoma in irradiated mice or after ITK-SYK induction, reduction of MCL-1 levels might serve as a mechanism to overcome chemo-resistance. It has been shown before, that high MCL-1 expression correlated with chemo-resistance in B-CLL cells (165), AML and ALL samples (76) and oral cancers (166). Furthermore resistance of solid tumor cells could be overcome by MCL-1 inhibition (49,166,167) and a synergistic effect of flavopiridol and vorinostat on survival of AML cells showed to be partially due to MCL-1 suppression (168). Furthermore down-regulation of MCL-1 showed to enhance rituximab-mediated apoptosis in primary CLL cells and ALL cell lines (169).

Consistent with this data, we found higher responsiveness to chemotherapeutic treatment of irradiation-induced T-NHL cells upon mono-allelic *Mcl-1* deletion ex *vivo*. All chemotherapeutics exhibited a reduced IC50 in *Mcl-1*$^{\Delta/+}$*CreER* T-NHL cells compared to *Mcl-1*$^{fl/+}$*CreER* T-NHL cells (Section 5.3.1). Complete *Bcl-x*$_L$ deletion sensitized T-NHL cells solely to treatment with doxorubicine, whereas mere CreER activation showed no effect on IC50 at all. These results were confirmed when cells were treated with doxorubicine over time. Whereas there was no synergistic effect between loss of *Bcl-x*$_L$ and the remaining chemotherapeutics, T-NHL cells heterozygous for *Mcl-1* showed significant higher responsiveness to cyclophosphamide, doxorubicine and etoposide. Doxorubicine showed the most efficient induction of cell death after 96 hours of treatment.

This was consistent with earlier findings, that *Mcl-1* is essential for Integrin-mediated doxorubicine resistance in T-ALL cells (170) and reduction of MCL-1 in PTEN$^{+/-}$-Eμ-myc lymphoma cells by translational inhibition resulted in increased sensitivity to doxorubicine treatment (171). Recently, it was found that targeting of IRAK1/4, which results in MCL-1 destabilization, caused higher responsiveness of T-ALL cells to vincristine and ABT-737 in a MCL-1 dependent manner (172). Our

data further support the notion that MCL-1 is a critical mediator for doxorubicine resistance, as mice transplanted with *Mcl-1*$^{fl/+}$*CreER* T-NHL cells show higher responsiveness to doxorubicine treatment and prolonged survival when *Mcl-1* was heterozygously deleted (Section 5.3.2).

Together, these data show that heterozygous loss of *Mcl-1* substantially impairs survival of lymphoma cells and sensitizes to drug treatment, consistent with a critical pro-survival function of this protein for sustained lymphoma growth. These data suggest that *Mcl-1* might serve as a potential target to overcome chemoresistance and MCL-1 inhibition combined with chemotherapy might be an efficient strategy for therapy of T-NHL.

6.4 There is a therapeutic window for the inhibition of *Mcl-1*

Although heterozygous deletion of *Mcl-1* proved to be sufficient to impair T-NHL cell survival, it still has to be solved if it is a suitable target for therapy. It was shown in the past, that complete loss of *Mcl-1* has toxic effects on the heart (164,173) and causes peri-implantation embryonic lethality in mice (26). Furthermore MCL-1 has been shown to be essential for survival of hematopoietic stem cells (27) and complete deletion of *Mcl-1* leads to a massive loss of T cells at multiple stages of development (28).

To see whether heterozygous deletion, which rather reflects the situation in a therapeutic context of inhibition, also has side effects on the normal T cell population or mouse survival, *Mcl-1* was ubiquitously deleted (Section 5.4). *Mcl-1*$^{\Delta/\Delta}$*CreER*^{T2} mice showed a profound loss of T cells in all lymphoid organs as published before (174,175). *Mcl-1*$^{\Delta/+}$*CreER*^{T2} mice, in contrast, exhibited T cell numbers, comparable to the control mice, even 4 weeks after *Mcl-1* deletion. Complete deletion of *Mcl-1* furthermore caused lethality of the mice within three

days, accompanied by loss of the spleen structure and massive apoptosis. As opposed to this, *Mcl-1*$^{\Delta/+}$*CreER*^{T2} mice showed only negligible changes in spleen structure and no signs of disease, also four weeks after *Mcl-1* deletion. The increase in relative T cells numbers in the blood and bone-marrow of *Mcl-1*$^{\Delta/\Delta}$*CreER*^{T2} mice was due to the more pronounced loss of B cells, which is consistent with previous findings (28). Although B cell numbers in the spleen of *Mcl-1*$^{\Delta/+}$*CreER*^{T2} mice were reduced, they still exhibited sufficient amounts. Still, the functionality of lymphocytes after heterozygous *Mcl-1* deletion remains a matter of investigation.

All together, heterozygous *Mcl-1* deletion had only a minor impact on the normal lymphocyte compartment and MCL-1 might therefore serve as an attractive pharmacological target.

6.5 The role of *Mcl-1* in mediating survival of human T-NHL cells

This work showed so far, that MCL-1 plays a pivotal role in the survival of murine T-NHL cells and could be a suitable target for therapy. Still, so far little is known about the function of MCL-1 in human T-NHL cells. Expression analysis of various PTCL samples have shown before that MCL-1 is the most abundant anti-apotpotic Bcl-2 protein and that MCL-1 expression correlates with proliferation (79). Furthermore human PTCL-NOS, ALTL and ALCL (Alk-/Alk+) exhibit genomic instabilities, by means of gain of chromosomal region 1q, were the *Mcl-1* gene is located (82,83,176). Gains of 1q12 were furthermore associated with more aggressive forms of CTCL (111) and ATL (177). Consistent with these findings, *Mcl-1* showed to be higher expressed at later stages of CTCL when expression level was measured at two different time points (115,156).

In this thesis, three different human CTCL cell lines (HH, Hut-78, MyLa) and one human T cell leukemia cell line (Jurkat) were used to test the effect of MCL-1 inhibition in a human context (Section 5.5). Transduction of the cell lines with doxycycline- (DOX) inducible BIM_S constructs, harboring distinct binding affinities to the anti-apoptotic Bcl-2 proteins, showed diverse dependencies. In Hut-78 cells BIM_S2A, which can only bind to MCL-1, showed to be as potent to induce apoptosis as BIM_SWT, which binds to all anti-apoptotic Bcl-2 proteins, and BIM_SBAD, which sequesters BCL-2, BCL-X_L and BCL-W. MyLa, in contrast, showed to be more dependent on BCL-2, BCL-X_L and BCL-W than on MCL-1. Still, BIM_SBAD was not as potent in inducing cell death as BIM_SWT, indicating that the presence of MCL-1 is still sufficient to rescue the cells partially. Interestingly, HH hardly showed any apoptosis, which can be explained by the bad overall viability of those cells. Still, BIM_S2A was the only construct leading to a significant reduction of viability in comparison to control cells. The T cell leukemia cell line Jurkat was also partially dependent on MCL-1. Still, the inhibition of BCL-2, BCL-X_L and BCL-W was more potent as it had the same effect as antagonizing all Bcl-2 proteins. In these cells apoptosis could not be prevented by residual MCL-1.

The differential dependency of the CTCL cell lines might be explainable by protein expression pattern. Western Blot analysis showed that Hut-78, which were more sensitive for MCL-1 inhibition, showed highest MCL-1 protein expression, whereas MyLa showed rather low levels of MCL-1 and higher BCL-X_L expression. HH exhibited general low Bcl-2 protein expression what explains the minor responsiveness to all BIM_S constructs and the bad overall viability. Also fitting with this hypothesis is that Jurkat cells also showed less MCL-1 and higher BCL-2 expression.

To find out whether MCL-1 or the other anti-apoptotic Bcl-2 proteins might serve as factors for chemo-resistance, BIM_S transduced cell lines were co-treated with chemotherapeutical drugs. Hut-78 cells and HH cells exhibited a synergy between BIM_S2A and etoposide. In MyLa and Jurkats cells, etoposide induced apotptosis was rather enhanced by BIM_SBAD.

Doxorubicine showed to be an efficient killer of HH and even more of Hut-78 cells and co-treament with the various BIM_S constructs showed no further apoptosis, whereas the effect of doxorubicine in MyLa could be enhanced only by BIM_SWT. Neither BIM_S2A nor BIM_SBAD were sufficient to sensitize the cells to doxorubicine. This indicates that presence of MCL-1 is as critical as the presence of BCL-2, BCL-XL and BCL-W together, to prevent complete cell death induced by doxorubicine. Jurkats showed only a minor responsiveness to doxorubicine, which could not be enhanced by the different BIM_S constructs. Resistance to doxorubicine in Jurkats might be therefore caused by a distinct factor than the anti-apotpotic Bcl-2 proteins.

Synergy of ABT-737 was seen in Hut-78, transfected with BIM_S2A, HH cells treated with BIM_SWT, BIM_S2A and BIM_SBAD and in Jurkats, transfected with BIM_S2A. This fits with previous observations that MCL-1 expression determines ABT-737 resistance (158,159). Still, the greatest effect was visible in Hut-78, co-treated with BIM_S2A, which again reflects their dependency on MCL-1. In MyLa, which showed to be more dependent on BCL-2 and BCL-X_L, the effect of ABT-737 could not be increased by additional MCL-1 inhibition.

In total, the effect of MCl-1 deletion on survival of T-NHL cell lines varies, most likely in dependence of the expression status of MCL-1. To get an idea whether MCL-1 might also be important in primary T-NHL, gene expression analysis on preexisting micro-array data on human T-NHL biopsies was performed (Section 5.6).

MCL-1 mRNA showed to be consistently highly expressed throughout all human T cell lymphoma subtypes ranging from immature precursor T lymphoblastic leukemia to mature peripheral T lymphocyte lymphoma (PTCL). This expression pattern was restricted to the anti-apoptotic splicing variant *MCL-1L*, as the pro-apoptotic *MCL-1S* only showed minor expression throughout all lymphoma entities. This indicates that apoptotic blockade by MCL-1 was a common denominator for all T-NHL subtypes. Despite the heterogeneity of T-NHL represented in the gene expression data, none of the alternative anti-apoptotic Bcl-2 proteins with the exception of *BCL2A1* (A1), which is structurally similar to MCL-1, showed to be

expressed in a meaningful way. The MCL-1 stabilizing proteins USP9X and KU70 also showed to be highly expressed, indicating that a post-translational stabilization of MCL-1 might lead to elevated MCL-1 protein levels in lymphoma tissues (178). As it is already known, MCL-1 is a highly regulated protein, with a short half-life were stabilization plays an important role in terms of cell survival (50,51,179,180), also for responsiveness to drugs (181). The functional relevance of this short-lived protein is underscored by the consistently high expression of MCL-1 on protein level in AITL, ALCL and PTCL-NOS patient samples. This is compatible with the finding that MCL-1 was the most abundant anti-apoptotic Bcl-2 family member in a histological study on various different human peripheral T-NHL samples (79) and on skin biopsies from patients with Mycosis fungoides or Sezary Syndrome (156). This argues that targeting MCL-1 for the re-activation of apoptosis might be beneficial for the treatment of many, if not all, subtypes of T-NHL.

Summary and Outlook

Targeting of MCL-1 was sufficient to suppress different types of hematologic malignancies (1,35,163). Although MCL-1 is an essential pro-survival factor of T cells at several stages of T cell development (2,28), it still remains a matter of investigation whether MCL-1 is also needed for survival of malignant T-NHL cells.

This work, together with previous findings (157), indicates that MCL-1 could be also a suitable target for therapy of T-NHL. Here we show that only a reduction of MCL-1 levels was sufficient to kill murine T-NHL cells and suppresses lymphoma development *in vivo* without having severe toxic effects on normal lymphocytes. Although the role of MCL-1 in human T-NHL cells is not entirely clear, expression data on human T-NHL samples support the idea of MCL-1 as an important driver of T-NHL cells survival. To solve this question further, additional MCL-1 inhibitors could be used to treat human T-NHL cell lines and maybe primary T-NHL cells. Although MCL-1 inhibitors are currently unavailable, the design and development of potential specific MCL-1 inhibitors is highly promoted (182). So far, there are some promising findings on small molecule inhibitors that bind exclusively MCL-1 which still have to be investigated further (183,184).

Although lymphoma cells gained resistance to MCL-1 inhibition, obviously by up-regulation of other anti-apoptotic Bcl-2 proteins, combination therapy consisting of MCL-1 inhibition and chemotherapy might be an efficient tool for therapy. This thesis showed that MCL-1 reduction sensitized murine and human T-NHL cells to chemotherapeutic treatment. To further solve this question T-NHL cell lines, resistant or sensitive to chemotherapeutic drugs should be confronted with MCL-1 inhibition to see whether sensitivity could be restored. Best, but also most difficult, would be to expose primary human T-NHL samples before chemotherapy and after relapse and co-treat them with MCL-1 inhibitors. Combining MCL-1 inhibition with chemotherapy has also shown to be an efficient tool in other lymphoid malignancies

(52,171,172). It also has to be kept in mind, that next to MCL-1, the role of A1 for survival of T-NHL is unknown. This work revealed, that besides MCL-1, A1 was the only anti-apoptotic Bcl-2 protein highly expressed in primary human T-NHL entities. A1 has a similar binding profile as MCL-1 and elevated A1 expression has been suggested as resistance mechanism against chemotherapy and BH3-mimetics similar to what was described for MCL-1 (21,185-187).

Due to the lack of appropriate loss-of-function models, the role of A1 in normal lymphocyte survival is still not resolved. However, some findings already demonstrated that A1 is essential at several stages of T cell development (36,188) and it plays a role for survival of activated T cells (37). It furthermore has already been shown to possess oncogenic potential as overexpression of A1 in HSCs of mice lead to leukemia/lymphoma of B cell origin (189). Supporting this notion, A1 has been implicated to contribute to T cell leukemia in humans (190). Therefore it might contribute to survival of at least a subgroup of T-NHL cells and is worthy to be further investigated.

Bibliography

1. Kelly GL, Grabow S, Glaser SP, Fitzsimmons L, Aubrey BJ, Okamoto T, et al. Targeting of MCL-1 kills MYC-driven mouse and human lymphomas even when they bear mutations in p53. Genes Dev. 2014 Jan 1;28(1):58–70.

2. Dzhagalov I, Dunkle A, He Y-W. The anti-apoptotic Bcl-2 family member Mcl-1 promotes T lymphocyte survival at multiple stages. J Immunol. 2008 Jul 1;181(1):521–8.

3. Grillot DA, Merino R, Núñez G. Bcl-XL displays restricted distribution during T cell development and inhibits multiple forms of apoptosis but not clonal deletion in transgenic mice. J Exp Med. Rockefeller Univ Press; 1995;182(6):1973–83.

4. Kaplan HS. Influence of Thymectomy, Splenectomy, and Gonadectomy on incidence of radiation-induced lymphoid tumors in strain C57 black mice. Journal of the National Cancer Institute (US) Changed to JNCI, J Natl Cancer Inst. 1950 Aug 1;Vol: 11.

5. Pechloff K, Holch J, Ferch U, Schweneker M, Brunner K, Kremer M, et al. The fusion kinase ITK-SYK mimics a T cell receptor signal and drives oncogenesis in conditional mouse models of peripheral T cell lymphoma. Journal of Experimental Medicine. 2010 May 10;207(5):1031–44.

6. Kerr JF, Wyllie AH, Currie AR. Apoptosis: a basic biological phenomenon with wide-ranging implications in tissue kinetics. Br J Cancer. Nature Publishing Group; 1972;26(4):239.

7. Nagata S, Hanayama R, Kawane K. Autoimmunity and the Clearance of Dead Cells. Cell. 2010 Mar;140(5):619–30.

8. Strasser A, Jost PJ, Nagata S. The Many Roles of FAS Receptor Signaling in the Immune System. Immunity. 2009 Feb 20;30(2):180–92.

9. Riedl SJ, Salvesen GS. The apoptosome: signalling platform of cell death. Nat Rev Mol Cell Biol. 2007 Mar 21;8(5):405–13.

10. Chen L, Willis SN, Wei A, Smith BJ, Fletcher JI, Hinds MG, et al. Differential targeting of prosurvival Bcl-2 proteins by their BH3-only ligands allows complementary apoptotic function. Mol Cell. Elsevier; 2005;17(3):393–403.

11. Chou JJ, Li H, Salvesen GS, Yuan J, Wagner G. Solution structure of BID, an intracellular amplifier of apoptotic signaling. Cell. Elsevier; 1999;96(5):615-24.

12. Scaffidi CC, Fulda SS, Srinivasan AA, Friesen CC, Li FF, Tomaselli KJK, et al. Two CD95 (APO-1/Fas) signaling pathways. EMBO J. 1998 Mar 15;17(6):1675–87.

13. Kaufmann T, Tai L, Ekert PG, Huang DCS, Norris F, Lindemann RK, et al. The BH3-Only Protein Bid Is Dispensable for DNA Damage- and Replicative Stress-Induced Apoptosis or Cell-Cycle Arrest. Cell. 2007 Apr;129(2):423–33.

14. Kuwana T, Bouchier-Hayes L, Chipuk JE, Bonzon C, Sullivan BA, Green DR, et al. BH3 domains of BH3-only proteins differentially regulate Bax-mediated mitochondrial membrane permeabilization both directly and indirectly. Mol Cell. 2005 Feb 18;17(4):525–35.

15. Kim H, Tu H-C, Ren D, Takeuchi O, Jeffers JR, Zambetti GP, et al. Stepwise activation of BAX and BAK by tBID, BIM, and PUMA initiates mitochondrial apoptosis. Mol Cell. Elsevier; 2009;36(3):487–99.

16. Willis SN, Fletcher JI, Kaufmann T, van Delft MF, Chen L, Czabotar PE, et al. Apoptosis Initiated When BH3 Ligands Engage Multiple Bcl-2 Homologs, Not Bax or Bak. Nature. 2007 Feb 9;315(5813):856–9.

17. Fletcher JI, Meusburger S, Hawkins CJ, Riglar DT, Lee EF, Fairlie WD, et al. Apoptosis is triggered when prosurvival Bcl-2 proteins cannot restrain Bax. Proc Natl Acad Sci USA. 2008 Dec 16;105(50):19792–6.

18. Czabotar PE, Lee EF, Thompson GV, Wardak AZ, Fairlie WD, Colman PM. Mutation to Bax beyond the BH3 domain disrupts interactions with pro-survival proteins and promotes apoptosis. Journal of Biological Chemistry. 2011 Mar 4;286(9):7123–31.

19. Mérino D, Giam M, Hughes PD, Siggs OM, Heger K, O'Reilly LA, et al. The role of BH3-only protein Bim extends beyond inhibiting Bcl-2-like prosurvival proteins. The Journal of Cell Biology. 2009 Aug 10;186(3):355–62.

20. Strasser A, Cory S, Adams JM. Deciphering the rules of programmed cell death to improve therapy of cancer and other diseases. EMBO J. 2011 Aug 23;30(18):3667–83.

21. Adams JM, Cory S. The Bcl-2 apoptotic switch in cancer development and therapy. Nature. 2007 Feb 26;26(9):1324–37.

22. Nakayama K, Nakayama K, Negishi I, Kuida K, Sawa H, Loh DY. Targeted disruption of Bcl-2 alpha beta in mice: occurrence of gray hair, polycystic kidney disease, and lymphocytopenia. Proc Natl Acad Sci, USA 1994; 91(9): 3700-3704.

23. Motoyama N, Wang F, Roth KA, Sawa H, Nakayama K, Nakayama K, et al. Massive cell death of immature hematopoietic cells and neurons in Bcl-x-deficient mice. Science. 1995 Mar 10;267(5203):1506–10.

24. Kasai S, Chuma S, Motoyama N, Nakatsuji N. Haploinsufficiency of Bcl-x leads to male-specific defects in fetal germ cells: differential regulation of germ cell apoptosis between the sexes. Developmental Biology. 2003 Dec;264(1):202–16.

25. Mason KD, Carpinelli MR, Fletcher JI, Collinge JE, Hilton AA, Ellis S, et al. Programmed Anuclear Cell Death Delimits Platelet Life Span. Cell. 2007 Mar;128(6):1173–86.

26. Rinkenberger JL, Horning S, Klocke B, Roth K, Korsmeyer SJ. Mcl-1 deficiency results in peri-implantation embryonic lethality. Genes Dev. 2000 Jan 1;14(1):23–7.

27. Opferman JT, Iwasaki H, Ong CC, Suh H, Mizuno S-I, Akashi K, et al. Obligate role of anti-apoptotic MCL-1 in the survival of hematopoietic stem cells. Science. 2005 Feb 18;307(5712):1101–4.

28. Opferman JT, Letai A, Beard C, Sorcinelli MD, Ong CC, Korsmeyer SJ. Development and maintenance of B and T lymphocytes requires antiapoptotic MCL-1. Nature. Nature Publishing Group; 2003;426(6967):671–6.

29. Vikstrom I, Carotta S, Luthje K, Peperzak V, Jost PJ, Glaser S, et al. Mcl-1 Is Essential for Germinal Center Formation and B Cell Memory. Science. 2010 Nov 18;330(6007):1095–9.

30. Steimer DA. Selective roles for antiapoptotic MCL-1 during granulocyte development and macrophage effector function. 2009 Mar 10;:1–11.

31. Print CGC, Loveland KLK, Gibson LL, Meehan TT, Stylianou AA, Wreford NN, et al. Apoptosis regulator bcl-w is essential for spermatogenesis but appears otherwise redundant. Proc Natl Acad Sci USA. 1998 Oct 12;95(21):12424–31.

32. Ross AJ, Waymire KG, Moss JE, Parlow AF, Skinner MK, Russell LD, et al. Testicular degeneration in Bclw-deficient mice. Nat Genet. Nature Publishing Group; 1998;18(3):251–6.

33. Pritchard DM, Print C, O'Reilly L, Adams JM, Potten CS, Hickman JA. Bcl-w is an important determinant of damage-induced apoptosis in epithelia of small and large intestine. Oncogene. 2000 Aug 10;19(34):3955–9.

34. Hamasaki A, Sendo F, Nakayama K, Ishida N, Negishi I, Nakayama K, et al. Accelerated neutrophil apoptosis in mice lacking A1-a, a subtype of the bcl-2-related A1 gene. J Exp Med. 1998 Dec 7;188(11):1985–92.

35. Xiang Z, Ahmed AA, Möller C, Nakayama K, Hatakeyama S, Nilsson G. Essential role of the prosurvival bcl-2 homologue A1 in mast cell survival after allergic activation. J Exp Med. 2001 Dec 3;194(11):1561–9.

36. Ottina E, Tischner D, Herold MJ, Villunger A. A1/Bfl-1 in leukocyte development and cell death. Experimental Cell Research. Elsevier B.V; 2012 Feb 13;:1–13.

37. Gonzalez J. A1 is a growth-permissive antiapoptotic factor mediating postactivation survival in T cells. Blood. 2002 Oct 24;101(7):2679–85.

38. Goldrath AW, Bevan MJ. Selecting and maintaining a diverse T-cell repertoire. Nature. 1999 Nov 18;402(6759):255–62.

39. Gratiot-Deans J, Merino R, Núñez G, Turka LA. Bcl-2 expression during T-cell development: early loss and late return occur at specific stages of commitment to differentiation and survival. Proc Natl Acad Sci USA. National Acad Sciences; 1994;91(22):10685–9.

40. Grayson JM, Murali-Krishna K, Altman JD, Ahmed R. Gene expression in antigen-specific CD8+ T cells during viral infection. J Immunol. 2001 Jan 15;166(2):795–9.

41. Wojciechowski S, Tripathi P, Bourdeau T, Acero L, Grimes HL, Katz JD, et al. Bim/Bcl-2 balance is critical for maintaining naive and memory T cell homeostasis. Nature. 2007 Jun 25.

42. Zhang N, He Y-W. The antiapoptotic protein Bcl-xL is dispensable for the development of effector and memory T lymphocytes. J Immunol. 2005 Jun 1;174(11):6967–73.

43. Dzhagalov I, St John A, He Y-W. The antiapoptotic protein Mcl-1 is essential for the survival of neutrophils but not macrophages. Cell Death Differ. 2007 Feb 15;109(4):1620–6.

44. Campbell KJ, Gray DHD, Anstee N, Strasser A, Cory S. Elevated Mcl-1 inhibits thymocyte apoptosis and alters thymic selection. Cell Death Differ. Nature Publishing Group; 2012 Jun 29;:1–10.

45. Dunkle A, Dzhagalov I, He Y-W. Mcl-1 promotes survival of thymocytes by inhibition of Bak in a pathway separate from Bcl-2. Cell Death Differ. 2010 Jan 8;17(6):994–1002.

46. Kozopas KM, Yang T, Buchan HL, Zhou P, Craig RW. MCL1, a gene expressed in programmed myeloid cell differentiation, has sequence similarity to BCL2. Proc Natl Acad Sci USA. 1993 Apr 15;90(8):3516–20.

47. Quinn BA, Dash R, Azab B, Sarkar S, Das SK, Kumar S, et al. Targeting Mcl-1 for the therapy of cancer. Expert Opin Investig Drugs. 2011;20(10):1397–411.

48. Ding Q, He X, Hsu J-M, Xia W, Chen C-T, Li L-Y, et al. Degradation of Mcl-1 by beta-TrCP mediates glycogen synthase kinase 3-induced tumor suppression and chemosensitization. Molecular and Cellular Biology. 2007 Jun;27(11):4006–17.

49. Wertz IE, Kusam S, Lam C, Okamoto T, Sandoval W, Anderson DJ, et al. Sensitivity to antitubulin chemotherapeutics is regulated by MCL1 and FBW7. Nature. 2011 Mar 3;471(7336):110–4.

50. Schwickart M, Huang X, Lill JR, Liu J, Ferrando R, French DM, et al. Deubiquitinase USP9X stabilizes MCL1 and promotes tumour cell survival. Nature. 2009 Dec 20;463(7277):103–7.

51. Mott JL, Kobayashi S, Bronk SF, Gores GJ. mir-29 regulates Mcl-1 protein expression and apoptosis. Oncogene. 2007 Apr 2;26(42):6133–40.

52. Garzon R, Heaphy CEA, Havelange V, Fabbri M, Volinia S, Tsao T, et al. MicroRNA 29b functions in acute myeloid leukemia. Blood. 2009 Dec 17;114(26):5331–41.

53. Bingle CD, Craig RW, Swales BM, Singleton V, Zhou P, Whyte MK. Exon skipping in Mcl-1 results in a bcl-2 homology domain 3 only gene product that promotes cell death. J Biol Chem. 2000;275(29):22136–46.

54. Huang C-R, Yang-Yen H-F. The fast-mobility isoform of mouse Mcl-1 is a mitochondrial matrix-localized protein with attenuated anti-apoptotic activity. FEBS Lett. 2010 Aug 3;584(15):3323–30.

55. Zhao Y, Altman BJ, Coloff JL, Herman CE, Jacobs SR, Wieman HL, et al. Glycogen Synthase Kinase 3 and 3 Mediate a Glucose-Sensitive Antiapoptotic Signaling Pathway To Stabilize Mcl-1. Cell Death Differ. American Society for Microbiology (ASM); 2007 May 25;27(12):4328–39.

56. Coloff JL, Macintyre AN, Nichols AG, Liu T, Gallo CA, Plas DR, et al. Akt-Dependent Glucose Metabolism Promotes Mcl-1 Synthesis to Maintain Cell Survival and Resistance to Bcl-2 Inhibition. Cancer Res. 2011 Jul 28;71(15):5204–13.

57. Peperzak V, Vikström I, Walker J, Glaser SP, LePage M, Coquery CM, et al. Mcl-1 is essential for the survival of plasma cells. Nat Immunol. 2013 Feb 3.

58. Wenzel S-S, Grau M, Mavis C, Hailfinger S, Wolf A, Madle H, et al. MCL1 is deregulated in subgroups of diffuse large B-cell lymphoma. Nature. 2012 Dec 21.

59. Hanahan D, Weinberg RA. Hallmarks of Cancer: The Next Generation. Cell. 2011 Mar 3;144(5):29–9.

60. Tsujimoto Y, Yunis J, Onorato-Showe L, Erikson J, Nowell PC, Croce CM. Molecular cloning of the chromosomal breakpoint of B-cell lymphomas and leukemias with the t(11;14) chromosome translocation. Science. 1984 Jun 29;224(4656):1403–6.

61. Vaux DL, Cory S, Adams JM. Bcl-2 gene promotes haemopoietic cell survival and cooperates with c-myc to immortalize pre-B cells. Nature. 1988 Sep 28;335(6189):440–2.

62. Strasser A, Harris AW, Bath ML, Cory S. Novel primitive lymphoid tumours induced in transgenic mice by cooperation between myc and bcl-2. Nature. Nature Publishing Group; 1990;348(6299):331–3.

63. Monni O, Joensuu H, Franssila K, Klefstrom J, Alitalo K, Knuutila S. BCL2 overexpression associated with chromosomal amplification in diffuse large B-cell lymphoma. Blood. 1997 Aug 1;90(3):1168–74.

64. Ikegaki N, Katsumata M, Minna J, Tsujimoto Y. Expression of bcl-2 in small cell lung carcinoma cells. Cancer Res. 1994 Jan 1;54(1):6–8.

65. Medan D, Luanpitpong S, Azad N, Wang L, Jiang B-H, Davis ME, et al. Multifunctional Role of Bcl-2 in Malignant Transformation and Tumorigenesis of Cr(VI)-Transformed Lung Cells. Tse W, editor. PLoS One. 2012 May 29;7(5):e37045.

66. Beroukhim R, Mermel CH, Porter D, Wei G, Raychaudhuri S, Donovan J, et al. The landscape of somatic copy-number alteration across human cancers. Nature. 2010 Feb 18;463(7283):899–905.

67. Swanson PJ, Kuslak SL, Fang W, Tze L, Gaffney P, Selby S, et al. Fatal acute lymphoblastic leukemia in mice transgenic for B cell-restricted bcl-xL and c-myc. J Immunol. 2004 Jun 1;172(11):6684–91.

68. Tang DG, Li L, Chopra DP, Porter AT. Extended survivability of prostate cancer cells in the absence of trophic factors: increased proliferation, evasion of apoptosis, and the role of apoptosis proteins. Cancer Res. 1998 Aug 1;58(15):3466–79.

69. Pallis M, Zhu Y-M, Russell NH. Bcl-x (L) is heterogenously expressed by acute myeloblastic leukaemia cells and is associated with autonomous growth in vitro and with P-glycoprotein expression. Leukemia. 1997;11(7):945.

70. Hermann M, Scholman HJ, Marafioti T, Stein H, Schriever F. Differential expression of apoptosis, Bcl‐x and c‐Myc in normal and malignant lymphoid tissues. European journal of haematology. Wiley Online Library; 1997;59(1):20–30.

71. Tu Y, Renner S, Xu F, Fleishman A, Taylor J, Weisz J, et al. BCL-X expression in multiple myeloma: possible indicator of chemoresistance. Cancer Res. 1998 Jan 15;58(2):256–62.

72. Kelly PN, Grabow S, Delbridge ARD, Strasser A, Adams JM. Endogenous Bcl-xL is essential for Myc-driven lymphomagenesis in mice. Blood. 2011 Dec 8;118(24):6380–6.

73. Wuillème-Toumi S, Robillard N, Gomez P, Moreau P, Le Gouill S, Avet-Loiseau H, et al. Mcl-1 is overexpressed in multiple myeloma and associated with relapse and shorter survival. Leukemia. 2005 May 5;19(7):1248–52.

74. Sieghart W, Losert D, Strommer S, Cejka D, Schmid K, Rasoul-Rockenschaub S, et al. Mcl-1 overexpression in hepatocellular carcinoma: A potential target for antisense therapy. Journal of Hepatology. 2006 Jan;44(1):151–7.

75. Xiang Z, Luo H, Payton JE, Cain J, Ley TJ, Opferman JT, et al. Mcl1 haploinsufficiency protects mice from Myc-induced acute myeloid leukemia. J Clin Invest. 2010 Jun 1;120(6):2109–18.

76. Kaufmann SH, Karp JE, Svingen PA, Krajewski S, Burke PJ, Gore SD, et al. Elevated expression of the apoptotic regulator Mcl-1 at the time of leukemic relapse. Blood. 1998 Feb 1;91(3):991–1000.

77. Cho-Vega JH, Rassidakis GZ, Admirand JH, Oyarzo M, Ramalingam P, Paraguya A, et al. MCL-1 expression in B-cell non-Hodgkin's lymphomas. Human Pathology. 2004 Sep;35(9):1095–100.

78. Zhou P, Levy NB, Xie H, Qian L, Lee CY, Gascoyne RD, et al. MCL1 transgenic mice exhibit a high incidence of B-cell lymphoma manifested as a spectrum of histologic subtypes. Blood. 2001 Jun 15;97(12):3902–9.

79. Rassidakis GZ, Jones D, Lai R, Ramalingam P, Sarris AH, McDonnell TJ, et al. BCL-2 family proteins in peripheral T-cell lymphomas: correlation with tumour apoptosis and proliferation. J Pathol. 2003;200(2):240–8.

80. Jaffe ESE. The 2008 WHO classification of lymphomas: implications for clinical practice and translational research. Hematology Am Soc Hematol Educ Program. 2008 Dec 31;:523–31.

81. Foss FM, Zinzani PL, Vose JM, Gascoyne RD, Rosen ST, Tobinai K. Peripheral T-cell lymphoma. Blood. 2011 Jun 23;117(25):6756–67.

82. Thorns C, Bastian B, Pinkel D, Roydasgupta R, Fridlyand J, Merz H, et al. Chromosomal aberrations in angioimmunoblastic T-cell lymphoma and peripheral T-cell lymphoma unspecified: A matrix-based CGH approach. Genes Chromosom Cancer. 2006;46(1):37–44.

83. Zettl A, Rüdiger T, Konrad M-A, Chott A, Simonitsch-Klupp I, Sonnen R, et al. Genomic profiling of peripheral T-cell lymphoma, unspecified, and anaplastic large T-cell lymphoma delineates novel recurrent chromosomal alterations. The American journal of pathology. Elsevier; 2004;164(5):1837–48.

84. Tan S-Y, Ooi A-S, Ang M-K, Koh M, Wong J-C, Dykema K, et al. leu2010295a. Leukemia. Nature Publishing Group; 2011 Jan 14;25(3):555–7.

85. Huang Y, de Reynies A, de Leval L, Ghazi B, Martin-Garcia N, Travert M, et al. Gene expression profiling identifies emerging oncogenic pathways operating in extranodal NK/T-cell lymphoma, nasal type. Blood. 2010 Feb 11;115(6):1226–37.

86. Lukk M, Kapushesky M, Nikkilä J, Parkinson H, Goncalves A, Huber W, et al. A global map of human gene expression. Nature Biotechnology. Nature Publishing Group; 2010 Apr 1;28(4):322–4.

87. Shah MV, Zhang R, Irby R, Kothapalli R, Liu X, Arrington T, et al. Molecular profiling of LGL leukemia reveals role of sphingolipid signaling in survival of cytotoxic lymphocytes. Blood. American Society of Hematology; 2008 Jul 23;112(3):770–81.

88. Rodríguez-Caballero A, García-Montero AC, Bárcena P, Almeida J, Ruiz-Cabello F, Tabernero MD, et al. Expanded cells in monoclonal TCR-alphabeta+/CD4+/NKa+/CD8-/+dim T-LGL lymphocytosis recognize hCMV antigens. Blood. 2008 Nov 30;112(12):4609–16.

89. Iqbal J, Weisenburger DD, Greiner TC, Vose JM, McKeithan T, Kucuk C, et al. Molecular signatures to improve diagnosis in peripheral T-cell lymphoma and prognostication in angioimmunoblastic T-cell lymphoma. Blood. 2010 Feb 4;115(5):1026–36.

90. Iqbal J, Wright G, Wang C, Rosenwald A, Gascoyne RD, Weisenburger DD, et al. Gene expression signatures delineate biologic and prognostic subgroups in peripheral T-cell lymphoma. Blood. 2014 Mar 14.

91. Piccaluga PP, Fuligni F, De Leo A, Bertuzzi C, Rossi M, Bacci F, et al. Molecular Profiling Improves Classification and Prognostication of Nodal Peripheral T-Cell Lymphomas: Results of a Phase III Diagnostic Accuracy Study. Journal of Clinical Oncology. 2013 Aug 16;31(24):3019–25.

92. Pileri SA, Piccaluga PP. New molecular insights into peripheral T cell lymphomas. J Clin Invest. 2012 Oct 1;122(10):3448–55.

93. International T-Cell Lymphoma Project. International Peripheral T-Cell and Natural Killer/T-Cell Lymphoma Study: Pathology Findings and Clinical Outcomes. Journal of Clinical Oncology. 2008 Aug 28;26(25):4124–30.

94. de Leval L. Pathology and biology of peripheral T-cell lymphomas. Ann Neurol. 2011 Feb 16;69(6):1060–1.

95. Savage KJ, Ferreri AJ, Zinzani PL, Pileri SA. Peripheral T-cell lymphoma–not otherwise specified. Critical reviews in oncology/hematology. Elsevier; 2011;79(3):321–9.

96. Piccaluga PP, Agostinelli C, Califano A, Rossi M, Basso K, Zupo S, et al. Gene expression analysis of peripheral T cell lymphoma, unspecified, reveals distinct profiles and new potential therapeutic targets. J Clin Invest. 2007 Mar 1;117(3):823–34.

97. Kaplan HS. The role of radiation on experimental Leukemogenesis. Natl Cancer Inst Monogr. 1964 May;14:207–20.

98. Newcomb EW, Diamond LE, Sloan SR, Corominas M, Guerrerro I, Pellicer A. Radiation and chemical activation of ras oncogenes in different mouse strains. Environ Health Perspect. 1989 Apr 30;81:33–7.

99. Jen K-Y, Song IY, Banta KL, Di Wu, Mao J-H, Balmain A. Sequential mutations in Notch1, Fbxw7, and Tp53 in radiation-induced mouse thymic lymphomas. Blood. 2012 Jan 18;119(3):805–9.

100. Kemp CJ, Wheldon T, Balmain A. p53-deficient mice are extremely susceptible to radiation-induced tumorigenesis. Nat Genet. 1994 Sep;8(1):66–9.

101. Kelly PN, White MJ, Goschnick MW, Fairfax KA, Tarlinton DM, Kinkel SA, et al. Individual and overlapping roles of BH3-only proteins Bim and Bad in apoptosis of lymphocytes and platelets and in suppression of thymic lymphoma development. Cell Death Differ. 2010 Apr 30;17(10):1655–64.

102. Streubel B, Vinatzer U, Willheim M, Raderer M, Chott A. Novel t(5;9)(q33;q22) fuses ITK to SYK in unspecified peripheral T-cell lymphoma. Leukemia. 2005 Dec 8;20(2):313–8.

103. Dierks C, Adrian F, Fisch P, Ma H, Maurer H, Herchenbach D, et al. The ITK-SYK Fusion Oncogene Induces a T-Cell Lymphoproliferative Disease in Mice Mimicking Human Disease. Cancer Res. 2010 Jul 28;70(15):6193–204.

104. Lee PP, Fitzpatrick DR, Beard C, Jessup HK, Lehar S, Makar KW, et al. A critical role for Dnmt1 and DNA methylation in T cell development, function, and survival. Immunity. 2001 Nov;15(5):763–74.

105. Burnette WN. “Western blotting”: electrophoretic transfer of proteins from sodium dodecyl sulfate--polyacrylamide gels to unmodified nitrocellulose and radiographic detection with antibody and radioiodinated protein A. Anal Biochem. 1981 Apr;112(2):195–203.

106. Seibler J. Rapid generation of inducible mouse mutants. Nucleic Acids Research. 2003 Feb 15;31(4):12e–12.

107. Wagner KU, Claudio E, Rucker EB, Riedlinger G, Broussard C, Schwartzberg PL, et al. Conditional deletion of the Bcl-x gene from erythroid cells results in hemolytic anemia and profound splenomegaly. Development. 2000 Nov;127(22):4949–58.

108. Ventura A, Kirsch DG, McLaughlin ME, Tuveson DA, Grimm J, Lintault L, et al. Restoration of p53 function leads to tumour regression in vivo. Nature. 2007 Jan 24;445(7128):661–5.

109. Machulla H-J, Blocher A, Kuntzsch M, Piert M, Wei R, Grierson JR. Simplified labeling approach for synthesizing 3′-deoxy-3′-[18F] fluorothymidine ([18F] FLT). Journal of Radioanalytical and Nuclear Chemistry. Springer; 2000;243(3):843–6.

110. Iqbal J, Weisenburger DD, Chowdhury A, Tsai MY, Srivastava G, Greiner TC, et al. leu2011102a. Leukemia. Nature Publishing Group; 2011 Aug 1;25(8):1377–7.

111. van Doorn R, van Kester MS, Dijkman R, Vermeer MH, Mulder AA, Szuhai K, et al. Oncogenomic analysis of mycosis fungoides reveals major differences with Sezary syndrome. Blood. 2009 Jan 2;113(1):127–36.

112. Travert M, Huang Y, de Leval L, Martin-Garcia N, Delfau-Larue MH, Berger F, et al. Molecular features of hepatosplenic T-cell lymphoma unravels potential novel therapeutic targets. Blood. 2012 Jun 14;119(24):5795–806.

113. de Leval L, Rickman DS, Thielen C, Reynies AD, Huang YL, Delsol G, et al. The gene expression profile of nodal peripheral T-cell lymphoma demonstrates a molecular link between angioimmunoblastic T-cell lymphoma (AITL) and follicular helper T (TFH) cells. Blood. 2007 Jun 1;109(11):4952–63.

114. Dürig J, Bug S, Klein-Hitpass L, Boes T, Jöns T, Martin-Subero JI, et al. Combined single nucleotide polymorphism-based genomic mapping and global gene expression profiling identifies novel chromosomal imbalances, mechanisms and candidate genes important in the pathogenesis of T-cell prolymphocytic leukemia with inv(14)(q11q32). Cell Death Differ. 2007 Aug 16;21(10):2153–63.

115. Shin J, Monti S, Aires DJ, Duvic M, Golub T, Jones DA, et al. Lesional gene expression profiling in cutaneous T-cell lymphoma reveals natural clusters associated with disease outcome. Blood. 2007 Oct 15;110(8):3015–27.

116. Eckerle S, Brune V, ring CDO, Tiacci E, Bohle V, m CSO, et al. leu2009161a. Leukemia. Nature Publishing Group; 2009 Aug 6;23(11):2129–38.

117. Lamant L, Reynies AD, Duplantier MM, Rickman DS, Sabourdy F, Giuriato S, et al. Gene-expression profiling of systemic anaplastic large-cell lymphoma reveals differences based on ALK status and two distinct morphologic ALK+ subtypes. Blood. 2007 Mar 1;109(5):2156–64.

118. Nakahata S, Ichikawa T, Maneesaay P, Saito Y, Nagai K, Tamura T, et al. Loss of NDRG2 expression activates PI3K-AKT signalling via PTEN phosphorylation in ATLL and other cancers. Nat Commun. 2013 Dec 31;5:3393–3.

119. Zhang J, Ding L, Holmfeldt L, Wu G, Heatley SL, Payne-Turner D, et al. The genetic basis of early T-cell precursor acute lymphoblastic leukaemia. Nature. Nature Publishing Group; 2012 Jan 4;481(7380):157–63.

120. Agostinelli C, Piccaluga PP, Went P, Rossi M, Gazzola A, Righi S, et al. Peripheral T cell lymphoma, not otherwise specified: the stuff of genes, dreams and therapies. Journal of Clinical Pathology. 2008 Oct 27;61(11):1160–7.

121. Cai Q, Deng H, Xie D, Lin T, Lin T. Phosphorylated AKT protein is overexpressed in human peripheral T-cell lymphomas and predicts decreased patient survival. Clin Lymphoma Myeloma Leuk. 2012 Mar 31;12(2):106–12.

122. Piva R, Agnelli L, Pellegrino E, Todoerti K, Grosso V, Tamagno I, et al. Gene Expression Profiling Uncovers Molecular Classifiers for the Recognition of Anaplastic Large-Cell Lymphoma Within Peripheral T-Cell Neoplasms. Journal of Clinical Oncology. 2010 Mar 18;28(9):1583–90.

123. Costello R, Sanchez C, Le Treut T. Peripheral T-cell lymphoma gene expression profiling and potential therapeutic exploitations - Costello - 2009 - British Journal of Haematology - Wiley Online Library. British journal of …. 2010.

124. Martinez-Delgado B. Peripheral T-cell lymphoma gene expression profiles. Hematol Oncol. 2006;24(3):113–9.

125. Murakami T, Ohtsuki M, Nakagawa H. Angioimmunoblastic lymphadenopathy-type peripheral T-cell lymphoma with cutaneous infiltration: report of a case and its gene expression profile. Br J Dermatol. 2001 Apr;144(4):878–84.

126. Foss HD, Anagnostopoulos I, Herbst H, Grebe M, Ziemann K, Hummel M, et al. Patterns of cytokine gene expression in peripheral T-cell lymphoma of angioimmunoblastic lymphadenopathy type. Blood. 1995 May 15;85(10):2862–9.

127. Bug S, DUrig J, Oyen F, Klein-Hitpass L, Martin-Subero JI, Harder L, et al. Recurrent loss, but lack of mutations, of the. Cancer Genetics and Cytogenetics. Elsevier Inc; 2009 Jul 1;192(1):44–7.

128. Nowak D, Le Toriellec E, Stern MH, Kawamata N, Akagi T, Dyer MJ, et al. Molecular allelokaryotyping of T-cell prolymphocytic leukemia cells with high density single nucleotide polymorphism arrays identifies novel common genomic lesions and acquired uniparental disomy. Haematologica. 2009 Apr 1;94(4):518–27.

129. Le Toriellec E, Despouy G, Pierron G, Gaye N, Joiner M, Bellanger D, et al. Haploinsufficiency of CDKN1B contributes to leukemogenesis in T-cell prolymphocytic leukemia. Blood. 2008 Feb 8;111(4):2321–8.

130. Brito-Babapulle V, Hamoudi R, Matutes E, Watson S, Kaczmarek P, Maljaie H, et al. p53 allele deletion and protein accumulation occurs in the absence of p53 gene mutation in T-prolymphocytic leukaemia and Sezary syndrome. British Journal of Haematology. 2000 Jul;110(1):180–7.

131. Mossafa H, Brizard A, Huret JL, Brizard F, Lessard M, Guilhot F, et al. Trisomy 8q due to i(8q) or der(8) t(8;8) is a frequent lesion in T-prolymphocytic leukaemia: four new cases and a review of the literature. British Journal of Haematology. 1994 Apr;86(4):780–5.

132. Maljaei SH, Brito-Babapulle V, Hiorns LR, Catovsky D. Abnormalities of chromosomes 8, 11, 14, and X in T-prolymphocytic leukemia studied by fluorescence in situ hybridization. Cancer Genetics and Cytogenetics. 1998 Jun;103(2):110–6.

133. Maljaie SH, Brito-Babapulle V, Matutes E, Hiorns LR, De Schouwer PJ, Catovsky D. Expression of c-myc oncoprotein in chronic T cell leukemias. Leukemia. 1995 Oct;9(10):1694–9.

134. Campbell JJ, Clark RA, Watanabe R, Kupper TS. Sezary syndrome and mycosis fungoides arise from distinct T-cell subsets: a biologic rationale for their distinct clinical behaviors. Blood. 2010 Aug 5;116(5):767–71.

135. Mahadevan D. Transcript profiling in peripheral T-cell lymphoma, not otherwise specified, and diffuse large B-cell lymphoma identifies distinct tumor profile signatures. Molecular Cancer Therapeutics. 2005 Dec 1;4(12):1867–79.

136. Bellavia D, Campese AF, Checquolo S, Balestri A, Biondi A, Cazzaniga G, et al. Combined expression of pTalpha and Notch3 in T cell leukemia identifies the requirement of preTCR for leukemogenesis. Proc Natl Acad Sci USA. 2002 Mar 19;99(6):3788–93.

137. Feldman AL, Sun DX, Law ME, Novak AJ, Attygalle AD, Thorland EC, et al. Overexpression of Syk tyrosine kinase in peripheral T-cell lymphomas. Leukemia. 2008 Apr 10;22(6):1139–43.

138. Üner AH MD, PhD, A, Sağlam A, Han Ü, Hayran M, Sungur A, Ruacan Ş. PTEN and p27 expression in mature T-cell and NK-cell neoplasms. Leuk Lymphoma. 2005 Jan;46(10):1463–70.

139. Martinez-Delgado B, Meléndez B, Cuadros M, Alvarez J, Castrillo JM, la Parte de AR, et al. Expression profiling of T-cell lymphomas differentiates peripheral and lymphoblastic lymphomas and defines survival related genes. Clinical Cancer Research. AACR; 2004;10(15):4971–82.

140. Ballester B, Ramuz O, Gisselbrecht C, Doucet G, Loï L, Loriod B, et al. Gene expression profiling identifies molecular subgroups among nodal peripheral T-cell lymphomas. Oncogene. 2005 Nov 14;25(10):1560–70.

141. Thompson MA, Stumph J, Henrickson SE, Rosenwald A, Wang Q, Olson S, et al. Differential gene expression in anaplastic lymphoma kinase–positive and anaplastic lymphoma kinase–negative anaplastic large cell lymphomas. Human Pathology. 2005 May;36(5):494–504.

142. Cuadros M, Dave SS, Jaffe ES, Honrado E, Milne R, Alves J, et al. Identification of a Proliferation Signature Related to Survival in Nodal Peripheral T-Cell Lymphomas. Journal of Clinical Oncology. 2007 Aug 1;25(22):3321–9.

143. Piccaluga PP, Agostinelli C, Zinzani PL, Baccarani M, Favera RD, Pileri SA. Expression of platelet-derived growth factor receptor in peripheral T-cell lymphoma not otherwise specified. Lancet Oncol. 2005 May 20;:1–1.

144. Piccaluga PP, Agostinelli C, Righi S, Zinzani PL, Pileri SA. Expression of CD52 in peripheral T-cell lymphoma. Haematologica. 2007 Apr;92(4):566–7.

145. Tracey L. Mycosis fungoides shows concurrent deregulation of multiple genes involved in the TNF signaling pathway: an expression profile study. Blood. 2003 Apr 3;102(3):1042–50.

146. Miyazaki K, Yamaguchi M, Imai H, Kobayashi T, Tamaru S, Nishii K, et al. Gene expression profiling of peripheral T-cell lymphoma including T-cell lymphoma. Blood. 2008 Sep 29;113(5):1071–4.

147. Kent WJ. BLAT--the BLAST-like alignment tool. Genome Res. 2002 Mar 31;12(4):656–64.

148. Oltersdorf T, Elmore SW, Shoemaker AR, Armstrong RC, Augeri DJ, Belli BA, et al. An inhibitor of Bcl-2 family proteins induces regression of solid tumours. Nature. 2005 May 15;435(7042):677–81.

149. Lee EF, Czabotar PE, van Delft MF, Michalak EM, Boyle MJ, Willis SN, et al. A novel BH3 ligand that selectively targets Mcl-1 reveals that apoptosis can proceed without Mcl-1 degradation. The Journal of Cell Biology. 2008 Jan 22;180(2):341–55.

150. Yip KW, Reed JC. Bcl-2 family proteins and cancer. Oncogene. 2008 Oct 27;27(50):6398–406.

151. Frenzel A, Grespi F, Chmelewskij W, Villunger A. Bcl2 family proteins in carcinogenesis and the treatment of cancer. Apoptosis. 2009 Apr;14(4):584–96.

152. Allen TD, Zhu CQ, Jones KD, Yanagawa N, Tsao M-S, Bishop JM. Interaction between MYC and MCL1 in the genesis and outcome of non-small-cell lung cancer. Cancer Res. 2011 Mar 15;71(6):2212–21.

153. Zhou P, Qian L, Bieszczad CK, Noelle R, Binder M, Levy NB, et al. Mcl-1 in Transgenic Mice Promotes Survival in a Spectrum of Hematopoietic Cell Types and Immortalization in the Myeloid Lineage. Blood. American Society of Hematology; 1998 Nov 1;92(9):3226–39.

154. Weyhenmeyer B, Murphy AC, Prehn J. Targeting the anti-apoptotic Bcl-2 family members for the treatment of cancer. Exp Oncology 2012; 34(3):192-9.

155. Thomas S, Quinn BA, Das SK, Dash R, Emdad L, Dasgupta S, et al. Targeting the Bcl-2 family for cancer therapy. Expert Opin Ther Targets. 2013 Jan;17(1):61–75.

156. Zhang C-L, Kamarashev J, Qin J-Z, Burg GN, Dummer R, D bbeling U. Expression of apoptosis regulators in cutaneous T-cell lymphoma (CTCL) cells. J Pathol. 2003;200(2):249–54.

157. Grabow S, Delbridge ARD, Valente LJ, Strasser A. MCL-1 but not BCL-XL is critical for the development and sustained expansion of thymic lymphoma in p53-deficient mice. Blood. 2014 Dec 17;124(26):3939–46.

158. Yecies D, Carlson NE, Deng J, Letai A. Acquired resistance to ABT-737 in lymphoma cells that up-regulate MCL-1 and BFL-1. Blood. 2010 Apr 22;115(16):3304–13.

159. Tromp JM, Geest CR, Breij ECW, Elias JA, van Laar J, Luijks DM, et al. Tipping the Noxa/Mcl-1 Balance Overcomes ABT-737 Resistance in Chronic Lymphocytic Leukemia. Clinical Cancer Research. 2012 Jan 16;18(2):487–98.

160. Keuling AM, Felton KEA, Parker AAM, Akbari M, Andrew SE, Tron VA. RNA silencing of Mcl-1 enhances ABT-737-mediated apoptosis in melanoma: role for a caspase-8-dependent pathway. PLoS One. 2009;4(8):e6651–1.

161. Mazumder S, Choudhary GS, Al-harbi S, Almasan A. Mcl-1 Phosphorylation Defines ABT-737 Resistance That Can Be Overcome by Increased NOXA Expression in Leukemic B cells. Cancer Res. 2012 Jun 14;72(12):3069–79.

162. Pobezinsky LA, Angelov GS, Tai X, Jeurling S, Van Laethem F, Feigenbaum L, et al. Clonal deletion and the fate of autoreactive thymocytes that survive negative selection. Nat Immunol. 2012 Apr 29;13(6):569–78.

163. Glaser SP, Lee EF, Trounson E, Bouillet P, Wei A, Fairlie WD, et al. Anti-apoptotic Mcl-1 is essential for the development and sustained growth of acute myeloid leukemia. Genes Dev. 2012 Jan 25;26(2):120–5.

164. Thomas RL, Roberts DJ, Kubli DA, Lee Y, Quinsay MN, Owens JB, et al. Loss of MCL-1 leads to impaired autophagy and rapid development of heart failure. Genes Dev. 2013 Jun 20;27(12):1365–77.

165. Kitada S, Andersen J, Akar S, Zapata JM, Takayama S, Krajewski S, et al. Expression of apoptosis-regulating proteins in chronic lymphocytic leukemia: correlations with In vitro and In vivo chemoresponses. Blood. 1998 May 1;91(9):3379–89.

166. Palve V, Mallick S, Ghaisas G, Kannan S, Teni T. Overexpression of Mcl-1L Splice Variant Is Associated with Poor Prognosis and Chemoresistance in Oral Cancers. Balaji KN, editor. PLoS One. 2014 Nov 19;9(11):e111927.

167. Michels J, Obrist F, Vitale I, Lissa D, Garcia P, Behnam-Motlagh P, et al. MCL-1 dependency of cisplatin-resistant cancer cells. Biochem Pharmacol. 2014 Aug 12.

168. Rosato RR, Almenara JA, Kolla SS, Maggio SC, Coe S, Gimenez MS, et al. Mechanism and functional role of XIAP and Mcl-1 down-regulation in flavopiridol/vorinostat antileukemic interactions. Molecular Cancer Therapeutics. 2007 Feb 1;6(2):692–702.

169. Hussain SRA, Cheney CM, Johnson AJ, Lin TS, Grever MR, Caligiuri MA, et al. Mcl-1 Is a Relevant Therapeutic Target in Acute and Chronic Lymphoid Malignancies: Down-Regulation Enhances Rituximab-Mediated Apoptosis and Complement-Dependent Cytotoxicity. Clinical Cancer Research. 2007 Apr 1;13(7):2144–50.

170. Naci D, Azreq El MA, Chetoui N, Lauden L, Sigaux F, Charron D, et al. 2 1 Integrin Promotes Chemoresistance against Doxorubicin in Cancer Cells through Extracellular Signal-regulated Kinase (ERK). Journal of Biological Chemistry. 2012 May 18;287(21):17065–76.

171. Cencic R, Hall DR, Robert F, Du Y, Min J, Li L, et al. Reversing chemoresistance by small molecule inhibition of the translation initiation complex eIF4F. Proc Natl Acad Sci USA. 2011 Jan 17;108(3):1046–51.

172. Li Z, Younger K, Gartenhaus R, Joseph AM, Hu F, Baer MR, et al. Inhibition of IRAK1/4 sensitizes T cell acute lymphoblastic leukemia to chemotherapies. J Clin Invest. 2015 Feb 2;125(3):1081–97.

173. Wang X, Bathina M, Lynch J, Koss B, Calabrese C, Frase S, et al. Deletion of MCL-1 causes lethal cardiac failure and mitochondrial dysfunction. Genes Dev. 2013 Jun 20;27(12):1351–64.

174. Opferman JT, Letai A, Beard C, Sorcinelli MD, Ong CC, Korsmeyer SJ. Development and maintenance of B and T lymphocytes requires antiapoptotic MCL-1. Nature. 2003;426(6967):671–6.

175. Dzhagalov I, Dunkle A, He Y-W. The anti-apoptotic Bcl-2 family member Mcl-1 promotes T lymphocyte survival at multiple stages. J Immunol. 2008;181(1):521–8.

176. Nelson M, Horsman DE, Weisenburger DD, Gascoyne RD, Dave BJ, Loberiza FR, et al. Cytogenetic abnormalities and clinical correlations in peripheral T-cell lymphoma. British Journal of Haematology. 2008 May;141(4):461–9.

177. Tsukasaki. Comparative genomic hybridization analysis in adult T-cell leukemia/lymphoma: correlation with clinical course. 2001 May 15;:1–7.

178. Wang B, Xie M, Li R, Owonikoko TK, Ramalingam SS, Khuri FR, et al. Role of Ku70 in deubiquitination of Mcl-1 and suppression of apoptosis. Cell Death Differ. Nature Publishing Group; 2014 Apr 25;21(7):1160–9.

179. Ertel F, Nguyen M, Roulston A, Shore GC. Programming cancer cells for high expression levels of Mcl1. Nature Publishing Group. Nature Publishing Group; 2013 Apr 1;14(4):328–36.

180. Inuzuka H, Fukushima H, Shaik S, Liu P, Lau AW, Wei W. Mcl-1 ubiquitination and destruction. Oncotarget. 2011 Mar;2(3):239–44.

181. Zhang C, Cai TY, Zhu H, Yang LQ, Jiang H, Dong XW, et al. Synergistic Antitumor Activity of Gemcitabine and ABT-737 In Vitro and In Vivo through Disrupting the Interaction of USP9X and Mcl-1. Molecular Cancer Therapeutics. 2011 Jul 6;10(7):1264–75.

182. Belmar J, Fesik SW. Small molecule Mcl-1 inhibitors for the treatment of cancer Pharmacology and Therapeutics. Elsevier B.V; 2014 Sep 1;:1–9.

183. Cohen NA, Stewart ML, Gavathiotis E, Tepper JL, Bruekner SR, Koss B, et al. A competitive stapled peptide screen identifies a selective small molecule that overcomes MCL-1-dependent leukemia cell survival. Chem Biol. 2012 Sep 20;19(9):1175–86.

184. Varadarajan S, Vogler M, Butterworth M, Dinsdale D, Walensky LD, Cohen GM. Evaluation and critical assessment of putative MCL-1 inhibitors. Nature Publishing Group; 2013 Jul 5;20(11):1475–84.

185. Chen L, Willis SN, Wei A, Smith BJ, Fletcher JI, Hinds MG, et al. Differential targeting of prosurvival Bcl-2 proteins by their BH3-only ligands allows complementary apoptotic function. Mol Cell. 2005 Feb 4;17(3):393–403.

186. Tse C, Shoemaker AR, Adickes J, Anderson MG, Chen J, Jin S, et al. ABT-263: A Potent and Orally Bioavailable Bcl-2 Family Inhibitor. Cancer Res. 2008 May 1;68(9):3421–8.

187. Vogler M. BCL2A1: the underdog in the BCL2 family. Nature Publishing Group; 2011 Nov 11;19(1):67–74.

188. Ottina E, Grespi F, Tischner D, Soratroi C, Geley S, Ploner A, et al. Targeting antiapoptotic A1/Bfl-1 by in vivo RNAi reveals multiple roles in leukocyte development in mice. Blood. 2012 Jun 20;119(25):6032–42.

189. Métais J-Y, Winkler T, Geyer JT, Calado RT, Aplan PD, Eckhaus MA, et al. BCL2A1a Over-Expression in Murine Hematopoietic Stem and Progenitor Cells Decreases Apoptosis and Results in Hematopoietic Transformation. PLoS One. Public Library of Science; 2012 Oct 30;7(10):e48267.

190. Mandal M, Borowski C, Palomero T, Ferrando AA, Oberdoerffer P, Meng F, et al. The BCL2A1 gene as a pre-T cell receptor-induced regulator of thymocyte survival. J Exp Med. 2005 Feb 21;201(4):603–14.